Microscale Process Characterisation of Oxidative Bioconversions

Claudia Ferreira-Torres

A thesis submitted for the degree of
Doctor of Philosophy to the
University of London

Department of Biochemical Engineering
University College London
Torrington Place
London
WC1E 7JE

ProQuest LLC
789 East Eisenhower Parkway
P.O. Box 1346
Ann Arbor, MI 48106-1346

Disclaimer

I, Claudia Ferreira-Torres, confirm that the work presented in this thesis is my own. Where information has been derived from other sources I confirm that this has been indicated in the thesis.

Claudia Ferreira-Torres

Abstract

In this work, the potential of automated microscale process sequences for the evaluation of recombinant biocatalysts and the use of microwell data to inform larger scale operations is examined. As a model bioconversion, the cyclohexanone monooxygenase (CHMO) Baeyer-Villiger oxidation of a range of cyclic ketone substrates was examined; cyclopentanone, cyclohexanone and bicyclo[3.2.0]hept-2-en-6-one. Three whole cell biocatalysts were evaluated which included two strains of *E. coli*: TOP10 [pQR239] and JM107 and *A. calcoaceticus* NCIMB 9871.

Initial studies to establish the microwell process used the well-characterised *E. coli* TOP10 [pQR239] biocatalyst that was previously prepared in our laboratory. It was shown that quantitative and reproducible data could be obtained for fermentation, enzyme induction and bioconversion operations carried out in 96 Deep Square Well (96 DSW) plate formats. It was possible to produce up to 5.8 $g_{DCW}.l^{-1}$ of the *E. coli* biocatalyst and support growth rates up to 0.55 h^{-1}. The biocatalyst had a specific CHMO activity of 11 $U.g_{DCW}^{-1}$ and could catalyse the conversion of bicyclo[3.2.0]hept-2-en-6-one at an initial rate of product formation of 62 $\mu mol.l^{-1}.min^{-1}$ with high yields of up to 92%.

The microscale process sequence was then operated in an automated fashion using a Multiprobe II EX liquid handling robot (Packard Instrument Company, Meriden, Connecticut, US). The process performance of the three biocatalysts was then examined following a combinatorial approach in which biocatalyst was produced at initial glycerol concentrations of 10 and 20 in fermentation and, following induction (when required), bioconversion rates were measured for each of the three ketone substrates at initial concentrations of 0.5 $g.l^{-1}$ and 1.0 $g.l^{-1}$. The *E. coli* TOP10 [pQR239] biocatalyst showed the best overall performance and the results obtained were comparable to those already reported in the literature.

Finally, the ability of microwell results to be predictive of larger scale operations was examined. Given the demand for molecular oxygen at both, the fermentation and bioconversion stages, the oxygen mass transfer coefficient, k_La, was considered as a basis for scale-up. k_La values in both shaken microwell plates and a 2 l stirred bioreactor were determined over a range of operating conditions. Values in the range 15 – 188 h^{-1} could be obtained at both scales. Processes carried out at the two scales at matched k_La values showed excellent agreement both in terms of the quantitative values of the results obtained and the way in which the process performance varied with k_La.

The results obtained in this thesis further show the potential of automated microwell experimentation to support rapid and more cost effective bioprocess development.

Acknowledgements

Firstly I would like to thank my supervisor, Dr. Gary Lye, for all his advice and support during my time at UCL and Dr. Paul Dalby for helpful discussions throughout the project. In addition I gratefully acknowledge the financial support provided by the Mexican Government through CONACYT and the ORS program. I would also like to thank all those people within the Department of Biochemical Engineering at UCL (past and present) who have helped me during my research. In particular I would like to thank Dr. Steve Doig for much practical discussion and advice regarding the Baeyer-Villiger bioconversion and microwells. Thank you, Nigel B. Jackson for our work together doing the microfiltration experiments. My thanks also go to Billy Doyle and Ian Buchanan for their invaluable technical support throughout the project. A special mention to Mike Hoare and Nigel Titchener-Hooker.

On a personal level I would like to thank all my fellow researchers with whom I shared the ups and downs of the PhD experience and who have made my time at UCL so enjoyable. To my friends in Mexico, I thoroughly miss you all. To Sarah, thank you for your support, help and shoulder, hope you'll visit!. Also my thanks and my love to my husband Tony, for keeping me sane in the bad times, and not so sane at others; to you Tony, the family we are about to start, and the family that saw me grow up, my mum Carmen and my sister Viris, I would like to dedicate this thesis.

A mi chiquito... I'm waiting for you, my baby!.

Index

Disclaimer	3
Abstract	4
Acknowledgements	5
List of figures	11
List of tables	22
Nomenclature	24
Abbreviations	27
1.0 Introduction	28
1.1 Bioconversions	28
1.1.1 The Baeyer-Villiger reaction	29
1.1.1.1 Baeyer-Villiger monooxygenase (BVMO)	31
1.1.1.2 Cyclohexanone monooxygenases (CHMOs)	32
1.1.2 Whole cell biocatalysis	33
1.1.3 Whole cell BVMO biocatalysis	36
1.2 Microscale bioprocessing	38
1.2.1 Microwell plates in bioscience applications	39
1.2.2 Biocatalytic microscale processing	41
1.2.3 Microscale bioreactors	43
1.2.4 Microscale process monitoring	45
1.2.5 Microscale process automation	48
1.2.6 Microscale downstream processing	49
1.3 Engineering characterisation of shaken microwells	49
1.3.1 Scale up fundamentals	49
1.3.2 Importance of oxygen mass transfer in scale-up	50
1.3.3 Oxygen mass transfer in microwells	52

1.3.4 Methods for quantifying k_La values 56
1.3.5 Modelling and prediction of engineering parameters in microwell plates 58
1.3.6 Methods to increase the oxygen transfer rate 59
1.4 Aims and Objectives 62

2.0 Materials and methods 66
2.1 Reagents and suppliers 66
2.2 Microorganisms 66
2.3 Analytical techniques 66
2.3.1 Substrate and product quantification by gas chromatography (GC) 67
2.3.1.1 Sample preparation for GC analysis 67
2.3.1.2 GC operation 67
2.3.1.3 Quantification of the GC response 68
2.3.1.4 Ketone and lactone evaporation curve 68
2.3.2 Biomass quantification 69
2.3.2.1 Dry cell weight (DCW) measurement 69
2.3.2.2 Optical density (OD) measurement 69
2.4. k_La measurements 70
2.4.1 Microscale k_La measurements 70
2.4.1.1. DOT probe 71
2.4.2 Bench scale k_La measurements 73
2.4.3 Bioprocess comparison under matching k_La at two scales 73
2.5 Microwell evaporation rate 74
2.6 Microscale processes sequence 75
2.6.1 *E. coli* TOP10 [pQR239] 75
2.6.1.1 Microorganism origin and culture 75
2.6.1.2 Inoculum preparation 76
2.6.1.3 Microscale fermentations 76

2.6.1.4 Microscale fermentation DOT monitoring 78
2.6.1.5 Microscale bioconversion 79
2.6.1.6 Bench scale fermentation 79
2.6.1.7 Fermentation data logging 82
2.6.2. *E. coli* JM107 [pQR210] 82
2.6.2.1 Microorganism origin and culture 82
2.6.2.2 Inoculum preparation 83
2.6.2.3 Microscale fermentations 83
2.6.2.4 Microscale bioconversion 85
2.6.3 *Acinetobacter calcoaceticus* NCIMB 9871 85
2.6.3.1 Microorganism origin and culture 85
2.6.3.2 Biocatalyst fermentation 86
2.6.3.3 Microscale bioconversion 87
2.6.4 Automated microscale process sequences 87
2.7 Microscale downstream processing 89
2.7.1 Microscale centrifugation 89
2.7.2 Microfiltration 90

3.0 Microscale unit operations and their characterisation 91
3.1 Aims of the chapter 91
3.2 Shake flask *E. coli* TOP10 [pQR239] process 92
3.2.1 Fermentation kinetics 92
3.2.2 Bioconversion kinetics 92
3.3 Microscale fermentation process characterisation 94
3.3.1 Effect of microwell geometry 94
3.3.2 Effect of inoculum concentration 99
3.3.3 Effect of temperature 101
3.3.4 Effect of evaporation in open microwells 101
3.4 Parallel fermentation and DOT monitoring 105

3.4.1 Oxygen sensing in 96 SRW microwell plates 105
3.4.2 Limitations in the use of oxygen sensing 96 SRB plate. 107
3.4.3 Illustration of high throughput potential 110
3.5 Microscale bioconversion process characterisation 113
3.5.1 Substrate and product evaporation rates 113
3.5.2 Effect of liquid fill volume 114
3.5.3 Effect of temperature and substrate concentration 118
3.6 Dry cell weight estimation at the microwell scale 121
3.7 Summary 126

4.0 Parallel microscale process sequences: fermentation, bioconversion and biocatalyst recovery 128
4.1 Aims of the chapter 128
4.2 Microscale processes calculations and evaluation 129
4.2.1 Automation of microscale processing techniques 129
4.2.2 Quantitative analysis of process performance 132
4.2.3 Reproducibility of microscale fermentation and bioconversion 133
4.3 Evaluation of different CHMO host strains 137
4.3.1 Microscale fermentation 137
4.3.2 Microscale whole cell bioconversion 140
4.3.3 Parallel fermentation and bioconversion process analysis 142
4.3.3.1 Microscale fermentation 142
4.3.3.2 Microscale bioconversion 144
4.4 Evaluation of biocatalyst recovery options 149
4.4.1 Microscale centrifugation 149
4.4.2 Microfiltration 150
4.5 Summary 155

5.0 Predictive scale-up of microwell results 157

5.1 Aims of the chapter 157
5.2 k_La as a basis for scale-up 158
5.2.1 Prediction of k_La values 158
5.2.2 Measurements of k_La values 161
5.2.2.1 96 DSW plate k_La values 161
5.2.2.2 Stirred bioreactor k_La values 167
5.3 Process variation at matched k_La values 171
5.3.1 Fermentation and bioconversion kinetics at typical k_La values 171
5.3.2 The need to investigate processes at different k_La values 177
5.3.3 Fermentation and bioconversion at "low" k_La value 177
5.3.4 Fermentation and bioconversion at "high" k_La value 181
5.3.5 Process comparison at different k_La values 185
5.4 Summary 187

6.0 Conclusions and future work 189
6.1 Microscale process design, characterisation and parallelisation 189
6.2 Predictive scale up of microwell results 193
6.3 Future work 196

7.0 References 199

Appendix I 219
Appendix II 223
Appendix III 230
Appendix IV 240
Appendix V 247

List of figures

Figure 1.1 Mechanism of the Baeyer-Villiger oxidation by peracids. Reproduced form Kamerbeek et al. (2003).

Figure 1.2 Model BVMO conversion reaction schemes: (A) CHMO-mediated regiodivergent oxidation of bicyclo[3.2.0]hept-2-en-6-one yielding (−)-(1*S*,5*R*)-2-oxabicyclo[3.3.0]oct-6-en-3-one and (−)-(1*R*,5*S*)-3-oxabicyclo[3.3.0]oct-6-en-2-one; (B) CHMO-mediated asymmetric oxidation of 4-methylcyclohexanone yielding (*S*)-5-methyl-oxepane-2-one; (C) CHMO-mediated oxidative resolution of 2-hexylcyclopentanone yielding (*S*)-6-hexyltetrahydropyran-2-one. (Doig et al., 2003). Note the requirement for molecular oxygen in each reaction scheme.

Figure 1.3 Example of a 24 SRW plate-based miniature stirred bioreactor. Turbidity was measured using probes A and B. This bioreactor presented similar characteristics to those of larger vessels such as pH and oxygen transfer probes, impellers and geometric ratios. Reproduced from Lamping et al. (2003).

Figure 1.4 Schematic diagram of the mechanism of PreSens sensing spot and probe. Reproduced from the manufacturer's internet page (www.presens.de, 31/04/06).

Figure 1.5 Photograph of 96 Standard Round Well (SRW) microwell plate with integrated fluorescence sensor for dissolved oxygen measurements.

Figure 1.6 Images of the liquid phase (water) during shaking at a shaking diameter of 25 mm and a fill volume of 200 µl at different shaking frequencies in a 96-well plate, where h_L is the liquid

height in the well. Images were obtained with a CCD camera installed on a shaking platform. Reproduced from Hermann et al. (2003).

Figure 1.7 Maximum oxygen transfer capacity (OTR_{max}) and specific mass transfer coefficient (k_La) in conventional 96 SRW plate at different shaking diameters and shaking frequencies with 200 µl fill volume. Measurements carried out using the sodium sulphite method. Reproduced from Hermann et al. (2002).

Figure 1.8 Images of the liquid phase (coloured water) during shaking at a shaking diameter of 6 mm and a fill volume of 400 µl at different shaking frequencies in a 96 DSW. Images were obtained with a NAC HSV-500 high-speed, analogue camera. Reproduced from Micheletti et al. (2006).

Figure 2.1 Schematic Diagram of a single well on the edge of a 96 DSW plate adapted for k_La measurements as described on Section 2.4.1.1.

Figure 2.2 Automated microscale sequence for the process evaluation of a recombinant *E. coli* TOP10 [pQR239] biocatalyst expressing cyclohexanone monooxygenase (CHMO).

Figure 2.3 Automated microscale sequence for the process evaluation of a recombinant *E. coli* JM107 [PQR210] biocatalyst expressing cyclohexanone monooxygenase (CHMO).

Figure 2.4 Automated microscale sequence for the process evaluation of a recombinant *A. calcoaceticus* NCIMB 9871 biocatalyst expressing cyclohexanone monooxygenase (CHMO).

Figure 3.1 Typical batch growth kinetics of *E. coli* TOP10 [pQR239] grown in shake flasks. Experiments performed as described in Section

2.3.2.2. Error bars represent the range of measured values about the mean.

Figure 3.2 Typical batch bioconversion kinetics in shake flask using a whole cell *E. coli* TOP10 [pQR239] biocatalysis with 1 $g.l^{-1}$ initial bicycloketone substrate concentration. This figure shows bicycloketone (♦) depletion over time and the corresponding bicyclolactone (■) production. Experiments performed as described in Section 2.6.1. Error bars represent the range of measured values about the mean.

Figure 3.3 Schematic diagrams of the 96 well plate geometries Standard Round Well (SRW) and Deep Square Well (DSW) used in this work (A) plan view, (B) cross section through single wells and (C) well working volume.

Figure 3.4 (A) Typical batch growth kinetics of *E. coli* TOP10 [pQR239] in two different microwell geometries: 96 SRW (■) and 96 DSW (▲). Experiments performed as described in Section 2.6.1.3. (B) Plot of the natural logarithm of biomass concentration against time used to calculate the growth rate kinetics in 96 DSW. Error bars represent the range of measured values about the mean.

Figure 3.5 (A) Effect of inoculum concentration on *E. coli* TOP10 [pQR239] batch fermentation kinetics in 96 DSW plates. (B) Growth rate calculations for different inoculum concentrations. Two inoculum concentrations were used, 5 % v/v (♦) and 10% v/v (■). Experiments performed as described in Section 2.6.1.3. Error bars represent the range of measured values about the mean.

Figure 3.6 Effect of temperature on batch growth kinetics of *E. coli* TOP10 [pQR239] in 96 DSW plates, using 5% v/v inoculum and 1000

rpm agitation. The temperatures investigated were 30°C (♦) and 37°C (■). Experiments performed as described in Section 2.6.1.3. Error bars represent the range of measured values about the mean.

Figure 3.7 Rate of water evaporation from a 96 DSW plate incubated at 37°C and agitation at 1000 rpm agitation speed. Experiments performed as described in Section 2.5. Error bars represent the range of measured values about the mean.

Figure 3.8 *In situ* dissolved oxygen concentration measurement in round-bottomed microtiter plates with an integrated optical sensor. F1, filter for excitation light (540 nm); F2, filter for fluorescence light (640 nm and 590 nm); SL, sensor layer; CB, culture broth. Figure adopted from Gernot et al. (2003).

Figure 3.9 Biomass growth kinetics and associated dissolved oxygen levels during *E. coli* TOP10 [pQR239] batch fermentations. Figure (A) shows the growth kinetics using 2.5 % v/v inoculum concentration, biomass concentration (▲) and DOT (♦, second y-axis). Figure (B) shows the profile using 5% v/v inoculum, biomass concentration (•) and DOT (■, second y-axis). Experiments were performed as described in Section 2.6.1.4. Error bars represent the range of measured values about the mean.

Figure 3.10 Parallel batch fermentation kinetics of *E. coli* TOP10 [pQR239] in standard 96 round bottomed microwell plates with integrated dissolved oxygen sensing using a FluoStar Optima microwell plate reader as incubator. This figure shows selected data from 96 parallel fermentations performed at different initial carbon source and inoculum concentrations: (Row A) 5 $g.l^{-1}$ glycerol, (Row B)

10 g.l^{-1} glycerol, (Column 1) 1% v/v inoculum, (Column 2) 2.5% v/v inoculum, (Column 3) 5% v/v inoculum. Smooth lines represent biomass dry cell weight data; dotted lines represent Dissolved Oxygen data. Experiments were performed as described in Section 2.6.1.4.

Figure 3.11 Evaporation rate of bicycloketone (♦) and bicyclolactone (●) from a 96 DSW plate with a fill volume of 1 ml. The initial concentration of bicycloketone and bicyclolactone was 1.0 g.l^{-1}. Measurements were performed at 30°C and 1000 rpm, as described in Section 2.3.1. Error bars represent the range of measured values about the mean.

Figure 3.12 Effect of liquid fill volume on whole cell *E. coli* TOP10 [pQR239] bioconversion kinetics. The bioconversion was carried out in 96 DSW using an initial concentration of 1 g.l^{-1} bicycloketone within each well, 30°C and 1000 rpm. Three different volumes were explored, 1000 µl (♦), 500 µl (▲) and 200 µl (●). Experiments performed as described in Section 2.6.1.5. Error bars represent the range of measured values about the mean.

Figure 3.13 Effect of initial bicycloketone concentration and temperature on whole cell *E. coli* TOP10 [pQR239] bioconversion kinetics. The bioconversion was carried out using 0.5 g.l^{-1} of bicycloketone within each well at 30°C and 1000 rpm. The solid symbols represent the bicycloketone utilisation kinetics, while the open symbols represent the bicyclolactone. Two different volumes were tested, 500 µl (▲) and 1000 µl (♦). Experiments performed as described in Section 2.6.1.5. Error bars represent the range of measured values about the mean.

Figure 4.1 The Multiprobe II EX liquid handling robot from Perkin Elmer and the Packard Instrument Company (Meriden, Connecticut, US). Image obtained from the Advanced Centre of Biochemical Engineering (ACBE) facilities in UCL. In this picture the robot is dispensing liquids into a 96 SRW plate using disposable tips.

Figure 4.2 Illustration of the WinPrep programme used to perform the microscale fermentation and bioconversion sequence described in Section 4.2.1. The left hand window illustrates the timed sequence of events involved in setting up the experimental protocol and shows user prompts at key stages in the process. The right hand window shows the deck layout used and the different labware geometries that can be addressed.

Figure 4.3 Reproducibility of independently replicated *E. coli* TOP10 [pQR239] batch microscale fermentations in a 96 DSW plate. All fermentations were induced by addition of L-arabinose 15% $w.v^{-1}$ three hours after inoculation. Experiments performed as described in Section 2.6.1.3 and 2.6.1.5. Error bars represent the range of measured values about the mean.

Figure 4.4 Reproducibility of independently replicated bioconversion kinetics of bicyclo[3.2.0]hept-2-en-6-one in 96 DSW plates using *E. coli* TOP10 [pQR239] as whole cell biocatalyst. Bioconversions were carried out at an initial ketone concentration of 0.4 $g.l^{-1}$: ketone depletion (●) and lactone formation (■). Experiments performed as described in Section 2.6.1.3 and 2.6.1.5. Error bars represent the range of measured values about the mean.

Figure 4.5 Reproducibility of bioconversion kinetics (past fermentation) across a single 96 DSW plate. After fifteen minutes of

bioconversion the average bicycloketone concentration (□) remaining across the plate was 0.1 ± 0.015 $g.l^{-1}$, while the average bicyclolactone (■) produced was 0.18 ± 0.02 $g.l^{-1}$. The error in product formation was of 12%. Experiments performed as described in Section 2.6.1.5. Dashed lines indicate the mean for ketone and lactone concentrations.

Figure 4.6 Comparative growth kinetics of different CHMO whole cell biocatalysts: *E. coli* TOP10 [pQR239] (♦), *E. coli* JM107 [pQR210] (■), *A. calcoaceticus* NCIMB 9871 (▲). Experiments performed as described in Sections 2.6.1.3, 2.6.2.2 and 2.6.3.2 respectively. *E. coli* TOP10 [pQR239] was induced by addition of L-arabinose 15% w/v three hours after inoculation. Error bars represent the range of measured values about the mean.

Figure 4.7 Comparative kinetics of bicyclolactone formation in 96 DSW plates using three different whole cell CHMO biocatalysts, *E. coli* TOP10 [pQR239] (♦), *E. coli* JM 107 [pQR210] (■) and *A. calcoaceticus* NCIMB 9871 (▲). Experiments performed using an initial concentration of bicycloketone of 1 $g.l^{-1}$. Experiments performed as described in Sections 2.6.1.5, 2.6.2.3 and 2.6.3.3 respectively. Error bars represent the range of measured values about the mean.

Figure 4.8 Parallel collection and evaluation of fermentation kinetic data in 96 DSW plates. Column 1 shows the growth curves of *E. coli* TOP10 [pQR239] (♦, yellow background), Column 2 shows the growth curves of *E. coli* JM107 [pQR210] (■, green background). Row A was filled with culture media containing 10 $g.l^{-1}$ of glycerol, while Row B was filled with culture media containing 20 $g.l^{-1}$ of glycerol. Experiments performed as

described in Section 2.6. Error bars represent the range of measured values about the mean.

Figure 4.9 Parallel characterisation of whole cell CHMO bioconversion. Rows A and C contain fermentations of *E. coli* TOP10 [pQR210] (yellow background), while rows B and D contain fermentations of *E. coli* JM107 [pQR210] (green background). Initial ketone substrate concentrations of 0.5 $g.l^{-1}$ (Rows A and B) and 1.0 $g.l^{-1}$ (Rows C and D) were used. Three different ketones (open symbols) were converted into their respective lactones (solid), bicycloketone (○, column 1), cyclohexanone (□, column 2) and cyclopentanone (△, column 3). Experiments performed as described in Section. 2.6. All bioconversions were carried out at an initial glycerol concentration of 10 $g.l^{-1}$ during the fermentation.

Figure 4.10 Fractional clarification (open bars) and product recovery (solid bars) by microcentrigation to harvest cells following whole cell bioconversion in a 96 DSW plate. Four gravitational forces or g-numbers (Z) were investigated, Z = 4 (black), Z = 16 (blue), Z = 97 (green) and Z = 249 (yellow) after three centrifugation times. Experiments performed as described in Section 2.7.1.

Figure 4.11 Microscale microfiltration of *E. coli* TOP10 [pQR23] following whole cell bioconversion in a 96 DSW plate. Experiments performed at 25 °C as described in Section 2.7.2. The results illustrate the fractional clarification (green bars), ketone (blue bars) and lactone transmission (yellow bars) using a variety of filters. Experiments performed as described in Section 2.7.2.

Figure 4.12 Specific cake resistance of *E. coli* TOP10 [pQR239] calculated for the use of different microfiltration membranes based on the data presented in Figure 4.11. Experiments performed as

described in Section 2.7.2.

Figure 5.1 Measurements of oxygen transfer rate in 96 DSW plates based upon the dynamic gassing out method. Representative curves are shown for various agitation speeds and liquid fill volumes: 1000 rpm, 1000 µl (♦), 1000 rpm, 600 µl (■), 1200 rpm, 200 µl (▲). Experiments performed in culture medium as described in Section 2.4.1.

Figure 5.2 Measured k_La values in a 96 DSW plate as a function of shaking speed. Figure shows k_La values measured with culture medium (solid line, filled symbols) and 10 $g.l^{-1}$ NaCl solution (dotted line, open symbols) at different liquid fill volumes: 1000 µl (♦), 600 µl (■) and 200 µl (▲). Lines were fitted by linear regression. Experiments performed as described in Section 2.4.1 and k_La values calculated according to Equations 2.1 and 2.2. Error bars represent the range of measured values about the mean.

Figure 5.3 Measured k_La values in a 2 l stirred bioreactor with culture media (solid line) and 10 $g.l^{-1}$ NaCl (dotted line). Lines were fitted by linear regression. Experiments performed as described in Section 2.4.2 and k_La values calculated according to Equations 2.1 and 2.2. Error bars represent the range of measured values about the mean.

Figure 5.4 Fermentation kinetics of *E. coli* TOP10 [pQR239] biocatalyst at a matched k_La value of 115 ± 10 h^{-1}: 96 DSW plate with 1000 µl fill volume (■) and 2 l stirred bioreactor (▲). Experiments performed as described in Sections 2.6.1.3 and 2.6.1.6 respectively. Error bars represent the range of measured values about the mean.

Figure 5.5 Bioconversion kinetics of bicyclo[3.2.0]hept-2-en-6-one at a matched k_La value of 115 ± 10 h^{-1} using a whole cell *E. coli* TOP10 [pQR239] biocatalyst: 96 DSW plate with a liquid fill volume of 500 µl (solid lines) showing bicycloketone (■) and bicyclolactone concentrations (□), 2 l stirred bioreactor (dotted lines) showing bicycloketone (▲) and bicyclolactone (Δ) concentrations. Experiments performed as described in Section 2.6.1.5 and 2.6.1.6 respectively. Error bars represent the range of measured values about the mean.

Figure 5.6 DOT profiles measured throughout the 96 DSW plate scale (gray line) and the 2 l stirred bioreactor scale (black line) fermentation and bioconversion processes operated at a matched k_La value of 115 ± 10 h^{-1}. Experiments performed as described in Section 2.4.3.

Figure 5.7 Fermentation kinetics of *E. coli* TOP10 [pQR239] biocatalyst at a matched k_La value of 45 ± 5 h^{-1}: 96 DSW plate with 1000 µl fill volume (■) and 2 l stirred bioreactor (♦). Experiments performed as described in Sections 2.6.1.3 and 2.6.1.6 respectively. Error bars represent the range of measured values about the mean.

Figure 5.8 Bioconversion kinetics of bicyclo[3.2.0]hept-2-en-6-one at a matched k_La value of 45 ± 5 h^{-1} using a whole cell *E. coli* TOP10 [pQR239] biocatalyst: 96 DSW plate with 1000 µl fill volume (■) and 2 l stirred bioreactor (♦). Experiments performed as described in Section 2.6.1.5 and 2.6.1.6 respectively. Error bars represent the range of measured values about the mean.

Figure 5.9 DOT profiles measured throughout the 96 DSW plate scale (gray line) and the 2 l stirred bioreactor scale (black line) fermentation and bioconversion processes performed at matched k_La of 45 ± 5

h^{-1}. Experiments performed as described in Section 2.4.3.

Figure 5.10 Fermentation kinetics of *E. coli* TOP10 [pQR239] biocatalyst at a matched k_La value of 180 ± 10 h^{-1}: 96 DSW plate with 500 µl fill volume (■) and 2 l stirred bioreactor (♦). Experiments performed as described in Sections 2.6.1.3 and 2.6.1.6 respectively. Error bars represent the range of measured values about the mean.

Figure 5.11 Bioconversion kinetics of bicyclo[3.2.0]hept-2-en-6-one at a matched k_La value of 180 ± 10 h^{-1} using a whole cell *E. coli* TOP10 [pQR239] biocatalyst: 96 DSW plate with 200 µl fill volume (■) and 2 l stirred bioreactor (♦). Experiments performed as described in Section 2.6.1.5 and 2.6.1.6 respectively. Error bars represent the range of measured values about the mean.

Figure 5.12 DOT profiles measured throughout the 96 DSW plate scale (gray line) and the 2 l stirred bioreactor scale (black line) fermentation and bioconversion processes performed at matched k_La of 180 ± 10 h^{-1}. Experiments performed as described in Section 2.4.3.

List of tables

Table 1.1 Properties that influence the oxygen transfer rate in stirred bioreactors and shaken microwell plates.

Table 2.1 Whole cell biocatalysis conditions for matched k_La values in 96 DSW plates and stirred vessels. Experiments were carried out as described in Section 2.4.3.

Table 2.2 Composition of the growth medium used in all *E. coli* TOP10 [pQR239] fermentations.

Table 2.3 Geometrical parameters of the 2 l total volume dual Rushton stirred vessel.

Table 2.4 Composition of the growth medium used in all *A. calcoaceticus* NCIMB 9871 fermentations.

Table 2.5 Correlation of gravitational force value and its corresponding speed.

Table 3.1 Comparison of microwell geometries in terms *E. coli* TOP10 [pQR239] fermentation kinetics and experimental throughput.

Table 4.1 Summary of microscale process results for sequential fermentation and bioconversion operations using three different CHMO-expressing whole cell biocatalysts. Fermentations performed at two different glycerol concentrations and subsequent bioconversions performed using three different ketone substrates each at two initial concentrations. Experiments performed as described in Section 2.6.

Table 5.1a Experimentally determined k_La values (h^{-1}) in 96 DSW plates measured using fermentation media described in Table 2.2. Experiments performed as described in Section 2.4.1.

Table 5.1b Experimentally determined k_La values (h^{-1}) in 96 DSW plates measured using a 10 $g.l^{-1}$ sodium chloride solution. Experiments performed as described in Section 2.4.1.

Table 5.2 Literature k_La values reported for a variety of microwell plates and shaking conditions determined using a number of conditions and techniques.

Table 5.3 Experimental k_La values in a 2 l stirred bioreactor measured using fermentation media as described in Table 2.2 and a solution of 10 $g.l^{-1}$ of sodium chloride. Experiments performed as described in Section 2.4.2.

Table 5.4 Comparison of kinetic parameters from microwell and laboratory scale processes performed at a matched k_La of 115 ± 10 h^{-1}. Fermentation parameters calculated from Figure 5.4. Bioconversion parameters calculated from Figure 5.5.

Table 5.5 Comparison of kinetic parameters from microwell and laboratory scale processes performed at matched k_La values. Fermentation and bioconversion parameters calculated as described in Section 2.6.1. Low, medium and high kinetic data taken from Figures 5.7 and 5.8, 5.4 and 5.5, 5.10 and 5.11 respectively.

Nomenclature

Roman Characters

Symbol		Units
a	Gas-liquid interfacial area	m^{-1}
a_i	Static gas-liquid interfacial area	m^{-1}
a_f	Final gas-liquid interfacial area	m^{-1}
B	Baffle width	m
Bo	Bond number	$(=\rho g d^2/W)$
C	Off-bottom clearance	m
C_L	Oxygen concentration in the liquid phase	$kg.m^{-3}$
C_L^*	Oxygen solubility in the liquid phase	$kg.m^{-3}$
ΔC	Spacing between impellers	m
D	Impeller diameter	m
	Oxygen diffusion coefficient	$m^2.s^{-1}$
d	Well diameter	m
d_t	Shaking diameter	m
FL_G	Gas flow number	$(= Q_G/ND^3)$

Fr	Froude number	$(=d_t(2\pi N)^2/2g)$
g	Gravity acceleration	$m.s^{-2}$
H_L	Liquid height	m
I	Fluorescence intensity	-
I_0	Fluorescence at zero oxygen concentration	-
K_L	Overall mass transfer coefficient	$m.s^{-1}$
k_L	Liquid mass transfer coefficient	$m.s^{-1}$
K_{SV}	Stern-Volmer constant	-
N	Impeller rotational speed	s^{-1}
OTR	Oxygen transfer rate	$kg.m^{-3}.s^{-1}$
OUR	Oxygen uptake rate	$kg.m^{-3}.s^{-1}$
Pg	Gassed power consumption	W
Q_G	Gas flow rate	$m^3.s^{-1}$
Re	Reynolds number	$(=\rho Nd^2/\mu)$
Sc	Schmidt number	$(=\rho/\mu D)$
T	Temperature	°C
T_V	Vessel internal diameter	m
t_b	Baffle thickness	m

V_L	Liquid volume	m^3
v_s	Superficial gas velocity	$m.s^{-1}$
W	Wetting tension	$N.m^{-1}$
X_f	Final biomass concentration	$kg.m^{-3}$

Greek characters

Symbol		**Units**
μ	Dynamic viscosity	$kg.m^{-1}.s^{-1}$
	Growth rate	h^{-1}
μ_{max}	Maximum growth rate	h^{-1}
ϕ	Orbital shaking radius	mm
ρ	Liquid density	$kg.m^{-3}$

Abbreviations

96 DSW	96 wells deep square microwell plate
96 SRW	96 wells standard round microwell plate
ATCC	American Type Culture Collection
BVMO	Baeyer-Villiger monooxygenase
CHMO	Cyclohexanone monooxygenase
DOT	Dissolved oxygen tension
DCW	Dry cell weight
FID	Flame ionisation detector
GC	Gas chromatography
g_{DCW}	Grams of dry cell weight
IPTG	Isopropyl β-D-thiogalacto pyranoside
MW	Molecular weight
NADPH	Nicotinamide adenine dinucleotide phosphate (reduced)
NCIMB	National Collections of Industrial, Marine and Food Bacteria
OD	Optical density
RO	Reverse osmosis
RPF	Rate of product formation
rpm	Revolutions per minute
SDS	Sodium dodecyl sulphate
U	Unit of activity (1 $\mu mol.min^{-1}$)
vvm	Vessel volumes per minute
v/v	Volume per unit volume
w/v	Weight per unit volume

1.0 Introduction

1.1 Bioconversions

Wang (1979) defined bioconversions as a process in which microorganisms convert a compound to a structurally related product. This process is comprised of only one or a small number of enzymatic reactions. The use of microbial cells or isolated enzymes in the production of fine chemicals, also known as biocatalysis, is becoming accepted as an indispensable tool in synthetic chemistry (Pollard and Woodley, 2007). Industrially, biocatalysis covers a broad range of applications, from the use of enzymes as a final product in detergents, to the development and production of pharmaceuticals and analytical tests and their use as processing aids in the paper, textile, brewing and dairy industries (Tramper, 1994).

Bioconversions have several advantages over chemical conversions such as specificity, operation under mild conditions, high chemoselectivity, regioselectivity and stereoselectivity, the potential to perform complex reactions with no equivalent in traditional chemistry, the potential for fewer reaction by-products due to biocatalyst selectivity and the possibility to avoid protection and de-protection steps (atoms are placed temporarily on parts of a molecule which need to be protected from a reagent to be used in one of the synthetic steps needed to make the final product. These protecting groups are removed afterwards.) (Liese et al., 1999). However, biocatalysts can show poor operational stability, and low volumetric productivities, their production may be expensive, bulk separation from water (if required) could make downstream processing challenging, the process may be inflexible due to high specificites, and there is a possibility of unwanted side reactions in whole cell biocatalysis (Cheetham, 1994). The specific nature of

bioconversions means that they can often be used as an alternative to chemical methods and can facilitate reactions not currently possible through chemistry, although several aspects of the process must be assessed before making the decision to switch from chemical to biological catalysis (Tramper, 1996).

Directed evolution methods are now widely used for the optimization of diverse enzyme properties, which include relevant characteristics like stability, regioselectivity and, in particular, enantioselectivity (Hibber et al., 2005). In principle, three different approaches are followed to optimize enantioselective reactions: the development of whole cell biocatalysts through the creation of designer organisms; the optimization of enzymes with existing enantioselectivity for process conditions; and the evolution of novel enantioselective biocatalysts starting from non-selective wild type enzymes (Jaeger et al., 2004).

In the development of whole cell biocatalysts development protein and cellular engineering techniques allow manipulations to improve activity and stability as well as to block or eliminate unwanted side reactions (Ishige et al., 2005). Protein engineering can be used to increase catalytic activity and stability, while cellular engineering can achieve greater expression of the enzyme or enable expression in a recombinant organism that is more convenient to handle and manipulate, such as *E. coli* (Mihovilovic et al., 2006).

1.1.1 The Baeyer-Villiger reaction

The conversion of ketones into esters or cyclic ketones into lactones was discovered more than a century ago by Adolf von Baeyer and Victor Villiger. In this reaction, the ketone is attacked by a nucleophilic peroxy acid (e.g. H_2O_2) to form the so-called tetrahedral Criegee intermediate (Figure 1.1). This unstable species

undergoes a rearrangement *via* expulsion of a carboxylate ion and migration of a carbon-carbon bond, yielding the ester and the acid. In general, the most substituted carbon centre migrates with retention of configuration. Steric, conformational, and electronic factors have an influence on the rate of rearrangement and the migration preferences. Migration is also influenced by the type of peroxy acid used. These features make the Baeyer-Villiger reaction an interesting tool for the synthesis of lactones and esters (Kamerbeek et al., 2003). If the starting material is chiral or prochiral the chemical reaction will produce a racemic mixture of the product enantiomers because the peroxide reagent can attack at either face of the molecule (Renz and Meunier, 1999). However, some limited enantioselectivity has been achieved in chemical Baeyer-Villiger reactions catalysed by various transition metal based reagents (Corma et al., 2001).

Figure 1.1 Mechanism of the Baeyer-Villiger oxidation by peracids. Reproduced from Kamerbeek et al. (2003).

Chemical synthesis of chiral molecules, however, is difficult and requires the use of very reactive and dangerous chemicals, making their handling difficult and their scale-up dangerous (Lorenz et al., 2004). It also produces large amounts of by-products which reduce the yields and the cost effectiveness of the reaction. The microbial Baeyer–Villiger oxidation thus represents a particularly useful tool for assessing and producing these asymmetric molecules. A biocatalytic process would also offer a more economic solution as it would reduce the purification costs and allow for higher yields.

1.1.1.1 Baeyer – Villiger monooxygenase (BVMO)

BVMOs are a group of monooxygenases which use a flavin coenzyme as an organic cofactor and either nicotinamide adenine dinucleotide (NADH) or nicotinamide adenine dinucleotide phosphate (NADPH) as a reductant (Willets, 1997). In addition to the Baeyer-Villiger type oxidation, BVMOs can also catalyse the electrophilic oxygenation of heteroatoms, e.g. to form sulfoxides from organosulfides (Walsh and Chen, 1988). The majority of the BVMOs discovered were originally described as a Baeyer-Villiger type activity in cells or cell extracts, and most are poorly characterised in terms of sequence, mechanism and natural function (Willets, 1997). An exception is the cyclohexanone monooxygenase (CHMO) used in this work (Section 1.1.1.2), which has been widely investigated. This was first discovered as an enzyme activity which allowed the *Acinetobacer calcoaceticus* NCIMB 9871 to grow on cyclohexanol and cyclohexanone (Donoghue and Trudgill, 1975). CHMO catalyses a key step in the metabolism of these compounds by converting cyclohexanone to ε-caprolactone, which can be catabolised further because the wild type *A. calcoecticus* contains a lactonase that subsequently opens up the lactone ring. The resulting compound can be

metabolised to adipate, from which acetyl-coA can be generated (Donoghue and Trudgill, 1975).

Advances in molecular biology have enabled access to an increasing number of novel BVMOs originating from various natural hosts, such as *A. calcoaceticus* NCIMB 9871 (Wright et al., 1994; Shipston et al., 1992; Roberts and Willets, 1993), *Pseudomonas putida* and *Rhodococcus fascians* (Shipston et al., 1992) amongst others. The utilization of strains engineered to overexpress a particular BVMO instead of wild type organisms minimizes problems with unwanted side reactions and low monooxygenase activity (Mihovilovic et al., 2006). These modificiations, teamed with some product removal strategies can help increase the bioconversion productivity and avoid substrate and product inhibition (Doig et al., 2002; Hilker et al., 2005; Hilker and Baldwin, 2005).

There has been much interest recently in BVMOs because they have the potential to be used in the synthesis of intermediates or precursors for many complex natural products such as pesticides (Carnell et al., 1991; Beauhaire et al., 1995), antibiotics (Konigsberger and Griengl, 1994; Taschner and Chen, 1991) and insect antifeedant (Gagnon et al., 1995; Petit and Furstoss, 1995)

1.1.1.2 Cyclohexanone monooxygenases (CHMOs)

Among the various BVMOs, the most studied to date is the cyclohexanone monooxygenases (CHMO) obtained from *A. calcoaceticus* NCIMB 9871, which is a flavoprotein type I monooxygenase and is therefore NADPH dependent using flavin adenine dinucleotide (FAD) as cofactor (Kamerbeek et al., 2003). The range of substrates known to be oxidized by CHMO include several representative heterocyclic ketones (Mihovilovic et al., 2001). Some authors (Mihovilovic et al.,

2001; Ottolina et al., 2005; Doig et al., 2002) have engineered *E. coli* strains to over express the CHMO gene from *A. calcoaceticus* NCIMB 9871, transforming them into whole cell CHMO biocatalysts. Mihovilovic et al. (2001) found that using the whole cells of the engineered *E. coli* strain allowed Baeyer-Villiger oxidations without the need for enzyme purification or cofactor regeneration. No side reactions of oxidation-sensitive functionalities such as sulfur or nitrogen were observed demonstrating that both native *E. coli* enzymes and CHMO possess high chemoselectivities. However Mihovilovic et al. (2001) stressed that while both electron-donating and withdrawing protecting groups were tolerated by CHMO, membrane penetration may be a limiting factor in some cases.

Ottolina et al. (2005) used cell extracts from *E. coli* TOP 10 [pQR239] expressing the CHMO from *A. calcoaceticus* in the conversion of various bicyclic diketones. They found that the enzyme presented a marked dependence on substrate structure. Substrates for this reaction include bicyclo[3.2.0]hept-2-en-6-one, which was used throughout this work, sulphides (Zambianchi et al., 2002), 4,4-disubstituted cyclohexanones and cyclohexenones (Mihovilovic et al., 2006), benzaldehydes (Moonen et al., 2005) and other bicyclic diketones (Ottolina et al., 2005). Figure 1.2 shows some of these reaction schemes.

1.1.2 Whole cell biocatalysis

The chemical industry has turned to use some partially or totally purified enzyme preparations, as they are easy to handle and generally show higher enantio-, chemo- and regio-selectivities, for example in the production of fine chemicals (Liese et al., 1999). Still, whole cell biocatalysts have been used in a wide range of processes such as: oil desulfurization (Setti et al., 1997); production of vitamins, aminoacids

Figure 1.2 Model BVMO conversion reaction schemes: (A) CHMO-mediated regiodivergent oxidation of bicyclo[3.2.0]hept-2-en-6-one yielding (−)-(1*S*,5*R*)-2-oxabicyclo[3.3.0]oct-6-en-3-one and (−)-(1*R*,5*S*)-3-oxabicyclo[3.3.0]oct-6-en-2-one; (B) CHMO-mediated asymmetric oxidation of 4-methylcyclohexanone yielding (*S*)-5-methyl-oxepane-2-one; (C) CHMO-mediated oxidative resolution of 2-hexylcyclopentanone yielding (*S*)-6-hexyltetrahydropyran-2-one. (Doig et al., 2003). Note the requirement for molecular oxygen in each reaction scheme.

and ribonucleotides (Hashimoto et al., 1999); fatty acids (Schneider, 1998); flavour enhancers, resins, antibiotics and other pharmaceuticals (Ishige, et al. 2005).

Duetz et al. (2001) identify four main reasons to use whole cell biocatalysis rather than purified enzymes. Whole cell biocatalysis is more economical as enzyme purification stages can be eliminated; it optimizes the use of membrane-bound enzymes, as the removal from the cell often leads to loss of activity; cascade enzymatic reactions may be too complicated to perform in any other ways; and NAD(P)H dependent reactions are more efficient inside the cells due to the recycling of cofactors. They concluded that whole cell biocatalysts therefore offer economic advantages over free enzymes; however, the unpredictability of reactions prevents many from being used at industrial levels.

Some problems with whole cell biocatalysis should be taken into consideration nonetheless. These include permeation of substrates across the cell membrane, side reactions causing degradation of products and accumulation of byproducts. (Ishige et al., 2005). To overcome these problems, the microorganisms used must go through an intensive screening or selection procedure. Furthermore, both enzymes and cells can be directly and efficiently developed because of progresses in molecular biotechnology such as directed evolution. As well as new technologies, traditional screening is still a powerful tool for finding promising biocatalysts (Lorenz et al., 2004).

Different strategies have been explored to increase productivity in whole cell biocatalytic processes apart from modifiying the microorganism or the enzyme. The use of absorbent resins inside the fermentation broth was proposed by Simpson et al. (2001). The addition of a resin can be considered as a two-phase system in which the product and reactant are removed from the reaction mixture via adsorption onto the solid resin phase, thus minimising the inhibition seen by a number of substrates

and products. Leon et al. (1998) also propose whole cell biocatalysis in organic media, when biotransformations involve sparingly water-soluble or toxic compounds; however the selection of a solvent combining adequate physicochemical properties with biocompatibility is a difficult task. Ni and Chen (2004) proposed to accelerate whole cell biocatalysis by molecular engineering of the permeability barrier of the outer membrane, although most current research is done regarding the modification of the enzyme rather the mechanism of interaction between the substrate and the cell.

1.1.3 Whole cell BVMO biocatalysis

The real breakthrough for the use of microbial BVMOs in asymmetric synthesis was the use of whole cell biocatalysts. Shipston et al. (1992) were the first to successfully carry out whole cell biocatalysis of bicyclo[3.2.0]hept-2-en-6-one using Baeyer-Villiger monooxygenases with the wild type organism as biocatalyst rather than recombinant ones.

Molecular biology techniques allowed the creation of recombinant strains expressing BVMO biocatalyst, particularly *E. coli*. This was a breakthrough as it was easier to handle the whole cell biocatalyst from *E. coli*, instead of type two pathogens like *A. calcoaceticus* and *P. putida* (Wright et al., 1994). This also allowed for more robust processes and eliminated problems with further modification of the reaction product by metabolic pathways present in the wild type host.

There are several reasons why it is desirable to clone BVMO from the wild type host and express it in a different host, particularly for large scale use. The wild type host, *A. calcoaceticus*, is a Class 2 pathogen, which makes it undesirable for large

scale fermentations. The fermentation protocol for *A. calcoaceticus* also involves growth on a toxic carbon source, cyclohexanol, in order to induce BVMO expression. Furthermore, *A. calcoaceticus* contains a lactone hydrolase with an activity 27 times greater than the BVMO. Therefore, in order to perform a bioconversion with these cells, either BVMO has to be purified or the hydrolase must be selectively inhibited using a toxic inhibitor such as tetraethyl-pyrophosphate (Alphand et al., 1990).

A recombinant whole cell BVMO biocatalyst was produced in previous research at UCL using the strain *E. coli* TOP10 pQR239, which expresses the BVMO from *A. calcoaceticus* upon induction with L-arabinose (Doig et al., 2001). BVMO expression is under the control of the *araBAD* promoter. This promoter was selected due to the low cost of the inducer, L-arabinose, the tight regulation of expression that can be achieved and the high level and rate of gene expression upon induction (Guzman et al., 1995). The selection marker used for the pBAD vector was ampicillin resistance. The *E. coli* TOP10 strain was chosen as the host organism because it is a strain that is capable of transporting, but not metabolising L-arabinose, has fast growth rates and short fermentation times. This is an important requirement because for L-arabinose inducible expression the level of L-arabinose inside the cell should not decrease over time (Doig et al., 2001).

Whole cell BVMO bioconversion can also be used in fed batch mode to increase productivity (Doig et al, 2002, Baldwin et al., 2005), for example by employing a strategy of feeding bicyclo[3.2.0]hept-2-en-6-one below that of the theoretical volumetric biocatalyst activity (275 $\mu mol.min^{-1}.l^{-1}$). Doig et al. (2002) maintained the reactant concentration in the bioreactor below the inhibitory concentration of 0.2 - 0.5 $g.l^{-1}$. They produced approximately 3.5 $g.l^{-1}$ of the combined regioisomeric lactones with a yield of product on reactant of 85-90 % $w.w^{-1}$. This approach was sensible as the BVMO is known to be inhibited by this particular substrate. These

authors later scaled up this process to 55 l, producing over 200 g of combined lactone product.

Other expression systems for CHMO have previously been created using *E. coli* (Chen et al., 1988; Chen et al., 1999) or *S. cerevisiae* (Stewart et al., 1996) as the host organism. The *E. coli* expression system developed by Chen and co-workers (1999) had an expression level of CHMO of approximately 20 % total cell protein which is substantially greater than the expression level in *A calcoaceticus*, where CHMO represents 4 % of the total cell protein (Chen et al., 1988). However, the production of the biocatalyst has not been characterised to any great extent for any of these systems, and they all require the inducer, isopropyl β-D-thiogalacto pyranoside (IPTG), which is relatively expensive for large scale biocatalyst production.

1.2 Microscale bioprocessing

Recently there has been considerable industrial innovation for the generation of larger compounds libraries and microorganisms with biocatalytic potential, however there has not been a concomitant expansion in the rate at which these can be evaluated as suitable candidates nor in the speed at which manufacturing processes can be designed for those compounds which are taken forward (Buckland et al., 2000). These areas are currently bottlenecks in the whole discovery and development process, and research is therefore starting to focus on ways of increasing the throughput of bioprocess experimentation and reducing costs. In order to achieve this it will be necessary to determine bioprocess constraints at small scale and find ways to relate the data generated to predict larger scale unit operations.

The discovery of compounds in the pharmaceutical industry has increased through the widespread application of High Throughput Screening (HTS) to the drug discovery process (Devlin, 1997). These increases have been driven by advances in combinatorial chemistry, genetic engineering and robotics technology which have enabled large numbers of chemical compounds to be synthesised and then screened past a target, such as an enzyme or a receptor, in order to identify compounds with a particular activity (Devlin, 1997). These processes are largely automated and can generate huge numbers of potential drugs. Similarly many companies have access to large banks of microorganisms which can be screened rapidly using automated techniques to locate particular catalytic activities (Stahl et al., 2000). As described in Section 1.4, the eventual goal of this thesis is to rapidly carry out whole process combinatorial experiments in microwells using robotic systems developed for HTS, and then to rapidly scale-up the optimised process for the production of candidate compounds.

1.2.1 Microwell plates in bioscience applications

The microwell plates, which are integral part of today's drug discovery programs, were first conceived of in the early 1960s. There are references to microwell plates being used as titration tools as early as 1974, when Miyamura et al. (1974) used them to titrate diphtheria toxin and antitoxin titres using VERO cells. Subsequently microwell plates have primarily been used as a way to facilitate the creation of novel assays and also in high throughput screening (HTS) for drug discovery (Lye et al., 2003). It is only recently that microwell plates have been considered as process research tools. Several manufactures of laboratory equipment produce microwell plates which vary in construction material, well geometry, number of wells per plate and application. The materials used include quartz, polypropylene and polystyrene and can be used in DNA quantification, PCR, ELISA, HTS and

studies of protein stability (Aucamp et al., 2005). Most of the published work regarding microwell plates is related to their use as a screening tool; consequently, there are published works which adapt assays to high density microwell plates, which contain 1536 wells per plate (Sullivan et al., 2000) in order to achieve the number of assays required per plate for HTS applications.

The general practice during screening of large microbial strain collections for new enzyme activities or bioactive compounds is that each strain is handled individually. The labour and time involved in separately reviving the stock cultures on agar plates and the subsequent inoculation of tubes or Erlenmeyer flasks are major limiting factors in the progress of such screening projects. This bottleneck led to the use of microwells as microscale processing tools in order to handle large numbers of microbial strains in parallel rather than in sequence.

In 2000, Duetz et al. proposed the use of 96 Deep Square Well (96 DSW) microwell plates as microbial bioreactions and addressed two major issues: how to obtain oxygen transfer rates (OTRs) similar to those achieved in regular growth systems while preventing cross-contamination and excessive evaporation, and how to set up a reliable and reproducible system for the inoculation of microwell plates with strains from frozen culture collections. Duetz et al. (2000) calculated a k_La of 188 h^{-1} for their plate format by following the growth curve of a strict aerobe under a range of agitation conditions (100 to 400 rpm, shaking throw 25 and 50 mm).

Until recently, microwell experiments used in screening applications would give only a "yes" or "no" answer. However, Doig et al. (2002) demonstrated that quantitative kinetic information regarding bioconversion kinetics and biocatalyst specific activity could be obtained under appropriately defined conditions.

1.2.2 Biocatalytic microscale processing

It can often be difficult to arrive at the best process design for a bioconversion even after key data has been collected (such as conversion rate and specific activity) because the design problems are frequently multivariate and complex. The factors affecting the outcome of a bioconversion process will usually be influenced earlier process steps such as biocatalyst production by fermentation, which in turn will depend on culture medium composition, timing, inducer and bioreactor correlation used.

In the chemical industries accurate and reliable mathematical models have been developed to describe the major unit operations and whole processes (Steffens et al., 2000). Using these models many design scenarios can be evaluated quickly in practical and economic terms. Mathematical models which accurately describe a biological process, or part of a process, have also been shown to be valuable design tools (Molinari et al., 1997; Hogan and Woodley, 2000). However, the variety and complexity of biological processes means that these models are often empirical and not always are able to predict interactions between individual unit operations. Thus these interactions are usually identified through thorough experimentation. In this situation, high throughput experimentation techniques could help generate more design data quicker than conventional experimentation. Such process interactions are tipically dependent upon the biocatalyst properties such as single or multienzymatic systems, cofactor requirements, coenzymes, location of enzyme activity and enzyme stability. Reaction properties needing to be investigated include equilibrium-pH/temperature dependence, Michaelis-Menten parameters, enantioselectivity, acid/base production, water and gas consumption or production and heat evolution. The physical and chemical properties of the substrate and product in biocatalytic reactions such as solubility, temperature, pH, stability and

volatility, and then the interaction of the biocatalyst with its substrate and product also need to be considered.

The requirements for early stage bioprocess design data have led to the increase in fermentation and bioconversion research being carried out using microwell plate formats because of their high throughput potential. Several microwell plate formats have been used and generally they have been agitated by orbital shaking to ensure reproducible performance in all the wells across the plate. Baminger et al. (2001) used a 12 well microtitre plate to evaluate redox mediators for the conjugated enzyme couple laccase/cellobiose dehydrogenase. The 24 microwell plate format was used for the biotransformation of cinnamic and ferulic acid using actinomycetes (Brunati et al., 2004) and for the screening for protein expression clones of *Pichia pastoris* (Boettner et al., 2002). However the most popular format for bioprocess applications appears to be the 96 microwell plate, particularly for systems with many process variables to be considered like the impact of variations in culture medium composition and the estimation of kinetic parameters (Duetz et al., 2000; Jansen et al., 2003; Reeves et al., 2004; Weis et al., 2004a; Weis et al., 2004b). Nonetheless all of this work was focused on the mechanics of fermentation, without further processing and without assessing other engineering parameters such as k_La and its effect in the process. Published research of biocatalysts processes in microwell plates is very rare.

Marques et al. (2007) developed multistep biotransformations and two-liquid biphasic processes using *Mycobacterium* sp. NRRL B-3805 in 24 standard round microwell plates (24 SRW). They suggested that microwell plates may be used for the characterisation of complex bioconversion systems to establish representative screening systems. Their experiments also demonstrated the feasibility of using microlitre and millilitre shaken bioreactors to evaluate organic/aqueous two-liquid bioconversion systems. They concluded that microwell plates are promising

representative screening systems for multistep biocatalysis, particularly in aqueous phase systems.

1.2.3 Microscale bioreactors

While most microwell studies have utilised shaking to promote mixing and oxygen transfer, a number of authors have established mechanically stirred microwell bioreactor design. One of the first was designed by Lamping et al. (2003) at UCL. The design was similar to that of a stirred tank but with dimensions equal to that of a single well of a 24-well plate and a working volume of 6 ml. Mixing was provided by a set of three impellers mechanically driven via a miniature electric motor and aeration was achieved with a single tube sparger. Parameter sensitive flourophors were used with fibre optic probes for continuous monitoring of dissolved oxygen tension and an optical based method was employed to monitor cell biomass concentration during growth (Figure 1.3). Lamping's bioreactor achieved volumetric oxygen mass transfer coefficients (k_La) of the order of 100 h^{-1} to 400 h^{-1}.

Many of the new miniature bioreactors follow the traditional profiles of larger vessels maintaining a proportion between parts of the vessels or the use of impellers; however, some are more closely related to microwell plates. A similar approach to Lamping's bioreactor design was used by Harms et al. (2005), but this was based on conventional microwells containing a magnetic stirrer bar. They created a series of parallelized bioreactors using the footprint of a well from a 24 microwell plate and a series of 24 independent stirred vessels. Each bioreactor had a working volume of 1 ml and achieved volumetric mass transfer coefficients of up to 490 h^{-1} at 2000 rpm.

In 2004, Maharbiz et al. designed a miniaturized bioreactor array with electrolytic gas generation as a key component to work as bubble columns. The array was assembled from commercial 96 SRW plates, Printed Circuit Boards (PCBs), and microfabricated components. Each of eight 250 µl wells continuously reported optical density, temperature, oxygen input, and has a modular area to allow additions. No mass transfer experiments were reported however. Additionally, Doig et al. (2004) designed a miniature 2 ml bubble column bioreactor consisting of a

Figure 1.3 Example of a 24 SRW plate-based miniature stirred bioreactor. Turbidity was measured using probes A and B. This bioreactor presented similar characteristics to those of larger vessels such as pH and oxygen transfer probes, impellers and geometric ratios. Reproduced from Lamping et al. (2003).

static deep well microwell plate inserted into the base of a 48 well plate. Air was supplied at a controlled flow rate from the bottom of each well forming bubbles in the liquid. A volumetric mass transfer coefficient for oxygen (k_La) of up to 220 h^{-1} was calculated. A combination of Lamping's and Maharbiz' approach was followed by Puskeiler et al. (2005). He created a millilitre-scale bioreactor equipped with a gas-inducing impeller. According to Puskeiler, this bioreactor reached oxygen transfer coefficients of >1440 h^{-1}.

All these additional miniature bioreactor design add to the understanding of mixing and mass transfer in such small vessels, and will enhance the engineering knowledge base for the design of microscale bioprocess experimentation.

1.2.4 Microscale process monitoring

Oxygen sensing is paramount in bioprocess research especially at the microwell scale. Online monitoring of shaken microwell plates has thus attracted special interest in recent years. In large bioreactors polarographic DOT probes are commonly used for oxygen measurements. The small culture volumes of microwell plates do not allow the use of conventional probes and therefore non-invasive optical measurements are preferable. Research in pH control strategies in microscale fermentations has also been reported for optimising the production of erythromycin (Elmahdi et al., 2003).

Recently such optical pH and dissolved oxygen monitoring systems have become commercially available. The German company PreSens manufactures adhesive attachable sensing "spots" containing immobilised pH and oxygen sensitive fluorescent dies (Figures 1.4 and 2.1) which are attached to the wall of individual microwells. This company also manufactures specific microwell plates for pH and

dissolved oxygen sensing. Girard et al. (2001) first proposed the use of Phenol Red dye as a pH indicator; however, the direct addition of such dyes to the culture medium may have an unpredictable influence on culture performance. Consequentially non intrusive means for oxygen and pH sensing are considered more suitable.

Samorski et al. (2005) designed a novel semi continuous measuring technique for optical density and dissolved oxygen measurements by a combined scattered light (for optical density) and fluorescence measurement (for oxygen sensing) approach. This approach relied on the well fitting a reading area at appropriate times; the problem with this is that the reader light does not reach the entire diameter of the well, making the readings prone to errors, and if the plates are not allocated correctly, the readings of two neighbouring wells may overlap, hence the need for online, non intrusive monitoring systems and can be fitted within the wells.

Figure 1.4 Schematic diagram of the mechanism of PreSens sensing spot and probe. Reproduced from the manufacturers internet page (www.presens.de, 31/04/06).

Gernot et al. (2003) created microwell plates with integrated optical sensing of dissolved oxygen by immobilization of two fluorophores at the bottom of 96-well polystyrene microwell plates. The relationship between fluorescence intensity and dissolved oxygen concentration was calculated using the Stern–Volmer correlation which describes the correlation of fluorescence values to oxygen concentration. Similar plates are commercially available, manufactured by BD Biosciences (Becton, Dickinson and Company, New Jersey, USA) (Figure 1.5). One of the major drawbacks of this type of plates is that it does not allow for continuous monitoring as the plate must be removed from the incubator and placed in a microplate reader. Additionally these microwell plates are only available in the standard 96 well geometry.

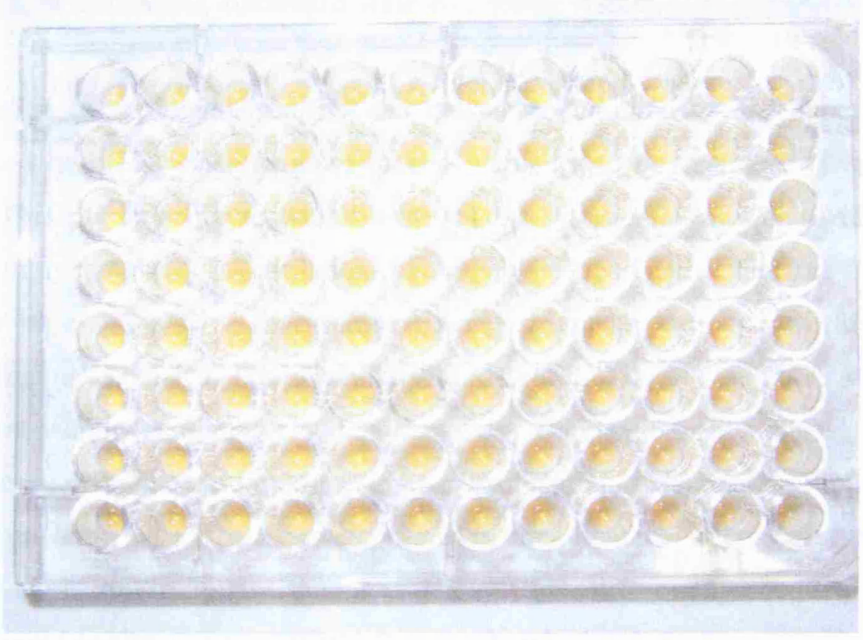

Figure 1.5 Photograph of 96 Standard Round Well (SRW) microwell plate with integrated fluorescence sensor for dissolved oxygen measurements.

1.2.5 Microscale process automation

As described in Section 1.2.1, microscale processing techniques are rapidly emerging as a means to increase the speed of bioprocess design and reduce material requirements. Underlying such experimentation is the ability to accurately and precisely add or remove specific volumes of liquid to each well of a plate. Burbaum (1998) identifies two main concerns regarding liquid handling at the microwell scale: reformatting (moving compounds into miniaturized formats) and dispensing (placing bioreagents into microwell plates). The key requirement for dispensing is the capability to place nearly identical volumes of aqueous solutions where required, while the key requirement for reformatting is to handle samples and dispensing without cross-contamination. These requirements can be satisfied with a washable, or disposable, automated sample-handling system.

Automation of the liquid handling can reduce labour intensity and experimental error, and enable a wider range of process variables to be examined (Lye et al., 2003). This can be achieved with the use robotic systems that can be divided into three main categories: workstations, single platforms, and integrated systems (Lamsa et al., 2004). Workstations are instruments which perform single specialized tasks, such as liquid handling, and are useful during the initial stages of process screening handling 50 to 100 plates a day. Single platform systems combine a number of tasks such as liquid handling, centrifugation, plate reading, storage and incubation, allowing a larger throughput and better automated microscale processes (Nealon et al., 2005). Finally, the integrated systems allow highly complex process development and have the capacity to process hundreds of plates per day (Lamsa et al., 2004).

1.2.6 Microscale downstream processing

For microscale processing techniques to be most effective they must ultimately address whole process sequences consequently it is necessary to integrate fermentation studies with appropriate downstream processing sequences also operated in microwell formats. Currently there exists very little work in the areas of cell separation and product recovery.

Regarding product recovery there have been initial reports on adsorption studies in microwell formats (Welch et al., 2002; Lye et al., 2003). Jackson et al. (2005) also established a microscale normal flow filtration (NFF) technique for the automated high throughput evaluation of complex biological feed streams, however little else has been done regarding downstream processing at the microscale. They used a commercially available 96-well filter plate (0.3 cm^2 per well) and a custom designed 8–24-well filter plate (0.8 cm^2 per well) to quantitatively study the microfiltration characteristics (such as cake resistance) of an *E. coli* TOP10 [pQR239] fermentation broth.

1.3 Engineering characterisation of shaken microwells

1.3.1 Scale-up fundamentals

Microbial fermentation process development has two main objectives: to improve existing processes by means of introducing better strains, more efficient culture conditions and better equipment and to transfer new processes discovered to the pilot plant scale. Ultimately the final microbial process must be able to produce a profit when developed from a bench scale to full industrial scale. For microwells to

be considered as an early process development tool, it must be possible to generate kinetic data that can be compared to larger scales of operations. The type and amount of data that is required is dependent upon the process to be examined and the size of the library to be evaluated.

There are several criteria for translating conventional laboratory scale process to larger scales (Wang et al., 1979), the main ones being:

- Constant volumetric oxygen transfer rate (k_La), where k_L is the volumetric oxygen transfer coefficient and a is the transfer area.
- Constant impeller tip speed (πND_i), where N is the stirrer speed and D_i is the impeller diameter.
- Constant volumetric power input (P_g/V_L), where P_g is the gassed power input and V_L is the volume.
- Equal mixing times

Wang et al. (1979) advise that in cases where dissolved oxygen is one of the critical process variables, constant k_La is a good basis for scale-up and is also a good way to compare two fermenters. Wang et al. (1979) also argue that when oxygen supply is limiting k_La is a useful guide in determining whether various changes in the equipment will result in a potential process improvement.

1.3.2 Importance of oxygen mass transfer in scale-up

Gas – liquid mass transfer is of paramount importance in bioprocessing because of the oxygen requirement of aerobic fermentations. Traditionally stirred tank bioreactors are the most commonly used vessel for aerobic culture. Oxygen is supplied to the microorganism by sparging air bubbles underneath the impellers. The impellers then disperse the gas throughout the vessel. Oxygen molecules must

overcome a series of transport resistances as they move from inside the air bubbles to the inside of the microorganism (Doran, 1999). These resistances are described by as diffusion from bulk gas to gas liquid interface, movement through the gas – liquid interface, diffusion of the solute through relatively unmixed liquid region near bubble, Transport of the solute through the bulk liquid to a second relatively unmixed liquid region surrounding cells, transport through second unmixed liquid region associated with cells, diffusion into the cellular floc and transport across cell envelope into intracellular reaction site (Bailey and Ollis, 1986).

Oxygen transfer in fermenters is driven by an oxygen concentration gradient that exists between the air bubbles and the fermentation broth. Convective mass transfer refers to mass transfer occurring in the presence of bulk fluid in motion. Equation 1.1 shows that the rate of mass transfer is proportional to the concentration gradient (the driving force for mass transfer) and the area available for transfer to take place:

$$N = k\, a\, \Delta C \qquad \text{[Eq. 1.1]}$$

where, N is the rate of mass transfer of the component, a is the area available for mass transfer, ΔC is the concentration gradient, and k is the mass transfer coefficient. The mass transfer coefficient is influenced by a number of variables like physical properties such as liquid hydrodynamics and also fluid properties such as diffusivity and viscosity (Doran, 1999).

Because of the high oxygen demands encountered with early antibiotic fermentations, some authors such as Bartholomew (1950) proposed that the volumetric oxygen transfer coefficient (k_La) should be kept constant during process scale-up. To calculate k_La, Van't Riet (1979) proposed the following correlation using water with high ionic concentration as the process fluid:

$$k_L a = 2.0x10^{-3}\left(\frac{P_g}{V_L}\right)^{0.7} v_s^{0.2} \qquad \text{[Eq. 1.2]}$$

where P_g is the gassed power input, V_L is the liquid volume and v_s is the gas superficial velocity. The addition of ions to water is known to reduce the average bubble size, by preventing coalescence, and consequently to increase the volumetric mass transfer coefficient (k_La). The error regarding k_La predictions with this correlation ranges from 20 to 40%.

The volumetric oxygen mass transfer coefficient (k_La) in gas-liquid dispersions has played a central role in the design and characterisation of bioreactors (Bailey and Ollis, 1986). This explains why the current focus of microwell bioprocess studies is on how to measure k_La and how reliable and reproducible the acquired data is. Ideally oxygen transfer rates should be measured in the bioreactor to be used and in the actual fermentation medium, thus measuring the dependence of k_La on aerodynamics (Bailey and Ollis, 1986). In production fermenters the value of k_La is typically in the range of 72 – 900 h^{-1} (0.02s^{-1} to 0.25 s^{-1}); this wide range is due mainly to variations in the transfer area a, result from different types and geometries of impellers and bioreactors and their impact on bubble size (Doran, 1999).

1.3.3 Oxygen mass transfer in microwells

In Section 1.3.1, the importance of oxygen mass transfer as a scale-up parameter was emphasized, however the knowledge of mass transfer in microwells systems is limited and further research is required. Several operational parameters have been identified that affect oxygen mass transfer in microwell plates namely: shape, size, material of construction (hydrophilic or hydrophobic) and fill volume of the well;

shaking angle, speed and diameter; physico-chemical properties of the liquid (viscosity, oxygen solubility and diffusivity).

Increasing shaking frequency enhances oxygen mass transfer and mixing in microtiter plates. According to Doig and Baganz (2005) the major factors affecting the volumetric mass transfer coefficient (k_La) in microwells are the shaking frequency and amplitude, interfacial properties and fluid properties. Doig et al. (2005) reported that for 96 standard well plates at 3 mm shaking amplitude, k_La ranged from 18 h^{-1} to 198 h^{-1} (0.005 to 0.055 s^{-1}) depending on the shaking speed.

Hermman et al. (2003) identified the surface tension of the liquid phase (σ) as a key factor in defining liquid flow and hence gas-liquid oxygen transfer in microwell plates. At a critical shaking frequency (n_{crit}) the surface tension of the liquid is overcome by the centrifugal force. Above n_{crit}, as the shaking frequency increases, so does the liquid height in the well, increasing the area available for mass transfer (Figure 1.6). The influence of surface tension, which tends to reduce fluid movement and thus reduce mass transfer, can be lessened by using wells with wider cross-sections (Hermann et al., 2003; Kensy et al., 2005). However, increasing shaking speed to improve mixing and mass transfer becomes less effective with decreases in size of wells, as capillary forces tend to play bigger roles so that free diffusion or forced motion of the liquid is hindered (Berg et al., 2001; Kensy et al., 2005).

Figure 1.6. Images of the liquid phase during shaking at a shaking diameter of 25 mm and fill volume of 200 µl at different shaking frequencies in a 96 SRW plate, where h_L is the liquid height in the well. Reproduced from Hermann et al. (2003).

Maier and Büchs (2001) described what was termed "out-of-phase" phenomenon that can be seen in shaken bioreactors. This phenomenon occurs at certain operating conditions and is characterised by an increasing amount of liquid not following the rotating movement of the shaker table, thus reducing the specific power consumption, mixing and gas/liquid mass transfer. The probability of the phenomenon occurring increases with lower shaking diameters, lower fill volumes, and higher viscosity values. Following their "in and out of phase" research, Lotter and Büchs (2004) observed that increasing the head space increased the maximum oxygen transfer rate (OTR_{max}). However Peter and Büchs (2006) report that as long as the fluid motion is "in-phase", volumetric power input is significantly higher and the volumetric power consumption is independent of the shaking diameter. Kensy et al. (2005) described how at 1 mm shaking diameter "out-of-phase" operating conditions were observed in microwell plates. This suggests that such a small shaking diameter should not be used when efficient mixing and gas-liquid mass transfer is required. Authors such as Hermman et al. (2003), Duetz et al. (2000) and Doig et al. (2005) have made several very comprehensive measurements and estimates of k_La values under a series of shaking conditions. Figure 1.7 shows the relationship between shaking speed and orbital diameter.

Figure 1.7 Maximum oxygen transfer capacity (OTR_{max}) and specific mass transfer coefficient (k_La) in conventional 96 SRW plate at different shaking diameters and shaking frequencies with 200 µl fill volume. Measurements carried out using the sodium sulphite method. Reproduced from Hermann et al. (2002).

A number of researchers have identified that deep-well plates with square-shaped wells provide the best combination for adequate oxygen supply and ability to keep cells in suspension. This can be explained by the shape of the well, with the corners giving a "baffle-like" effect (Duetz et al., 2000; Duetz & Witholt, 2001; Hermann et al., 2003). They also suggested that oxygen transfer mostly occurs at the gas liquid interface, rather than by entrained bubbles which have not been observed under any shaking conditions to date. Duetz et al. (2004) demonstrated that larger square vessels (18mm×18mm and 50mm×50 mm) yielded high oxygen transfer rates and a regular shaking pattern, demonstrating that vessels in this size range could be a viable, space-efficient alternative to baffled or unbaffled Erlenmeyer shaking flasks. Figure 1.8 demonstrates how the gas-liquid surface area is affected by shaking speed in 96 DSW plats. At higher shaking speeds the liquid height increases as well as the area available for oxygen transfer while the fluid mantains an "in-phase" pattern of movement. Round vessels (internal diameter 6.6 mm) resulted in OTRs that were approximately 50% of those measured for square vessels in the same size range (Duetz et al., 2004).

Figure 1.8 Images of the liquid phase (coloured water) during shaking at a shaking diameter of 6 mm and a fill volume of 400 µl at different shaking frequencies in a 96 DSW. Images were obtained with a NAC HSV-500 high-speed, analogue camera. Reproduced from Micheletti et al. (2006).

1.3.4 Methods for quantifying k_La values

As discussed in Section 1.3.3, one of the main unit operations in bioprocessing is mixing. Rapid and efficient mixing is crucial in this respect to ensure the generation of quantitative and reproducible data. Hermann et al. (2003) and later Doig et al. (2005) used high speed video techniques with shaken microwells to observe the fluid motion and study its impact on measurements of oxygen transfer rates.

Hermann et al. (2001; 2002) designed a method to measure oxygen transfer rates based on sulfite oxidation. The sharp decrease of the pH at the end of the oxidation, which is typical for this reaction, is visualized by adding a pH indicator dye which is measured throughout the reaction. The oxygen transfer capacity can then be calculated by the oxygen consumed during the complete stoichiometric transformation of sodium sulfite and the visually determined reaction time. A similar method was used by Kensy et al. (2005), who reported calculated volumetric mass transfer coefficients of up 1600 h^{-1} and oxygen transfer rates of up to 0.28 $mol.l^{-1}.h^{-1}$ in 48 SRW plates. However, Linek et al. (2006) demonstrated that the mass transfer rates measured by the optical sulfite oxidation method are overestimated by about 1.4 times, and therefore the results obtained with them should be treated more carefully or avoided if possible.

Some authors have devised novel methods to measure OTR. Many of these methods are based on zero order enzymatic oxidations. Duetz and Witholt (2004) created an enzymatic method involving glucose oxidase, horseradish peroxidase (HRP), and 2,2-azino-bis3-ethybenz-thiazoline-6-sulfonic acid (ABTS). The product of the reaction, a blue compound, was measured using a spectrophotometer at a wavelength of 725nm. This method is considered a colourimetric method as the

intensity of colour is directly correlated to the amount of oxygen consumed for the reaction of zero order kinetics. These authors used this technique to characterize the transfer rate in deepwell microplates. They concluded that in comparison to non-shaking conditions (3.2 $mmolO_2.l^{-1}.h^{-1}$), OTRs in 4mm × 4mm vessels (corresponding to wells in 384-square deepwell microwell plates) at a working volume of 0.125 ml could only be significantly enhanced at 300 rpm if a shaking diameter of 50mm was applied (25 mmol $O_2.l^{-1}.h^{-1}$) instead of 25mm (6.7 mmol $O_2.l^{-1}.h^{-1}$).

Following a similar approach, Ortiz-Ochoa et al. (2005) also designed a colourimetric method for the measurement of the volumetric oxygen transfer coefficient, k_La, using the catechol-2,3-dioxygenase (XylE) bio-oxidation of catechol yielding 2-hydroxymuconic semialdehyde (2-HS). When the enzyme concentration was in excess and the bio-oxidation rate was mass transfer limited, the oxygen transfer rate was determined from the linear increase in product concentration with time. The bio-oxidation was monitored by taking samples every minute and recording the optical density at 425 nm.

Doig et al. (2005) used an adaptation of the gassing out method to measure k_La values in microwell plates, where a superficial blanket of nitrogen was placed over the well until the dissolved oxygen value reached zero. Oxygen uptake rates were then measured using the fluorescent probes described in Section 1.2.4. The same gassing out method is used in this work since it most closely resembles the type of k_La measurements that can be performed in larger scale stirred bioreactors.

1.3.5 Modelling and prediction of engineering parameters in microwell plates

Only a limited number of attempts have been made to relate engineering parameters such as k_La to the conditions used during shaking of microwell plates. As mentioned in Section 1.3.3., Hermann et al. (2003) concluded that a critical shaking frequency had to be reached in order to overcome the surface tension (σ) of the liquid in a microwell. They developed a correlation to calculate the critical frequency. They postulated that "the critical shaking frequency (n_{crit}) is reached when the work delivered by the centrifugal force is equal to the surface tension of the liquid in a microwell plate well (Equation 1.3). This correlation for n_{crit} depended on the shaking diameter (d_O) and the physical and geometric parameters such as surface tension (σ), liquid density (ρ_L), well diameter (D_W), and well fill volume (V_{fill}). This information is important to establish as it helps to develop the microwell experimental methodologies and verify that the shaking correlations ensure adequate fluid motion.

$$n_{crit} = \sqrt{\frac{\sigma \cdot D_W}{4 \cdot \pi \cdot V_{fill} \cdot \rho_L \cdot d_O}} \qquad \text{[Eq. 1.3]}$$

Later Doig et al. (2005) presented a more comprehensive correlation based on dimensionless numbers, in order to calculate the volumetric oxygen mass transfer coefficient for surface aerated vessels (Equation 1.4). The flow characteristics of the liquid (Reynolds number, Re) and the physico-chemical properties of the fluid (Schmidt number, Sc) were considered important in modeling the liquid side oxygen transfer coefficient (k_L); the axial inertia (Froude number, Fr) and surface forces (Bond number, Bo) were considered critical in determining the final air–liquid surface area (a_f). The Sherwood number and a ratio of final (a_f) and initial

specific (a_i) surface areas (a_f /a_i) contained the two objective functions, k_L and a_f . The final equation for 96 microwells plates was as illustrated below, the values of y and z changing according to the well geometry:

$$k_La = 31.35\ D_{O2}\ a_i\ Re^{0.68}\ Sc^{0.36}\ Fr^{Y}\ Bo^{Z} \qquad \text{[Eq. 1.4]}$$

This correlation was created in order to predict k_La values over a wide range of operating conditions, providing an engineering basis for the selection of operating conditions for microplate scale cell cultivation.

1.3.6 Methods to increase the oxygen transfer rate

The rate of oxygen transfer in fermentation broths is influenced by several physical and chemical properties that affect either the mass transfer coefficient (k_L), the interfacial area (a), or the saturation concentration of oxygen (C^*). Table 1.1 lists these properties. Changing these variables can either increase or decrease the oxygen transfer rate; however, some of these properties cannot be altered systematically to increase the oxygen transfer rate e.g. the media composition and the interfacial tension (Doran, 1997). The properties in bold print are the most easily altered variables in order to increase the oxygen transfer rate.

For stirred vessels the impeller speed and geometry determine the power input, which in turn influences the mass transfer coefficient (k_L) and the interfacial area (a). At higher power inputs the turbulence in the liquid is greater, reducing the boundary layer surrounding the air bubbles to a minimum and therefore minimising the resistance to mass transfer. The interfacial area is increased because small bubbles have a higher surface area and also a slower rise velocity, which means they stay in the liquid longer allowing more time for the oxygen to transfer to the

aqueous phase (Doran, 1997). However, if the impeller speed is increased too much, the shear forces will cause the microorganism to disintegrate, and the higher power input required can make the process economically unfeasible (Nienow, 1998). The air flow rate determines the volume of gas in the reactor (gas hold-up), which influences the interfacial area. The airflow rate has a minor effect on the oxygen transfer rate compared to the impeller speed.

Table 1.1 Properties that influence the oxygen transfer rate in stirred bioreactors and shaken microwell plates.

Parameter	**Properties**	
	Stirred bioreactor	**Shaken microwell**
Mass transfer coefficient (k_L)	Viscosity	Viscosity
	Media composition	Medium composition
	Temperature	Temperature
	Power input	Density
Interfacial area (a)	**Gas hold-up**	**Shaking speed**
	Power input	**Shaking diameter**
	Interfacial tension	**Fill volume**
		Well format
		Liquid height
		Surface tension
Driving force (C^*)	**Partial pressure of oxygen**	**Diffusion**
	Temperature	Temperature
	Media composition	Media composition

Microwell plates rely on other mechanisms to promote oxygen mass transfer; Table 1.1 demonstrates that while it is feasible to change the values of k_L or a in a microwell plate, it would always be easier to achieve the desired levels of k_La by changing the transfer area (a), as there are many more mechanical variables that can be manipulated to affect a with minimum impact in the overall process, for example changing medium composition or temperature may affect the outcome of the fermentation or bioconversion and the impact may or may not be a positive one.

Mechanically stirred bioreactors are fed air through the sparger, pressurising the interior of the vessel, this in turns affects oxygen solubility and therefore oxygen mass transfer. There is a linear relationship between the oxygen partial pressure and the aqueous phase oxygen concentration. The equilibrium relationship obeys Henry's Law:

$$p_{O2} = p_T y_{O2} = H C^* \qquad \text{[Eq. 1.5]}$$

where, p_{O2} is the partial pressure of oxygen, p_T is the gas pressure, y_{O2} is the mole fraction of oxygen in the gas, H is the Henry's Law constant, and C^* is the saturation concentration of oxygen in the aqueous phase. If the total pressure of the gas is increased the driving force will be greater (Matsui et al., 1989). If the volume fraction of oxygen in the air entering the reactor is increased the driving force for mass transfer will increase. In stirred vessels the use of pure oxygen and oxygen-enriched air will increase the oxygen transfer rate (Castan et al., 2002). Nonetheless this is not the case for commercial microwell plates as there are no aeration systems within the well, unless they are custom designs like microscale bubble colum bioreactors (Doig et al., 2004). There is the possibility of incubating the plate in an oxygen rich environment; however, this presents other constrains, such as the need for a contained area to maintain a constant oxygen partial pressure.

1.4 Aims and Objectives

As described in Section 1.2 there is growing interest in the use of microwell systems for the rapid generation of quantitative bioprocess design data. Such methods could be particularly useful to support the rapid design and optimisation of bioconversion processes. This is due to the large number of variables required to be investigated and the strong influence of upstream operations, fermentation and/or enzyme purification, on bioconversion performance (Sections 1.1.3 and 1.2.2). Fernandez and Cabral (2006) reached a similar conclusion in their recent review of the area noting that in the near future automated, fully monitored and controlled bioreactor systems based on the use of small and microscale reactors will be widely used in bioprocess research and development.

To date the majority of microwell studies have focussed on the creation of assays for use in drug discovery and on a relatively small number of microbial fermentation processes (Section 1.2.1). There remains, however, a need to identify a generic set of microwell culture conditions for the most commonly used industrial microorganisms and to illustrate the high throughput potential of this approach. There is also a need for better monitoring and control of microwell cultures and the need to introduce feeding strategies in order to attain higher biomass levels. In contrast there are very few publications dealing with the study of bioconversion kinetics in microwell systems (Section 1.2.2). Here there is a need to show that quantitative bioconversion kinetic can be reliably obtained and to expand the classes of bioconversions studied (Doig et al., 2002; Brunatti et al., 2004; Marques et al., 2007).

A better understanding of the engineering environment within shaken microwells is

urgently required in order to ensure the generation of reliable and quantitative bioconversion kinetic data. While there have been some attempts to define mixing and oxygen transfer characteristics within the wells (Section 1.3.3) further investigation is required in order to establish useful correlations for the better specification of microwell experimental conditions. Going further, effective bases need to be established in order that knowledge generated from microwell experiments can be predictive of larger scale performance.

Finally, the limited number of unit operations established in microwell formats is currently holding back the creation of automated whole process sequences at the microwell scale (Section 1.2.6). Once such experimental protocols are established it will be possible to exploit the potential of laboratory robotic platforms to truly enable parallel and high throughput bioprocess experimentation. Such platforms will enable the 'whole process' evaluation of recombinant biocatalysts and the generation of bioprocess data for the modelling and evaluation of different process routes.

Although a wide range of microwell scale studies are still required, this thesis focused on the establishment of automated whole process sequences and the generation of scalable bioconversion data in microwell formats. **The overall aim of the thesis was thus to establish an automated microscale platform for the generation of quantitative and scalable biocatalytic bioprocess design data.** The approach was illustrated using advanced Baeyer–Villiger monooxygenases (BVMOs) which mediate the nucleophilic oxygenation of linear or cyclic ketones, yielding the corresponding esters or lactones (Section 1.1.3). These have application in the synthesis of a broad range of compounds with different industrial applications, from synthesis of antitumor compounds to the production of intermediaries for potent drugs for the treatment of glaucoma and hypertension, amongst others (Alphand et al., 2003). The use of whole cell BVMO biocatalysts

facilitated the use of mild process conditions for the reaction and promoted *in vivo* recycling of the necessary enzyme cofactors.

The initial objective was to establish the microscale fermentation and bioconversion methodologies and to generate an understanding on how microscale experimental conditions impact on process performance. To illustrate the approach production of a whole cell *E. coli* TOP10 [pQR239] biocatalyst was used expressing the CHMO activity from *A. calcoaceticus* NCIMB 9871 (Section 1.1.3). The subsequent use of these cells for the bioconversion of bicyclo[3.2.0]hept-2-ene-6-one into its corresponding lactones (-)-(1*S*,5*R*)-2-oxabicyclo[3.3.0]oct-6-en-3-one and (-)-(1*R*,5*S*)-3-oxabicyclo[3.3.0]oct-6-en-2-one was examined (Figure 1.2). The advantage of using the whole cell *E. coli* TOP10 [pQR239] biocatalyst is that fermentation and bioconversion data at a range of conventional scales already exists (Doig et al., 2000; 2002a; 2002b; 2003). Specific objectives were to reproduce the quantitative results of these previous studies, to understand how microscale experimental conditions impact on process performance at each stage and to optimise the conditions used for microwell experimentation so that data comparable to that obtained in typical shaken flasks is obtained. This work is described in Chapter 3 along with an example of high throughput data collection on both cell growth and oxygen utilisation kinetics.

Having established the experimental methodology the next objective was to establish automated microscale process sequences, for the operation of linked fermentation, bioconversion and primary product recovery stages. A small library of different recombinant whole cell CHMO expressing biocatalysts was used in order to test that the microwell process can quantitatively discriminate the performance of each biocatalyst at each stage in the process sequence. This work is described in Chapter 4.

The output of Chapter 4 will be identification of the optimum conditions for biocatalyst production and bioconversion. **The final objective will be to establish a suitable basis for the scale-up of these microwell results in order to show that the data obtained can be predictive of larger scale performance.** Given the demand of both the fermentation and bioconversion steps for molecular oxygen it was hypothesised that k_La will be the most appropriate basis for scale-up (Sections 1.3.2 and 1.3.3). Consequently k_La was measured in both microwell and stirred bioreactor geometries and combined fermentation-bioconversion processes performed at a range of matched k_La values between the two scales. This work is described in Chapter 5.

The experimental findings in Chapters 3 to 5 are summarised in Chapter 6 and the overall findings of this study discussed. A series of recommendation for further work are also made (Section 6.3) in order to verify the results obtained and to consider the wider implementation of the experimental platform.

2.0 Materials and methods

2.1 Reagents and suppliers

Reverse osmosis (RO) water was used in all experimental work. Tryptone, yeast extract, glycerol, sodium chloride, ampicillin, arabinose, cyclohexanone and caprolactone were obtained from Sigma Chemical Co. (Poole, Dorset, UK). Cyclopentanone, monosodium glutamate, sodium hydrogen phosphate, potassium dihydrogen phosphate, ammonium sulphate and (1R, 5S)-2-oxabicyclo[3.3.0]oct-6-en-3-one were obtained from Fluka Chemie AG (Buchs, Switzerland). Bicyclo[3.2.0]hept-2-en-6-one (bicycloketone) was a kind donation from Fluka. All chemicals were of analytical grade.

2.2 Microorganisms

Acinetobacter calcoaceticus NCIMB 9871 and *E. coli* TOP10 were obtained from NCIMB (Aberdeen, Scotland, UK) and Invitrogen (Groningen, The Netherlands) respectively. The CHMO gene from *A. calcoaceticus* was cloned into *E. coli* TOP10 using an L-arabinose inducible vector, pQR239, as described by Doig, et al. (2001). The strain of *E. coli* JM107 was constructed by Dr. Sejal Patel from UCL using the same monooxygenase as the one contained in *E. coli* TOP10 [pQR239]. This strain was inserted with a pQR210 plasmid, as reported by Barclay (2001).

2.3 Analytical techniques

2.3.1 Substrate and product quantification by gas chromatography (GC)

2.3.1.1 Sample preparation for GC analysis

The following technique was applied to extract cyclohexanone, cyclopentanone and bicycloketone, which were all the bioconversion substrates used in this work. The ethyl acetate and naphthalene (1 $mg.ml^{-1}$) solution was used to extract all samples. Equal volumes of the fermentation broth sample (without prior removal of cells) and ethyl acetate were vortex mixed for 30 seconds in a 1.5 ml Eppendorf tube. Naphthalene was used as an internal standard for the Gas Chromatography. This was determined to be long enough for extraction equilibrium to be reached (data not shown). The sample was then centrifuged at 13000 rpm for 2 minutes (Biofuge 13, Heraeus Sepatech, Brentwood, UK) and the top solvent layer was transferred into a separate vial, diluted appropriately with ethyl acetate (if required) and analysed by GC, as described in Section 2.3.1.2. This technique is adequate for samples with low concentrations of substrate and product. This technique was previously reported by Lander (2000).

2.3.1.2 GC operation

Detection and quantification of the ketone substrate and lactone products of the bioconversion was performed simultaneously using a Perkin-Elmer autosystem XL-2 gas chromatograph (Perkin-Elmer, Connecticut, USA), fitted with an AT-1701 column (reverse phase silica, 30 m x 0.54 mm) (Alltech, Carnforth, UK). 1 µl samples were injected onto the column at 200 °C using the integrated autosampler and compounds exiting the column were detected by a flame ionisation detector (FID). The oven temperature programme included an initial holding step at 100 °C

for 5 minutes and then the temperature was ramped at 10 °C per minute until it reached 240 °C. Data capture and analysis was made using Perkin-Elmer Nelson Turbochrom™ software.

2.3.1.3 Quantification of the GC response

The FID response to a particular solute concentration in a sample was measured as an integrated peak area on a GC chromatogram. External calibration curves were used to quantify these responses for the ketone substrate and lactone products. Pure bicyclo[3.2.0]hept-2-en-6-one, cyclohexanone or cyclopentanone were used for the ketone standard and pure (1R,5S)-2-oxabicyclo[3.3.0]oct-6-en-3-one, caprolactone and δ-valerolactone were used for the lactone standard. The results are shown in a graph of ketone or lactone concentration *vs.* time (Appendix II). Typical calibration curves of concentration against FID response and sample chromatograms are shown in Appendix III for all the types of sample analysed. For each type of sample the coefficient of variance for a single peak area measurement was determined from triplicate measurements of six sample solutions (concentration range 0.1-1 $g.l^{-1}$), and was found to be ± 2.5 %. The error in preparation of a 1 $g.l^{-1}$ standard solution was taken as ± 0.5 %.

2.3.1.4 Ketone and lactone evaporation curve

Bioconversion substrate evaporation curves were carried out to assess whether substrate was being consumed by the cells or it was going to the atmosphere. These curves were made for all the substrates that were used in this work.

These experiments were carried out in two modes, with the plate covered and uncovered. 1000 µl of a solution of 1 $g.l^{-1}$ of ketone was dispensed inside the whole plate. The plates were incubated at 30°C and 1000 rpm for 1 hour. Four samples were "cherry picked" from the borders and the centre of the plate every 10 minutes and analyzed by GC (Section 2.3.1).

2.3.2 Biomass quantification

2.3.2.1 Dry cell weight (DCW) measurement

Two millilitre aliquots of cell culture were added to pre-dried and pre-weighed 2.2 ml Eppendorf tubes, and the tubes centrifuged at 13000 rpm for 2 minutes. The supernatant was discarded and the process was repeated for a further 2 ml aliquot and then a 1 ml aliquot in the same vial. After the final supernatant was discarded, the tubes were dried in an oven at 100 °C until they achieved a constant weight. The DCW of the culture could then be calculated. All the biomass concentrations subsequently reported in this thesis are on a DCW basis. The coefficient of variance for an individual DCW measurement was determined from triplicate measurements of each of nine cell suspensions (concentration range 1.0 - 6.0 $g.l^{-1}$) and found to be ± 2.5 %.

2.3.2.2 Optical density (OD) measurement

The optical density of fermentation broth samples (200 µl) was measured in polystyrene 96-Standard Round Well plates (SRW) (Fisher Scientific, Loughborough, Leicestershire, UK) using a SpectraCount microplate reader

(Packard Instrument Company, Meriden, Connecticut, US) at 600 nm (OD_{600}), using reverse osmosis water as blank and for dilutions so that the optical density measurement was between 0.1-1 absorbance unit. External calibration curves were produced for each microorganism-broth combination in order to relate OD values to biomass dry cell weight ($g_{DCW}.l^{-1}$). All OD measurements were performed in triplicate and the coefficient of variance of typical OD readings determined as ± 5%. A calibration curve linking the OD_{600} measurement from before and after induction (when required) to the DCW measurement was constructed and is shown in Appendix I (Amanullah et al., 2002, 2003). The measurements were taken from a dilution series of a typical fermentation culture medium (Section 2.4.2.1).

2.4. k_La measurements

2.4.1 Microscale k_La measurements

All k_La measurements were performed in a well from a 96 DSW plate adapted to fit the oxygen probe and cable (Section 2.4.1.1, Figure 2.1), using a matrix of mixing speeds (800 – 1200 rpm) and filling volumes (200 – 1000 µl). The dynamic gassing out method was used for these experiments (Doig et al. 2005). A superficial stream of N_2 was used to calibrate 0% DOT. In order to measure the probe response time (PRT), the probe was left to stabilize up to 100%, then the stream of N_2 was placed on the surface of the well. This stream was maintained up to when DOT reached ≈ 10%. PRT was considered as the time required for the well to reach 37% DOT from 100%. Typical Probe Response Times (PRT) were of 10.4 s ± 1.2 s.

The culture media described in Table 2.2 was used for all k_La experiments. To measure k_La, the well was first depleted of oxygen by a superficial stream of N_2 up

to the 0% DOT. This current was removed at this point and the well was allowed to transfer air by superficial mass transfer. As k_La is a first order lag process, individual k_La values were calculated using Eq. 2.1 at different DOT data points between 10% and 70% and the average was obtained, depending of the linearity of the points. In Eq. 2.1 k_P is equal to the PRT and t is the time at which individual DOT data points were measured; Y_P is also defined in Eq. 2.2.

This same technique was applied using NaCl 10 $g.l^{-1}$ as filling liquid, in order to assess the coalescent effects of high ionic concentration solutions in microwells.

$$Y_P = \frac{1}{\left(\frac{1}{k_La}\right)-\left(\frac{1}{k_P}\right)}\left[\left(\left(\frac{1}{k_La}\right)\exp\left(\frac{-t}{\frac{1}{k_La}}\right)\right)-\left(\left(\frac{1}{k_P}\right)\exp\left(\frac{-t}{\left(\frac{1}{k_P}\right)}\right)\right)\right] \qquad \text{[Eq. 2.1]}$$

Where

$$Y_P = \exp\left(\frac{-t}{\frac{1}{k_P}}\right) \qquad \text{[Eq. 2.2]}$$

2.4.1.1. DOT probe

Semi-continuous measurements (every two seconds for k_La experiments and every minute for fermentation profiles) of dissolved oxygen levels during microwell fermentations were made using 96 DSW plates containing an oxygen sensitive fluorescent patch connected through a fibre optic cable to the Oxy4- Oxygen-metre

from PreSens (Regensburg, Germany). The microwell plate was drilled up to the wall of a well nearest to the border of the plate. A 3 mm diameter hole was drilled through the outer wall of a 96 DSW and into one of the outer wells and sealed from the outside with Perspex to create a window into the well. This window was later covered with the O_2 probe which would be quenched by the available oxygen in the liquid and create a fluorescent pulse, recorded into a computer using the software provided by the manufacturer PreSens (www.presens.de). The software further converts the fluorescent signal into a DOT values using the Stern-Volmer correlation. A schematic diagram of the arrangement can be seen in Figure 2.1. The gassing out method was chosen because it is a well established method, being flexible, robust and able to be carried out at small scales. Shaking for these experiments was achieved using the same Eppendorf Thermomixer Comfort (Eppendorf AG, Hamburg, Germany) used in other microwell fermentations and bioconversions (Sections 2.6.1, 2.6.2). The plate with the DOT sensor was cleaned after bioconversion with deionised water and alcohol and stored in a dark place to preserve the oxygen probe (Figure 2.1).

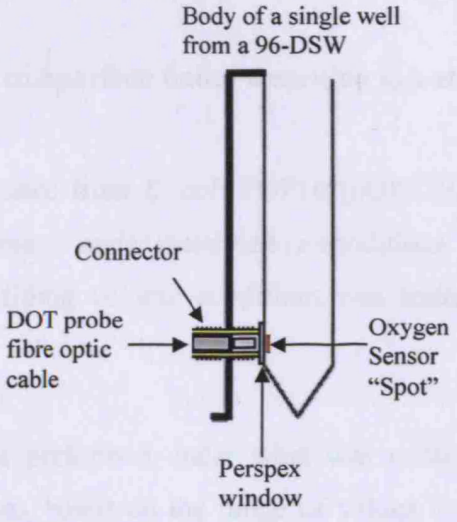

Figure 2.1 Schematic Diagram of a single well on the edge of a 96 DSW plate adapted for k_La measurements as described on Section 2.4.1.1.

2.4.2 Bench scale k_La measurements

Culture media and a 10 $g.l^{-1}$ sodium chloride solution were used to measure the k_La values of an array of mixing conditions. The gassing out method was used for these experiments. To measure the probe response time (PRT), the DOT probe was subjected to a N_2 gas flow until its reading reached 0% and then it was submerged in the vessel, which had been pre-saturated with air. PRT was considered as the time required for the well to reach 63% DOT from 0% (Van't Riet, 1979).

In order to measure k_La, the air inside the vessel was removed by a feed of N_2 into the vessel. When the DOT was $\approx$ 0%, the N_2 feed was disconnected to allow the vessel to release excess gas. After 3 minutes a 1 $l.min^{-1}$ feed of air was attached to the vessel. The k_La was calculated using the same procedure described in Section 2.4.1, by using Equations 2.1 and 2.2.

2.4.3 Bioprocess comparison under matching k_La at two scales

The process sequence from *E. coli* TOP10 [pQR239] was chosen to perform the bioprocess experiments under matched k_La conditions. A combination from a range of agitation and filling volume conditions was tested for both fermentation and bioconversion.

Experiments were performed under what was considered "low", "medium" and "high" k_La regimes, based on the range of values obtained from the experiments performed in Section 2.4.1 and 2.4.2. Several process parameters were measured for each matched k_La condition at both scales, such as growth rate, final biomass

concentration, rate of lactone formation, specific activity and yield. The process parameters used to match k_La values in 96 DSW plates and stirred vessels are presented in Table 2.1.

Table 2.1 Whole cell biocatalysis conditions for matched k_La values in 96 DSW plates and stirred vessels. Experiments were carried out as described in Section 2.4.3.

k_La value (h^{-1})	96 DSW plate		Stirred vessel agitation speed (rpm)
	Agitation speed (rpm)	Liquid fill volume (µl)	
"Low" k_La 45 ± 5	1000	1000	700
"Medium" k_La 115 ± 10	1000	500	900
"High" k_La 180 ± 10	1200	200	1000

2.5 Microwell evaporation rate

The weight of a single 96 DSW plate was measured and recorded. A volume of 1 ml of water was added to 20 randomly distributed wells and weighed again to record the weight at time zero and to verify a weight increase of 20 g. The 96 DSW plate was then incubated uncovered at 37°C and 1000 rpm for seven hours. The plate was reweighed hourly, the value recorded and the difference between the hourly weight and the initial weight calculated. These values were plotted and the overall rate of evaporation was calculated. The average rate of evaporation was determined to be 0.039 $g_{water}.h^{-1}$ with a R^2 value of 0.992 and a variance of ± 1%.

2.6 Microscale processes sequence

2.6.1 *E. coli* TOP10 [pQR239]

2.6.1.1 Microorganism origin and culture

The *E. coli* TOP10 [pQR239] strain was a kind gift from Dr John Ward (Department of Biochemistry and Molecular Biology, University College London). Working stock cultures of *E. coli* TOP10 [pQR239] were prepared initially from a 50% v/v glycerol master stock, stored at -70 °C. Two master stock vials were inoculated into two sterile 500 ml shake flask containing 100 ml of the growth medium described in Table 2.2, to which 100 $mg.l^{-1}$ ampicillin had been added via a 0.2 μm filter (Pall, MI, USA). This culture was left for 12 hours and a 5 ml aliquot of each shake flask was then used to inoculate two 1 l shake flasks with a further 100 ml of the media described in Table 2.2. When the culture had grown for four hours, 50 % v/v of sterile glycerol was mixed in aseptically and 1 ml aliquots were frozen at -70 °C. These working stock cultures were then used throughout all the work reported in this thesis.

Table 2.2 Composition of the growth medium used in all *E. coli* TOP10 [pQR239] fermentations.

Media component	Concentration ($g.l^{-1}$)
Yeast extract	10.0
Peptone	10.0
Glycerol	10.0
NaCl	10.0

2.6.1.2 Inoculum preparation

A 500 ml shake flask containing 100 ml of the medium described in Table 2.2 was first autoclaved at 121 °C for 20 minutes. When the flask had cooled, ampicillin was added via a 0.2 μm filter to a concentration of 50 $mg.l^{-1}$. A 1 ml frozen stock aliquot, as described in Section 2.6.1.1, was then thawed and inoculated into the shake flask aseptically and was subsequently incubated overnight at 37 °C in an orbital shaker at 200 rpm (New Brunswick Scientific, Edison, USA).

2.6.1.3 Microscale fermentations

Figure 2.2 shows a schematic diagram of the microscale process sequence which consisted of fermentations followed by whole cell bioconversions. Fermentations were carried out in polypropylene 96-deep square well plates (96-DSW, Becton Dickenson, Franklin Lakes, NJ, USA) in a contained environment. Each well was filled with 950 μl of the same culture medium described in Table 2.2 and then inoculated with 50 μl of overnight culture (Section 2.6.1.1). The plate was incubated at 37°C and 1000 rpm using a microwell plate thermomixer (Eppendorf Thermomixer Comfort, Eppendorf AG, Hamburg, Germany). The mixing was in an orbital pattern with a throw of 3 mm. The plates were left unsealed to allow efficient oxygen transfer. Samples (200 μl) were withdrawn periodically using a sacrificial well approach as described by Doig et al. (2002), where after a sample was taken from a well, that well was not reused. Samples were transferred to standard 96-round well (96-SRW, Fisher Scientific, Epsom, UK) plates for optical density measurements (Section 2.3.2.2).

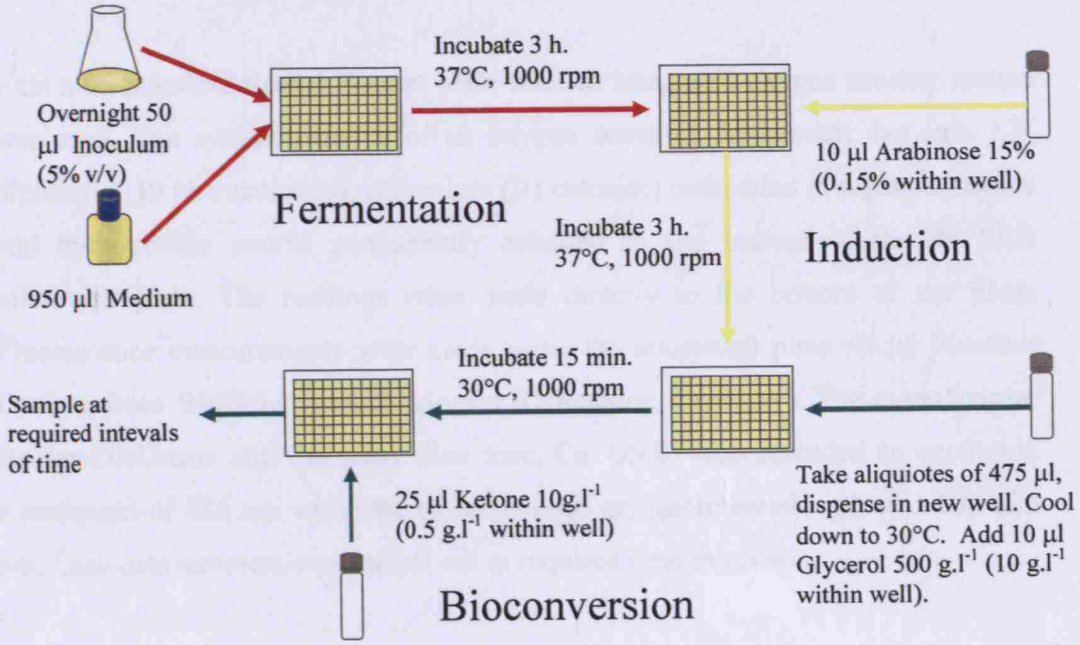

Figure 2.2 Automated microscale sequence for the process evaluation of a recombinant *E. coli* TOP10 [pQR239] biocatalyst expressing cyclohexanone monooxygenase (CHMO).

2.6.1.4 Microscale fermentation DOT monitoring

Microscale fermentations were carried out to acquire DOT data from *E. coli* TOP10 [pQR239]. The fermentations were carried out using the conditions described in Section 2.6.1.3. Two different microscale oxygen probes were used in these experiments.

First a 96 Standard Round Bottom plate with an integrated oxygen sensing system was used. The system consists of an oxygen sensitive fluorescent dye (tris 1,7-diphenyl-1,10 phenanthroline ruthenium (II) chloride) embedded in a gas permeable and hydrophobic matrix permanently attached to the bottom of the 96 SRB microwell plate. The readings were made directly to the bottom of the plate. Fluorescence measurements were made using the microwell plate reader FluoStar Optima, from BMG Laboratechnologies (Offenburg, Germany). The manufacturer Becton-Dickinson and Company (San Jose, Ca. USA) recommended an excitation wavelength of 485 nm while the recommended emission wavelength was 590-630 nm. Each measurement was carried out at required time intervals.

The fermentation conditions were at 37 °C and pH 7 and the inoculum concentrations used were between 1 to 5 % v/v. Agitation and temperature control were achieved using the incubator integrated to the microwell plate reader from FluoStar Optima. The radius was selected as it was required to achieve a shaking speed from the variable radius/shaking speeds this equipment provides. FluoStar Optima does not have a choice for stirring speed and instead this parameter is controlled by selecting a shaking radius (ϕ), where 1mm was 350 rpm and 6mm was 40 rpm. In order to quantify the fluorescence results, zero oxygen conditions microwells were required as a base line. This was achieved by the addition of a 100 mM solution of sodium sulfite to the corresponding wells. Fluorescent data was

later translated into DOT values using Stern-Volmer correlation. Further dissolved oxygen tension measurements in microscale fermentation (Section 2.6.1.3) and bioconversion (Section 2.6.1.5) were carried out with the oxygen probe described in Section 2.4.1.1

2.6.1.5 Microscale bioconversion

Bioconversions using whole cell biocatalysts were performed in 96-DSW plates using cyclohexanone, bicycloketone and cyclopentanone as substrates. For *E. coli* TOP10 [pQR239], induction of CHMO activity and quantification of bioconversion kinetics were carried out as first reported by Doig et al. (2002). CHMO induction took place after three hours of fermentation by adding 10 µl from a stock solution of L-arabinose (15% w/v) into each well. Three hours after induction, aliquots of 475 µl were taken from each well and added to wells in a new 96 DSW plate along with 10 µl of a glycerol stock solution (500 $g.l^{-1}$) to promote regeneration of the NADPH cofactor required for this bioconversion (Doig et al. 2003). The temperature was allowed to cool to 30°C, and the cells incubated for an additional 15 minutes to allow glycerol uptake and metabolism before the appropriate substrate solution was added to each well to give the desired initial concentration (Figure 2.2). Samples were taken at the required intervals in duplicate.

2.6.1.6 Bench scale fermentation

The laboratory scale fermentation, induction and bioconversion process sequence was performed using *E. coli* TOP10 [pQR239] with bicycloketone as the bioconversion substrate. For the fermentation, 100 ml of overnight culture, prepared as described in Section 2.6.1.2, was used to inoculate a 2 l stirred bioreactor

(Bioprocess Engineering Services, Charing, Kent, UK), having an internal diameter of 120 mm (T) and filled with a total liquid volume V_L = 1.4 l (liquid height H_{LT}). The vessel was equipped with four equally spaced vertical baffles of width B = T/10 and thickness t_b = T/100 and was stirred by two standard Rushton turbines (diameter D = T/3). The bottom impeller was located at a clearance C = 0.15*T* from the vessel bottom while the spacing between the two impellers was $\Delta C = 1.235D$. Further details can are available in Table 2.3

The impeller speed was set at 900 rpm throughout most of the fermentation only being altered slightly (±10 rpm) prior to enzyme induction to ensure the DOT was at an optimal level of 5-10%, for inducing CHMO activity (Doig et al. 2003). The vessel was aerated with 0.7 vvm sterile air via a submerged sparger and the temperature was maintained at 37 °C using a temperature probe and heating element. In the laboratory scale bioreactor pH was not controlled in order to provide a fair comparison with corresponding microwell studies.

After three hours of fermentation 1.5 ml of a 15% w/v L-arabinose solution was added to the vessel to induce CHMO activity. Enzyme synthesis proceeded for a further three hours, as in the microwell process (Section 2.4.1.4), before 6 ml of a glycerol solution (500 $g.l^{-1}$) was added to enable NADPH regeneration. After a further 15 minutes of incubation, 70 ml of bicycloketone (10 $g.l^{-1}$) was added to give an initial substrate concentration of 0.5 $g.l^{-1}$. Agitation throughout the subsequent bioconversion was maintained at 900 rpm, with an air flow rate of 0.7 vvm. Samples were taken from the bioreactor at the required intervals and monitored for substrate and product concentrations by GC (Section 2.3.1).

Table 2.3 Geometrical parameters of the 2 l total volume dual Rushton stirred vessel.

Parameter	Value (mm)	Characteristic Ratio
Vessel		
Internal Diameter (T)	120	
Vessel Height (H)	200	
Liquid Height (H_L)	124	H~T
Baffles		
Height (H_b)	93	
Width (B)	11	0.09T
Thickness (t_b)	1	0.0089T
Rushton Turbine		
Diameter, D	40	0.33T
Width (parallel to shaft), W	7	0.175D
Length, L	10	0.25D
Disk thickness, t_d	1.3	0.0325D
Impeller thickness, t	0.7	0.025D
Hub width	11	
Shaft diameter, D_{sh}	10	
Spacing between impellers, ΔC	53	1.325D
Clearance of bottom impeller, C	18	0.15T

2.6.1.7 Fermentation data logging

The inlet and exhaust gases were filtered through 0.2 μm filters (Gelman Sciences, Ann Arbor, MI, USA) and the composition of the exhaust gas was determined by mass spectrometry (Prima 600, VG Gas Analysis, Cheshire, UK). Data logged from the fermenter itself, e.g. impeller speed, pH, DOT and exhaust gas measurements were recorded with the RT-DAS program (Acquisition Systems, Guildford, Surrey, UK).

2.6.2. *E. coli* JM107 [pQR210]

2.6.2.1 Microorganism origin and culture

The *E. coli* JM107 [PQR210] strain was also a kind donation from Dr John Ward (Department of Biochemistry and Molecular Biology). Working stock cultures were prepared initially from a 50% glycerol master stock, stored at -70 °C. Two master stock vials were inoculated into two sterile 500 ml shake flasks containing 100 ml of the growth medium described in Table 2.2, to which 100 $mg.l^{-1}$ ampicillin had been added via a 0.2 μm filter (Pall, MI, USA). This culture was left for 12 hours and a 5 ml aliquot of each shake flask was then used to inoculate two 1 l shake flasks with a further 100 ml of the media described in Table 2.2. When the culture had grown for four hours, 50 % v/v of sterile glycerol was mixed in aseptically and 1 ml aliquots were frozen at -70 °C. These working stock cultures were then used throughout all the work reported in this thesis.

2.6.2.2 Inoculum preparation

As described in Section 2.6.1.2 for *E. coli* TOP10, a 500 ml shake flask containing 100 ml of a similar medium to that described in Table 2.2, but with 20 $g.l^{-1}$ of glycerol instead of 10, was used. The shake flask was autoclaved at 121 °C for 20 minutes. Once the shake flask had cooled, ampicillin was added via a 0.2 µm filter to a concentration of 50 $mg.l^{-1}$. A 1 ml frozen stock aliquot, as described in Section 2.6.2.1, was then thawed and inoculated into the shake flask aseptically, which was subsequently incubated overnight at 37 °C in an orbital shaker at 200 rpm (New Brunswick Scientific, Edison, USA).

2.6.2.3 Microscale fermentations

Figure 2.3 shows a schematic diagram of the process sequence which involves fermentation and whole cell bioconversion. As described in Section 2.6.1.3 for *E. coli* TOP10 [pQR239], fermentations were carried out in polypropylene 96-deep square well plates (96 DSW plates, Becton Dickenson Franklin Lakes, NJ, USA) in a contained environment. Each well was filled with 950 µl of the same culture medium described in Table 2.2 and then inoculated with 50 µl of overnight culture (Section 2.6.1.1). The plate was incubated at 37°C and 1000 rpm using a microwell plate thermomixer (Eppendorf Thermomixer Comfort; Eppendorf AG, Hamburg, Germany). The mixing was in an orbital pattern with a throw of 3 mm. The plates were left unsealed to allow efficient oxygen transfer. Samples (200 µl) were withdrawn periodically using a sacrificial well approach (Doig et al. 2002), where after a sample was taken from a well; that well was not reused. These were transferred to standard 96-round well (96-SRW, Fisher Scientific, Epsom, UK) plates for optical density measurements (Section 2.3.2.2).

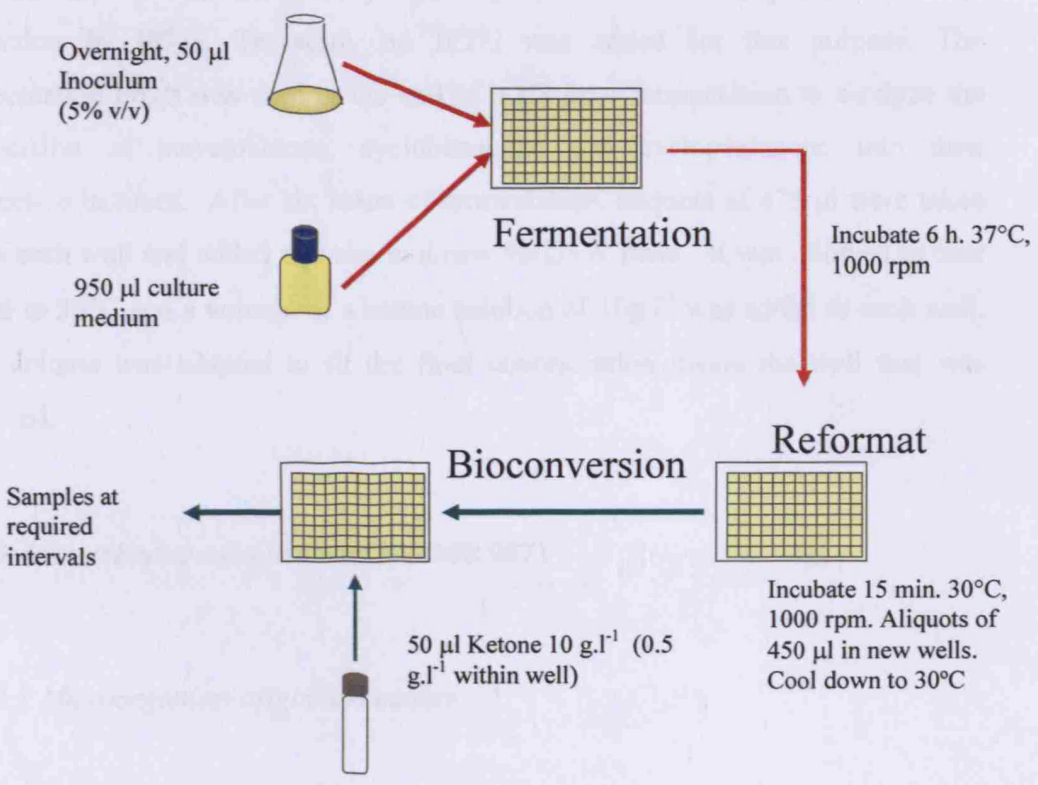

Figure 2.3 Automated microscale sequence for the process evaluation of a recombinant *E. coli* JM107 [PQR210] biocatalyst expressing cyclohexanone monooxygenase (CHMO).

2.6.2.4 Microscale bioconversion

The *E. coli* JM107 [PQR210] strain was engineered to express the CHMO from *A. calcoaceticus* using an IPTG induced plasmid. Preliminary studies, however, showed that the CHMO activity was expressed at satisfactory levels without induction by IPTG. Therefore, no IPTG was added for this purpose. The fermentation broth was used at the end of a six hour fermentation to catalyze the conversion of bicycloketone, cyclohexanone and cyclopentanone into their respective lactones. After six hours of fermentation, aliquots of 475 µl were taken from each well and added to wells in a new 96-DSW plate. It was allowed to cool down to 30°C and a volume of a ketone solution of $10 g.l^{-1}$ was added to each well. The volume was adapted to fit the final concentration inside the well that was required.

2.6.3 *Acinetobacter calcoaceticus* NCIMB 9871

2.6.3.1 Microorganism origin and culture

The *A. calcoaceticus* NCIMB 9871 strain was obtained from NCIMB (Aberdeen, Scotland, UK). A master stock culture was prepared from a lyophilised vial, as per the manufacturer's procedures. A working stock was created as two vials from the master stock were inoculated into two sterile 500 ml shake flask containing 100 ml of the growth medium described in Table 2.4. When the culture had grown to reach the exponential phase and biomass levels of $4 g.l^{-1}$, 30 % v/v of sterile glycerol was mixed in aseptically and 1 ml aliquots were frozen at -70 °C. These working stock cultures were used throughout this work.

2.6.3.2 Biocatalyst fermentation

A 500 ml shake flask containing 100 ml of the media described in Table 2.4 was sterilised without the trace elements, at 121 °C for 21 minutes. Cyclohexanol and 400 µl of trace elements solution were then added under aseptic conditions prior to inoculation. Cyclohexanol was weighed and dispensed to achieve a concentration of 1 $g.l^{-1}$ inside the vessel. The flask was then inoculated with one frozen stock sample, as described in Section 2.6.3.1. Samples were taken every two hours to measure optical density (Section 2.3.2.2) and cyclohexanol concentration by GC (Section 2.3.1). Whenever cyclohexanol was depleted, a further aliquot was weighed and added to achieve 1 $g.l^{-1}$, as described by Barclay (1999).

Table 2.4 Composition of the growth medium used in all *A. calcoaceticus* NCIMB 9871 fermentations.

Anhydrous constituent	**g. l^{-1}**
Sodium hydrogen phosphate (Na_2HPO_4)	4.0
Potassium dihydrogen phosphate (KH_2PO_4)	2.0
Ammonium sulphate ($(NH_4)_2SO_4$)	2.0
Trace elements (4ml)	**g. l^{-1}**
Magnesium sulphate ($MgSO_4 \bullet 7H_2O$)	19.6
Iron sulphate ($FeSO_4 \bullet 7H_2O$)	5.6
Calcium carbonate ($CaCO_3$)	2.0
Zinc Sulphate ($ZnSO_4 \bullet 7H_2O$)	1.4
Manganese chloride ($MnCl_2 \bullet 4H_2O$)	1.1
Cobalt chloride ($CoCl_2$)	0.28
Copper sulphate ($CuSO_4$)	0.25
Boric acid	0.06
Hydrochloric acid	53 ml

2.6.3.3 Microscale bioconversion

Aliquots of 475 µl from the fermentation broth described in Section 2.6.3.2 were dispensed in a 96 DSW. Three different ketones were used for the bioconversion: cyclohexanone, cyclopentanone and bicycloketone. Volumes of 25 – 50 µl from a solution of 10 $g.l^{-1}$ ketone were added to each well, depending on the final concentration required. Samples were taken at the required time intervals and analysed by GC as described in Section 2.3.1.

2.6.4 Automated microscale process sequences

Figures 2.2, 2.3 and 2.4 show schematic diagrams of the automated microscale process sequences, involving the linked fermentation, induction and bioconversion operations established for each of the biocatalyst-substrate combinations described in Sections 2.6.1, 2.6.2 and 2.6.3. Automation was achieved using a Multiprobe II EX liquid handling robot (Packard Instrument Company, Meriden, Connecticut, US) as previously described by Lye et al. (2003). Small micro-conductive tips, either fixed or disposable (Packard), depending on the stage of the process, were used for reagent addition. The performance files, which determine the accuracy and precision of pipetting, were optimised as previously described by Nealon et al. (2006). For the low viscosity liquids and dispense volumes used in this work the error in the accuracy and precision of all liquid additions is expected to be less than 5%.

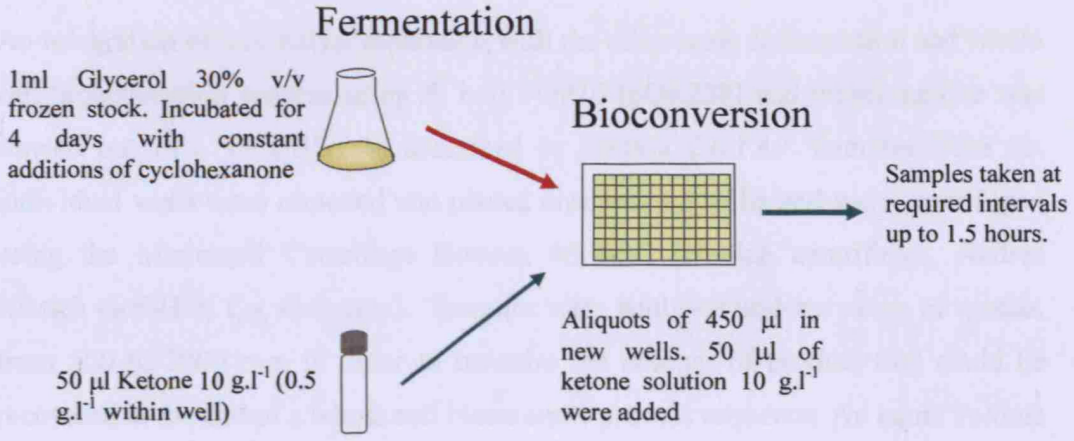

Figure 2.4 Automated microscale sequence for the process evaluation of a recombinant *A. calcoaceticus* NCIMB 9871 biocatalyst expressing cyclohexanone monooxygenase (CHMO).

2.7 Microscale downstream processing

2.7.1 Microscale centrifugation

An integration of biocatalyst separation with the microscale fermentation and whole cell bioconversion process using *E. coli* TOP10 [pQR239] and bicycloketone was carried out in a 96 DSW, as described in Section 2.6.1.4. Samples from six individual wells were removed and placed onto unused wells and were centrifuged using the Microwell Centrifuge Rotanta 46 RSC (Hettich centrifuges, Andres Hettich GmbH & Co, Germany). Samples were analysed under a range of speeds, from 500 to 2000 rpm in order to measure the amount of product that could be recovered at the end of a whole cell biocatalytic process sequence. An equal volume of water was dispensed in the same position as the samples in another 96 DSW to be used as a counter balance inside the centrifuge. The supernatant from three of these wells was used to measure OD_{600}, as described in Section 2.3.2.2, in order to quantify the fractional clarification and cell removal. The supernatant of the remaining three wells was used to measure bicycloketone and lactone concentration with gas chromatography, as described in Section 2.3.1, in order to quantify the fractional product recovery. Four different gravitational forces values (Z) were investigated. Table 2.5 translates such Z values into rpms.

Table 2.5. Correlation of gravitational force value and its corresponding speed.

Z values	Centrifugation (rpm)
4	500
16	1000
97	2500
249	4000

2.7.2 Microfiltration

An integration of biocatalyst separation with the microscale fermentation and whole cell bioconversion process using *E. coli* TOP10 [pQR239] and bicycloketone was carried out in a 96 DSW, as described in Section 2.6.1.4. The content of the wells was then dispensed into a new vessel in order to mix them and have a homogeneous initial feed.

The culture broth of a typical microscale whole cell biocatalysis of bicycloketone, using *E. coli* TOP10 [pQR239] as the biocatalyst, was used to perform these experiments. Several types of membranes were investigated: Millipore Durapore PVDF 0.1 μm, Millipore Durapore 0.22 μm, Millipore Durapore PVDF 0.4 μm, Millipore Durapore PVDF 0.65 μm, Millipore Nylon 0.2 μm and Whatman Cellulose Nitrate 0.2 μm. A filtration time of 90 seconds and a pressure of 60kPa was used. Six samples were analysed *per* membrane. All microfiltration experiments were carried out at 25 °C (room temperature). This technique was reported by Jackson et al. (2005).

This chapter described the procedures to carry out the work presented in this thesis. The following chapters will focus on the results from this work and their implications.

3.0 Microscale unit operations and their characterisation

3.1 Aims of the chapter

As described in Section 1.4, the aim of this chapter was to establish the microscale fermentation and bioconversion methodologies for the model BVMO bioconversion and to generate an understanding of how microscale experimental conditions impact on BVMO process performance. In particular, the specific objectives were to:

- Establish microscale experimental methods for the quantification of *E. coli* TOP10 [pQR239] fermentation and bioconversion kinetics.
- Generate an understanding of how microscale experimental conditions impact on fermentation and bioconversion performance.
- Illustrate the potential for high throughput data collection with the parallel collection of cell growth and DOT data.
- Compare the kinetic data obtained from the optimised microscale culture conditions with previously published work and replicated shake flask experiments.

The fermentation and bioconversion processes were characterised using an *E. coli* TOP10 [pQR239] strain expressing cyclohexanone monooxygenase (CHMO) from *A. calcoaceticus* NCIMB 91839, as described in Section 1.1.3. This enzyme catalysed the bioconversion of the ketone substrate bicyclo[3.2.0]hept-2-en-6-one (hereafter referred to as bicycloketone) into its corresponding lactone products (1R,5S)-3-oxabicyclo[3.3.0]oct-6-en-2-one and (1S,5R)-2-oxabicyclo[3.3.0]oct-6-en-3-one (hereafter referred to as bicyclolactone). The reaction scheme can be seen in Figure 1.2.

3.2 Shake flask *E. coli* TOP10 [pQR239] process

3.2.1 Fermentation kinetics

A number of previous laboratory scale studies have investigated the fermentation of *E. coli* TOP10 [pQR239] and the kinetics of the CHMO bioconversion using bicyclo[3.2.0]hept-2-en-6-one as substrate (Simpson et al., 2001; Doig et al., 2001). The standard fermentation and bioconversion conditions established in these previous studies were first repeated in order to verify their results and provide a reference data set against which to compare subsequent microscale process results. *E. coli* TOP10 [pQR239] fermentations were carried out in 500 ml shake flasks containing 100 ml of the medium described in Table 2.2. The inoculum was prepared as described in Section 2.6.1.2. The fermentation was carried out at pH 7 and 37 °C with shaking at 200 rpm. Figure 3.1 shows typical batch fermentation kinetics with a final biomass concentration of 4.5 $g.l^{-1}$ and a maximum growth rate (μ_{max}) of 0.69 h^{-1}. The results compare well with those reported by Doig et al. (2001) who reported a biomass concentration of $\approx$ 5 $g.l^{-1}$ and a maximum growth rate of 0.9 h^{-1} in a 1.5 l aerated stirred tank reactor.

3.2.2 Bioconversion kinetics

Subsequent bioconversion using whole cells of *E. coli* TOP10 [pQR239] were carried out using the medium described in Table 2.2 in 500 ml shake flasks with a working volume of 100 ml (Figure 3.2). The cells from a typical fermentation (Figure 3.1) were first induced with 100 µl of a solution 15 % w/w L-arabinose three hours after inoculation. The bioconversion was then carried out using the

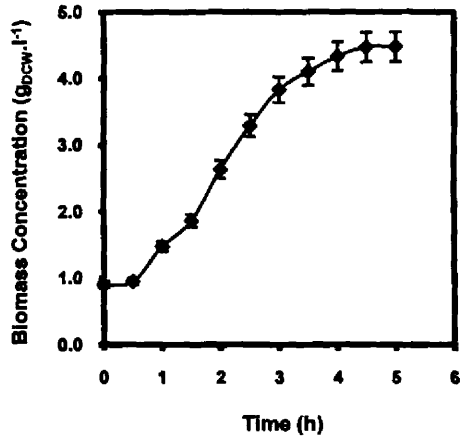

Figure 3.1 Typical batch growth kinetics of *E. coli* TOP10 [pQR239] grown in shake flasks. Experiments performed as described in Section 2.3.2.2. Error bars represent the range of measured values about the mean.

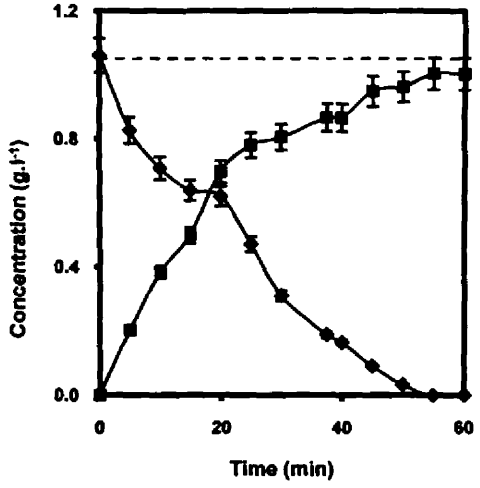

Figure 3.2 Typical batch bioconversion kinetics in shake flask using a whole cell *E. coli* TOP10 [pQR239] biocatalysis with 1 $g.l^{-1}$ initial bicycloketone substrate concentration. This figure shows bicycloketone (♦) depletion over time and the corresponding bicyclolactone (■) production. Experiments performed as described in Section 2.6.1. Error bars represent the range of measured values about the mean.

same conditions as for fermentation, i.e. pH 7 and 37 °C and 200 rpm. Samples were taken every five minutes over one hour to enable accurate determination of the bioconversion kinetics. Figure 3.2 shows bicycloketone consumption and the corresponding bicyclolactone production over time. The results show quantitative conversions of the bicycloketone into the corresponding bicyclolactone products. The mass balance on bicycloketone and bicyclolactone in the supernatant comes to within 98%, suggesting there is little or no accumulation of these solutes within the cell.

3.3 Microscale fermentation process characterisation

3.3.1 Effect of microwell geometry

Microscale fermentations performed as described in Section 2.6.1.3, were initially carried out in various microwell plate geometries to examine which yielded the best *E. coli* TOP10 [pQR239] growth kinetics and had an appropriate balance between working volume and sample volume. As described in Section 1.3.3, microwell geometry can have a major influence on oxygen transfer into the wells and hence on cell growth kinetics (Duetz et al., 2000; Doig et al., 2005). The number of wells also impacts on total plate volume, the possibility of sampling from individual wells or the need to adopt a "sacrificial well" approach as used by Doig et al. (2002) and Elmahdi et al. (2003).

Two different well geometries were assessed based on those previous studies: a 96 Standard Round Well plate (96 SRW) and a 96 Deep Square Well plate (96 DSW).

The differences in geometry and size of these wells can be seen in Figure 3.3. The 96 SRW has a flat base to facilitate spectroscopic measurements while the 96 DSW has a conical base. The working volume is the maximum amount of fluid that a well can contain without spilling or splashing, in the case of low viscosity fluids. In this case, the working volume in each well was 200 µl for the 96 SRW plate and 1000 µl for the 96 DSW plate. Sampling was carried out using the sacrificial well strategy reported by Doig et al. (2003). *E. coli* TOP10 [pQR239] fermentations were carried out using a 5% v/v inoculum, as also recommended by Doig et al. (2002).

Figure 3.4(A) shows typical *E. coli* TOP10 [pQR239] batch growth kinetics in each microwell geometry. The culture in the 96 DSW plate is seen to attain the highest biomass concentration of 4 ± 0.3 $g.l^{-1}$ which is close to the 4.5 $g.l^{-1}$ obtained in shake flaks (Section 3.2.1). The calculated maximum growth rate (μ_{max}) for the 96 DSW plate was 0.73 ± 0.03 h^{-1} which is also close to that determined in the earlier shake flask experiments. Figure 3.4(B) shows the growth calculations for the 96 DSW plate geometry.

The exponential phase in the growth kinetics in the 96 SRW plate was short and the maximum biomass concentration at the end of the fermentation was only 2.5 ± 0.2 $g.l^{-1}$. Calculations of the cell growth rate in the 96 SRW plate gave unrealistically high values (≈ 65% higher than the 96 DSW plate). This may be explained by liquid evaporation from the wells or cell sedimentation at the bottom of the well when the plate was not subjected to rigorous agitation (Marques et al., 2007), like during spectroscopic readings. In each case these would lead to increased optical density measurements and lead to the overestimation of μ_{max}.

Duetz et al. (2001) characterised several custom made deep square vessels, which indicates their increasing importance in microscale bioprocessing research. These

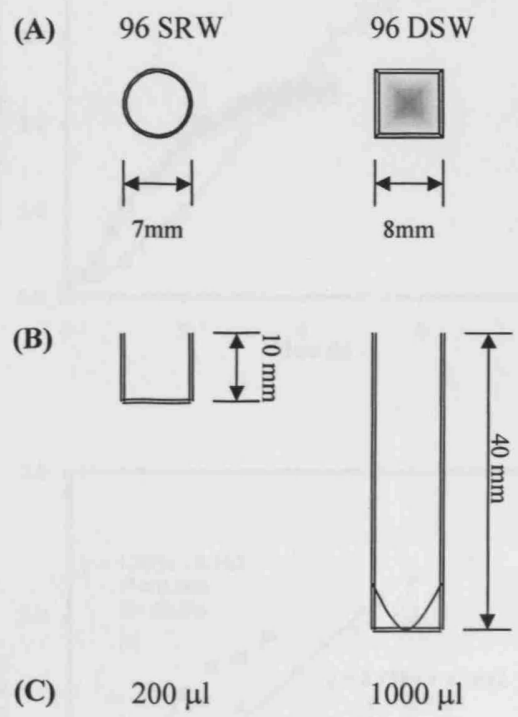

Figure 3.3 Schematic diagrams of the 96 well plate geometries Standard Round Well (SRW) and Deep Square Well (DSW) used in this work (A) plan view, (B) cross section through single wells and (C) well working volume.

(A)

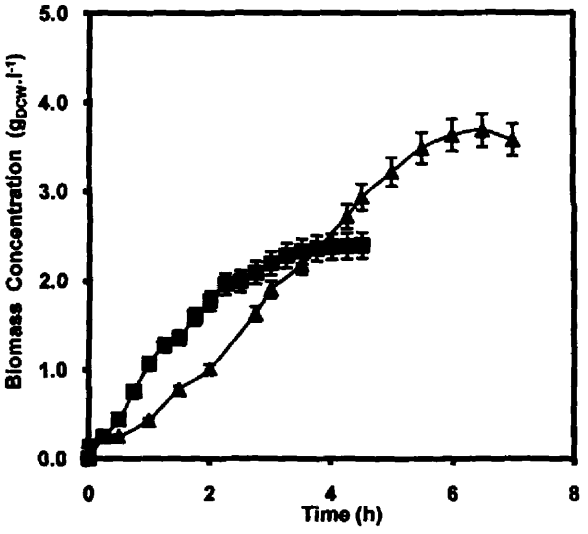

(B)

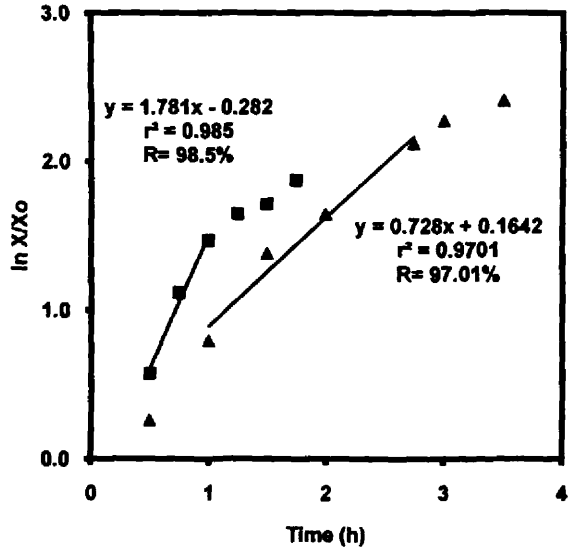

Figure 3.4 (A) Typical batch growth kinetics of *E. coli* TOP10 [pQR239] in two different microwell geometries: 96 SRW (■) and 96 DSW (▲). Experiments performed as described in Section 2.6.1.3. (B) Plot of the natural logarithm of biomass concentration against time used to calculate the growth rate kinetics in 96 DSW. Error bars represent the range of measured values about the mean.

authors found that the 8 mm square well, as used here, had an Oxygen Transfer Rate (OTR) of up to 33 ± 4.4 $mmol.l^{-1}.h^{-1}$ when larger shaking orbital diameters were used. They also found that wider square vessels have even higher OTR values (nearly double) but with an associated decrease in experimental throughput as the plate contains only 24 wells; 96 DSW is well suited to meet most requirements, however. Well geometry is thus an important factor to consider when developing microscale processes (Sections 1.3.3 and 1.3.6) as different well formats can impact on oxygen mass transfer (Doig et al., 2005), and may directly impact on the kinetics of oxygen acquiring unit operations such as aerobic fermentation or bioconversions catalysed by BVMO which also require molecular oxygen. This has been illustrated by Doig et al. (2002) who found that the 96 DSW geometry allowed a 400 $U.l^{-1}$ increase in measured BVMO activity in *E. coli* TOP10 [pQR239] when compared to the 96 SRW geometry, from 500 $U.l^{-1}$ to 900 $U.l^{-1}$.

Table 3.1 summarises the results of the microwell fermentations described here and the calculated kinetic parameters. The results from the 96 DSW plate are closest to those reported in the shake flask fermentations described in Section 3.2. The deep well geometry also has the advantage of larger working volumes and better mass transfer (Duetz et al., 2001) and will thus be the geometry used for the majority of the microscale fermentations reported in this thesis.

Table 3.1 Comparison of microwell geometries in terms *E. coli* TOP10 [pQR239] fermentation kinetics and experimental throughput.

No. wells	Well Geometry	Working Vol. per well (µl)	Max. Sampling Vol. per well (µl)	Maximum Growth Rate (h^{-1})	Final Biomass Concentration ($g_{DCW}.l^{-1}$)
96	SRW	200	160	1.78*	2.5
96	DSW	1000	800	0.73	4.0

*Apparent value due to evaporation and biomass settling.

3.3.2 Effect of inoculum concentration

The effect of inoculum concentration on fermentation performance was assessed by carrying out fermentations of *E. coli* TOP10 [pQR239] at 5% v/v and 10% v/v inoculum concentrations using a 96 DSW plate agitated at 1000 rpm, as described in Section 2.6.1.3. Typical fermentation kinetics are shown in Figure 3.5(A), while growth rate calculations are shown in Figure 3.5(B). Growth rates were calculated using the values between 1 h to 3 h of fermentation for both growth curves, when both fermentations reached their exponential phase.

The final biomass concentration obtained in both cases was in the range of $\approx 3.5 - 3.8$ g.l^{-1}. The maximum growth rate for the fermentation carried out at 5% v/v inoculum was 0.70 ± 0.04 h^{-1} while the one at 10% v/v had a growth rate of 0.50 ± 0.02 h^{-1}. As expected, the fermentation with the higher inoculum concentration, 10% v/v inoculum had a shorter lag and exponential phases due to the higher initial number of cells growing rapidly and exceeding the oxygen transfer capacity of the wells (Duetz et al., 2000).

Based on these results, all subsequent fermentations were carried out at 5% v/v inoculum unless stated otherwise. Although the lag phase was slightly longer, these fermentation conditions exhibited the highest growth rate and final biomass concentrations similar to those obtained in shake flask (Section 3.2.1). This is considered important for later studies where the oxygen consumption rate of the culture will also be considered and scale-up comparisons are made.

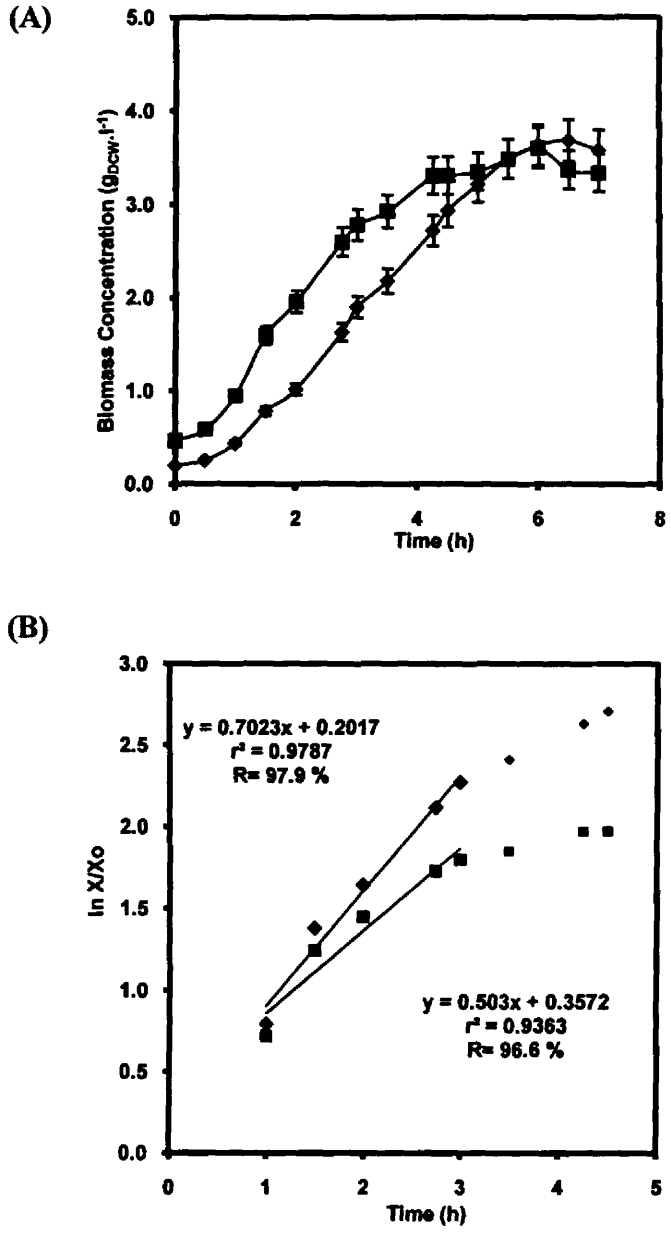

Figure 3.5 (A) Effect of inoculum concentration on *E. coli* TOP10 [pQR239] batch fermentation kinetics in 96 DSW plates. (B) Growth rate calculations for different inoculum concentrations. Two inoculum concentrations were used, 5 % v/v (♦) and 10% v/v (■). Experiments performed as described in Section 2.6.1.3. Error bars represent the range of measured values about the mean.

3.3.3 Effect of temperature

Initial *E. coli* TOP10 [pQR239] fermentations in 96 DSW plates using a 5% v/v inoculum and agitated at 1000 rpm were carried out at 30 and 37°C to assess the impact of temperature on cell growth rate and final biomass concentrations achieved (Figure 3.6). Growth rates were calculated between 2 to 3.5 hours of fermentation carried out at 30°C and between 3 to 4.5 hours of fermentation carried out at 37°C.

The final biomass concentration was 3.5 ± 0.3 $g.l^{-1}$ at 30°C, in comparison to 4.5 $g.l^{-1}$ at 37°C; the final biomass produced at 37°C is closest to 4.5 ± 0.4 $g.l^{-1}$ reported in shake flask (Section 3.2.1) and 5.5 $g.l^{-1}$ obtained in stirred tank bioreactors, as reported by Doig et al. (2003). The growth rate at 30°C was 0.53 ± 0.02 h^{-1} while at 37°C it was 0.57 ± 0.04 h^{-1}. While the growth rate is not greatly different, the biomass concentration obtained at higher temperatures was enhanced by nearly 30%; this is desirable as it would affect subsequent bioconversion process stages. This result is to be expected as the optimal growth temperature of *E. coli* TOP10 [pQR239] is reported to be 37°C (Doig et al., 2000, 2002). This temperature is also recommended by ATCC for the culture of most of its *E. coli* strains (www.atcc.com). Based on these findings, all later fermentations were performed 37°C.

3.3.4 Effect of evaporation in open microwells

As described in Section 2.6.1.3 microwell fermentations carried out with open microwells. It was necessary to quantify and account for the rate of evaporation since this can cause a steady increase in solute concentration within each well.

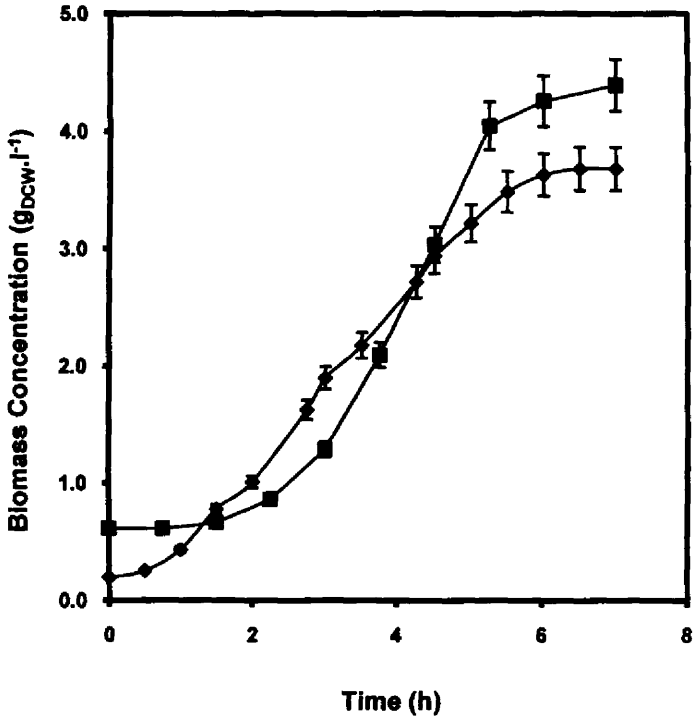

Figure 3.6 Effect of temperature on batch growth kinetics of *E. coli* TOP10 [pQR239] in 96 DSW plates, using 5% v/v inoculum and 1000 rpm agitation. The temperatures investigated were 30°C (♦) and 37°C (■). Experiments performed as described in Section 2.6.1.3. Error bars represent the range of measured values about the mean.

Water evaporation rates were quantified as described in Section 2.5. The rate of water loss was observed to be linear with an average rate of 0.039 $g_{water}.h^{-1}$ per well with an R^2 value of 0.994. This represents ≈ 39 µl per hour in each well (Figure 3.6). Water loss was not considered to have significant impact on 96 DSW fermentations; the majority of maximum growth rate calculations were performed within the first two hours of growth thus water losses due to evaporation would be less than 8% of the total volume and therefore insignificant.

Culture sterility was tested by ensuring that 1 well on each plate contained culture medium but without being inoculated. No microbial growth occurred in the well during any of the fermentations reported here as determined by optical density measurements. This is in part due to the use of antibiotics on the culture medium.

Open wells have been used throughout this work in order to facilitate the highest rates of oxygen transfer (Doig et al. 2002, Hermann et al., 2002). This was further proved by Zimmermman et al. (2003) who tested eight commercially available microwell plate sealing tapes and 10 other suitable materials (transparent wound dressings) and compared them semi quantitatively in terms of their ability to minimize water evaporation and maintain sterility while maintaining the oxygen supply as high as possible. They found oxygen transfer through the sealing films was slower, but the water retention capability was higher in all but one sealant (Mölnlycke Tendra Mefilm). Berg et al. (2001) found that a 96 SRW showed 50% v/v evaporation after 30 hours at room temperature and normal atmospheric pressure. This is due to lower filling volumes as well as smaller distance between the liquid meniscus and the top of the well in this well format. Berg et al. (2001) concluded that evaporation would be more significant with the higher well density formats used in drug discovery applications.

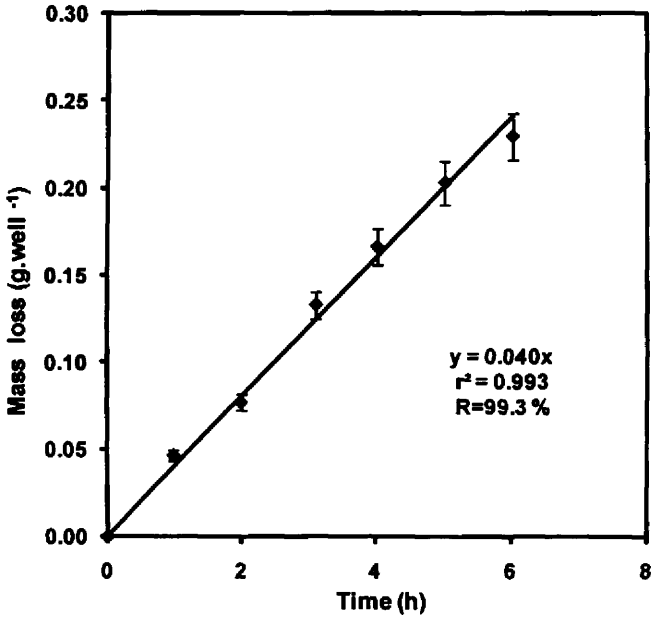

Figure 3.7 Rate of water evaporation from a 96 DSW plate incubated at 37°C and agitation at 1000 rpm agitation speed. Experiments performed as described in Section 2.5. Error bars represent the range of measured values about the mean.

3.4 Parallel fermentation and DOT monitoring

3.4.1 Oxygen sensing in 96 SRW microwell plates

While representative growth kinetics for *E. coli* TOP10 [pQR239] can be achieved in 96 DSW plates (Figure 3.4), this geometry has the disadvantage that it cannot be fitted into any commercially available microwell plate reader. This is because microwell plate readers are based on standard wells with a height of 10 mm. Also the 96 DSW design does not have a clear flat base to allow any light beam through it, rendering it unsuitable to make readings from.

Advances in parallel microwell measuring technologies have been developed using 96 Standard Round Bottom plates (96 SRB). During the course of these studies Becton-Dickinson and Company released a new 96 SRB plate with an integrated oxygen sensing system (Figure 1.5, Section 2.6.1.4). These plates were used to monitor the DOT profiles during microscale fermentations of *E. coli* TOP10 [pQR239], as this is one of the most important parameter in fermentations to ensure oxygen availability for growth and any other oxygen requiring processes like oxidative bioconversions.

The concentration of oxygen in the vicinity of the immobilised fluorescent dye is in equilibrium with that in the liquid media. Oxygen quenches the dye in a predictable concentration dependent manner. The amount of fluorescence correlates directly to the rate of oxygen consumption in the well which, in turn, can relate to any sort of reaction that can be linked to oxygen consumption. As oxygen is consumed, the biosensor fluoresces providing a signal that can be directly correlated to cell growth or oxygen consumption.

The behaviour of fluorophores quenched in this way follow the Stern-Volmer equation (3.1). At its simplest, the Stern-Volmer equation takes the following form (Pritchard and Servedio, 1975; Amao et al., 2000):

$$I_0 / I = 1 + K_{SV} * [O_2] \qquad \text{[Eq. 3.1]}$$

Where $[O_2]$ is the oxygen concentration in the liquid medium, K_{SV} is the Stern-Volmer constant, I is the fluorescence intensity under the presence of oxygen , $[O_2]$ is the oxygen concentration and I_0 is the fluorescence intensity at the reference condition of zero oxygen (Timmins, 2002). Gernot et al. (2003) have developed a similar oxygen sensing plate as shown in Figure 3.8.

Figure 3.8 *In situ* dissolved oxygen concentration measurement in round-bottomed microtiter plates with an integrated optical sensor. F1, filter for excitation light (540 nm); F2, filter for fluorescence light (640 nm and 590 nm); SL, sensor layer; CB, culture broth. Figure adopted from Gernot et al. (2003).

Fluorescence values vary from plate to plate and well to well and therefore need to be standardised against the fluorescence values of each individual empty well before they are translated into DOT values.

Also, the mechanism for reading the plates in the readers gives a margin of error in the oxygen readings as it is not carried out "in line" during the fermentation process but rather as an "off line" reading, as the plate reader has to stop agitation and relocate the plate to carry out the reading. However, these plates can be used for other type of reactions and can be a useful tool in understanding oxygen mass transfer in microlitre scale processes.

3.4.2 Limitations in the use of oxygen sensing 96 SRB plate.

Fermentation profiles comprising both cell growth (OD) and dissolved oxygen (fluorescence) for *E. coli* TOP10 [pQR239] were carried out using the oxygen sensing microwell plates described in Section 3.4.1. The fermentations were carried out using a shaking orbital throw (ϕ) of 3mm, which is the same in the Thermomixer Control previously used (Section 3.3). However the Fluostar Optima (the microwell plate reader on which fluorescence measurements were made) controls shaking speed by increasing or decreasing the shaking throw, unlike Thermomixer Control where both parameters are controlled independently. The shaking orbital throw used in these (3mm) experiments yields a shaking speed of 175 rpm. Two inoculum concentrations have previously been shown to result in different growth rates (Figure 3.5) and in this case they were used to allow clearer oxygen profiles.

Figure 3.9 shows the growth kinetics and oxygen consumption of *E. coli* TOP10 [pQR239] fermentations using the oxygen sensing BD 96 SRB plate at different

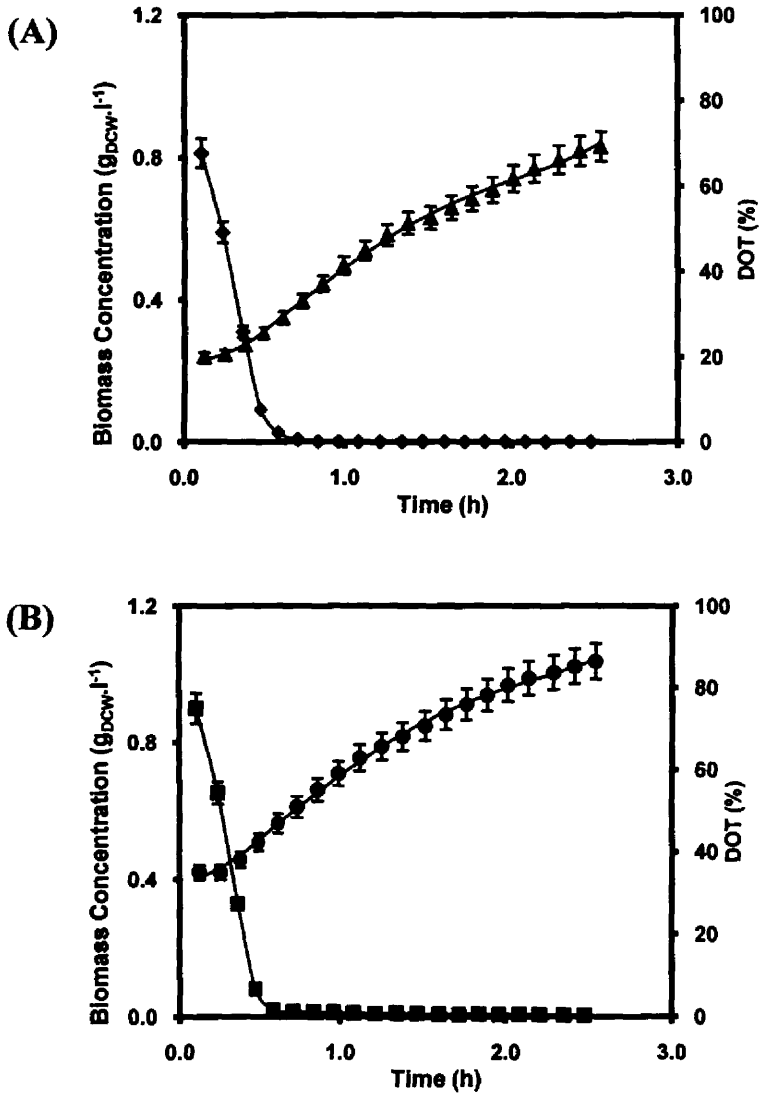

Figure 3.9 Biomass growth kinetics and associated dissolved oxygen levels during *E. coli* TOP10 [pQR239] batch fermentations. Figure (A) shows the growth kinetics using 2.5 % v/v inoculum concentration, biomass concentration (▲) and DOT (♦, second y-axis). Figure (B) shows the profile using 5% v/v inoculum, biomass concentration (●) and DOT (■, second y-axis). Experiments were performed as described in Section 2.6.1.4. Error bars represent the range of measured values about the mean.

initial inoculum concentrations. The growth rate in the fermentation with an initial inoculum concentration of 2.5% v/v had a growth rate of 0.98 ± 0.05 h^{-1} while the fermentation with initial inoculum concentration of 5% v/v had a growth rate of 0.76 ± 0.04 h^{-1}; Figure 3.5 presents a similar trend in that the higher inoculum concentration yields lower growth rates. These high values of growth rates are artificial however, as calculations are limited to the first half hour of fermentation, when cells are adapting to its environment. Dissolved oxygen levels (DOT) had a steep decline from the inoculation time until they reached zero after the first 40 minutes of the fermentation indicating that oxygen transfer rate was limited thus limiting fast aerobic growth to the first hour of fermentation since *E. coli* is a facultative aerobe (Clements et al., 2002).

DOT is seen to rapidly reach zero in both fermentations. This is due to the limitations in agitation, as the FluoStar Optima's highest shaking speed is 350 rpm using a shaking diameter of 1 mm, 2 mm less than in Thermomixer Control and while they cannot be compared due to equipment restrictions, it is important to demonstrate the influence of agitation conditions in microwell plate fermentations. Additionally, this particular geometry of microwell plates has a lower mass transfer rate, therefore limiting the amount of oxygen that can be used for cell growth. For 96 SRW plates Hermann et al. (2002) report an Oxygen Transfer Rate capacity (OTR_{max}) of ≈ 0.005 $mol.l^{-1}.h^{-1}$ for a 200 µl fill volume and 200 rpm agitation speed, close to that of a static well. While Gernot et al. (2003) report a k_La of 12 h^{-1} for this type of microwell plate with 200 µl fill volume which is in the lower range of typical values for shake flasks. This means that oxygen transfer limitations are likely to occur in the 96 SRW plates under the shaking conditions used here, making mass transfer more reliant upon diffusion forces in this case. This can be better observed if these results are compared to those obtained in a 96 DSW plate, as shown in Figure 3.4.

During oxygen limited fermentations alternative electron acceptors such as nitrate, fumarate, or dimethylsufoxide are used. Mixed–acid fermentation, where pyruvate acts as the final electron acceptor, occurs if no alternative electron acceptors are available (Cotter et al., 1992). This results in the production of compounds such as acetate, formate and succinate (Lee, 1996) and explains why both growth curves have two different slopes. The first growth rate, for both fermentations, reached its highest point after 1 hour of fermentation, after this point oxygen limitation could have induced a mixed acid fermentation; this change is gradual and while some cells have been oxygen deprived before this point, others may still have an aerobe metabolism even after this point was reached as the fermentation was carried out in open wells. The complete change from aerobic to anaerobic can take as much as 9 hours if no oxygen is supplied (O'Bairne and Hamer, 2000). *E. coli* has a lower growth rate in its anaerobic metabolism, as can be appreciated in the second part of growth, achieving only a difference of $\approx$ 0.4 $g.l^{-1}$ in biomass after 2 hours of fermentation. Gernot et al. (2003) attempted fermentations of *C. glutamicum* ATTC 21253 using these microwell plates and FluoStar Optima microwell plate reader as incubator. They found that and dissolved oxygen dropped to zero value rather quickly, as seen in this work.

3.4.3 Illustration of high throughput potential

The previous section demonstrated that the 96 SRW BD oxygen sensing plates have poor oxygen transfer capacity. However, they have the significant advantage that both optical density and fluorescence can be measured *in situ* during fermentations without the need to remove samples. To illustrate the potential of the microwell approach for high throughput fermentation process development, *E. coli* TOP10 [pQR239] fermentations were carried out in the 96 SRW BD oxygen sensing plates.

Figure 3.10 shows various graphs of kinetic data of parallel cell growth and DOT profiles for a series of *E. coli* TOP10 [pQR239] fermentations performed at different carbon source concentrations (Rows A and B), and inoculum levels (Columns 1 to 3). The growth rates for the fermentations carried out at 5 $g.l^{-1}$ of glycerol are 1.68 ± 0.07 h^{-1} for 1% inoculum, 1.67 ± 0.08 h^{-1} for 2.5% inoculum and 1.36 ± 0.06 h^{-1} for 5% inoculum, while the growth rates for the fermentations carried out at 10 $g.l^{-1}$ of glycerol are 1.66 ± 0.06 h^{-1} for 1% inoculums, 1.65 ± 0.07 h^{-1} for 2.5% inoculum and 1.38 ± 0.05 h^{-1} for 5% inoculum. The carbon source concentration made no significant difference to the growth rate, but the initial inoculum concentration was seen to be a relevant factor, as demonstrated previously in Section 3.4.2. Growth rates using 1 and 2.5% inoculum concentrations were similar while the growth rate at 5% was slightly slower. However, all growth rates were artificially high, as observed in Section 3.3.1.

DOT levels in all cases are seen to fall to zero at a rate that increases with inoculum concentration. The corresponding growth curves show two distinct growth rates. The latter one, which begins shortly after DOT = 0, is approximately constant for each fermentation signifying oxygen limited culture conditions. Given the significantly lower k_La values of 96 SRW plates of ≈ 36 h^{-1} (0.01 s^{-1}) (Doig et al., 2005), it is not surprising that the rapidly growing *E. coli* cultures quickly become oxygen transfer limited in these particular experiments.

While the oxygen sensing plates have clear advantages for parallel operation and simultaneous collection of both growth data and oxygen uptake kinetics of the culture, the oxygen limited culture conditions make them unsuitable for bioprocess studies, especially for scale-up purposes. Consequently all subsequent work was performed in 96 DSW plates, already shown to support higher density culture conditions (Sections 3.3.1 and 3.3.2).

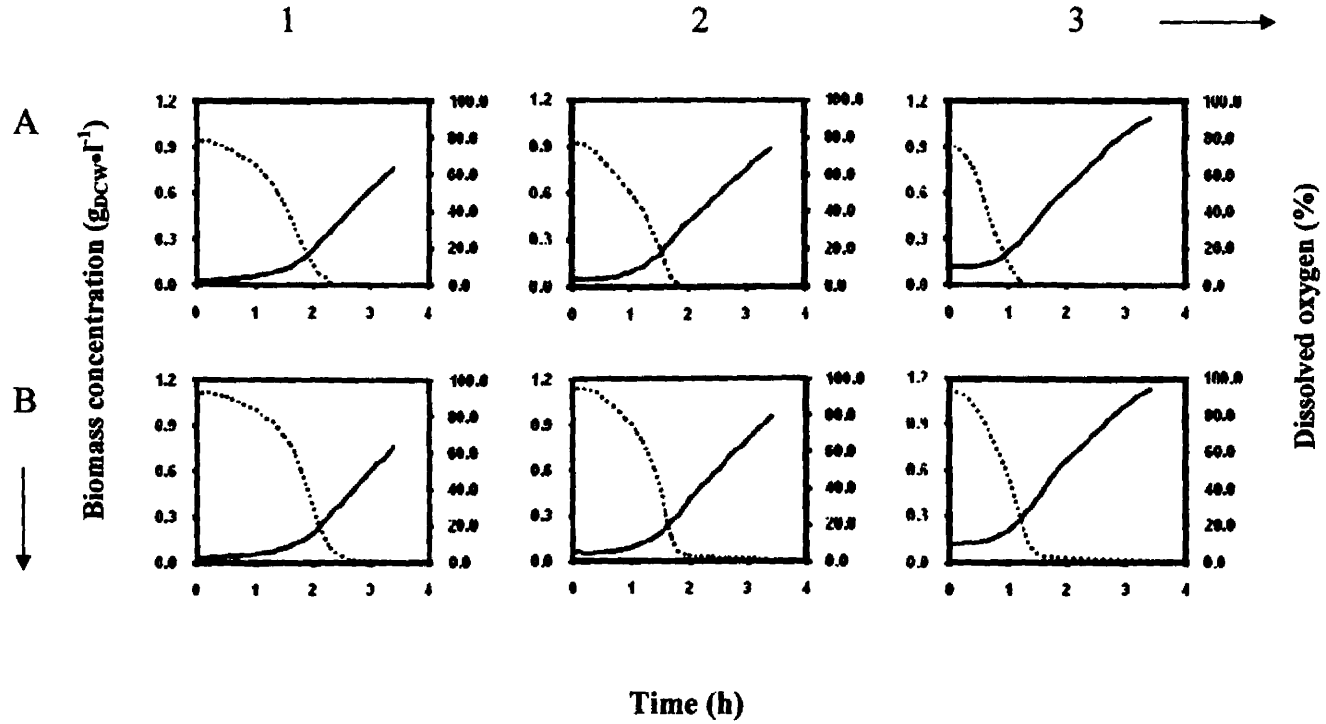

Figure 3.10 Parallel batch fermentation kinetics of *E. coli* TOP10 [pQR239] in standard 96 round bottomed microwell plates with integrated dissolved oxygen sensing using a FluoStar Optima microwell plate reader as incubator. This figure shows selected data from 96 parallel fermentations performed at different initial carbon source and inoculum concentrations: (Row A) 5 $g.l^{-1}$ glycerol, (Row B) 10 $g.l^{-1}$ glycerol, (Column 1) 1% v/v inoculum, (Column 2) 2.5% v/v inoculum, (Column 3) 5% v/v inoculum. Smooth lines represent biomass dry cell weight data; dotted lines represent Dissolved Oxygen data. Experiments were performed as described in Section 2.6.1.4.

3.5 Microscale bioconversion process characterisation

3.5.1 Substrate and product evaporation rates

Experiments in the previous sections have focused on production of the whole cell *E. coli* TOP10 [pQR239] biocatalyst. In this section the CHMO activity of the biocatalyst is considered. As with the evaporation of water during fermentation, previously considered in Section 3.3.4, it is important here to also consider the evaporation of the reaction substrate and product during the bioconversion time course.

The reaction substrate, bicycloketone, and the reaction lactone products, are uncharged, low molecular weight, organic compounds. The bicycloketone is a liquid at room temperature and has the molecular formula of C_7H_8O with a molecular weight of 108. The lactone products are regioisomers and have the molecular formula of $C_7H_8O_2$, each with a molecular weight of 124. The lactone products are not commercially available, but the enantiomer of (1S,5R)-2-oxabicyclo[3.3.0]oct-6-en-3-one can be purchased from Fluka. This enantiomer was then used as a reference in substitution of the other two isomers; (1R,5S)-2-oxabicyclo[3.3.0]oct-6-en-3-one is a white solid with a melting point of 45-47 °C and a purity > 99%.

The bicycloketone substrate and bicyclolactone were analysed throughout this work by GC, as described in Section 2.3.1. The bicycloketone had a retention time on the GC column of 6.3 minutes and was visualised as a single peak on the chromatogram. The bicyclolactone products were visualised as two unseparated

peaks on the chromatogram with a retention time on the GC column of 13.4 minutes (Appendix III). Throughout this work the concentration of the bicyclolactone products were combined in order to give a total value for the product concentration.

The solubility of the bicycloketone in water is 15.2 ± 0.1 $g.l^{-1}$ and the solubility of the bicyclolactone in water is 49.6 ± 0.1 $g.l^{-1}$ (Lander, 2002). The initial rate of evaporation of bicycloketone aqueous solution of 1 $g.l^{-1}$ was determined to be 16.2 $mg.l^{-1}.min^{-1}$; however, from a concentration of the aqueous solution of 0.5 $g.l^{-1}$ bicycloketone the evaporation rate was greatly reduced to 5.1 $mg.l^{-1}$ indicating that a higher initial concentration of bicycloketone in the aqueous solution will generate a higher evaporation rate of the substrate. The initial rate of evaporation of bicyclolactone was determined to be 2.3 $mg.l^{-1}.min^{-1}$ (Figure 3.11). Further experiments were carried out at an initial aqueous concentration of 0.5 $g.l^{-1}$ of bicycloketone, to avoid high levels of substrate evaporation; this is also in keeping with Doig et al. (2003) assessment that at substrate concentrations higher than 0.5 $g.l^{-1}$, bicycloketone becomes toxic for the cells.

3.5.2 Effect of liquid fill volume

Bioconversions using whole cell *E. coli* TOP10 [pQR239] as biocatalyst have previously been reported in 96 DSW plates by Doig et al. (2002). In this early work; however, the cells were harvested and then resuspended in a buffer solution. For the work described in this thesis the ultimate aim was to carry out the bioconversion as part of a process sequence comprising three stages: fermentation, characterised by the addition of inoculum; induction, characterised by the addition of 10 µl of 15% v/v L-arabinose as inducer, and bioconversion, characterised by the addition of bicycloketone substrate. Consequently the bioconversion here was

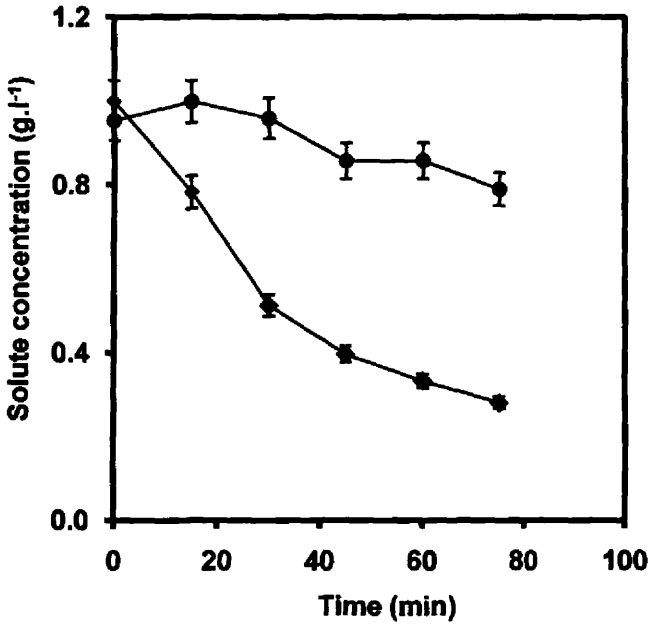

Figure 3.11 Evaporation rate of bicycloketone (♦) and bicyclolactone (●) from a 96 DSW plate with a fill volume of 1 ml. The initial concentration of bicycloketone and bicyclolactone was 1.0 $g.l^{-1}$. Measurements were performed at 30°C and 1000 rpm, as described in Section 2.3.1. Error bars represent the range of measured values about the mean.

carried out in the fermentation broth. The effect of working volume on the bioconversion was studied, using 96 DSW plates, with bioconversion conditions of 1 $g.l^{-1}$ initial bicycloketone concentration, 37°C and 1000 rpm. This high substrate concentration was chosen as it would lead to the highest initial rates of evaporation and therefore impact most significantly on quantification of bioconversion kinetics.

The reaction (Figure 1.2) is stoichiometricaly equal, meaning that the ratio of bicyclolactone product formed to the initial amount of substrate is very close to 1. Figure 3.12 shows the bioconversion kinetics of bicycloketone at three different fill volumes. The initial Rate of Product Formation (RPF) using 1000 µl as working volume inside the well was 34.0 ± 1.9 $\mu mol.l^{-1}.min^{-1}$. However, a working volume of 500 µl had a RPF of 45.5 ± 2.1 $\mu mol.l^{-1}.min^{-1}$, while a working volume of 200 µl had a RPF of 42.1 ± 2.4 $\mu mol.l^{-1}.min^{-1}$. These rates are comparable to those reported by Doig et al. (2002). The reactions were operated for up to 60 minutes and while bicycloketone had reached zero after 40 minutes they did not achieve 100 % conversion as bicyclolactone did not reach 1 $g.l^{-1}$. This can be explained by considerable evaporation of the bicycloketone (Section 3.5.1).

Doig et al. (2002) established that to produce 1 mol of lactone product, 6.91 mol of oxygen were required, therefore bioconversion stages will require a supply of oxygen far higher than that of a fermentation in order to be carried out. As explained in Section 1.3.6, mass transfer is microwell plates is highly dependent on fill volume to control the levels of oxygen transfer, therefore to allow higher levels of oxygen transfer in the wells, the fill volume was reduced for bioconversion reactions.

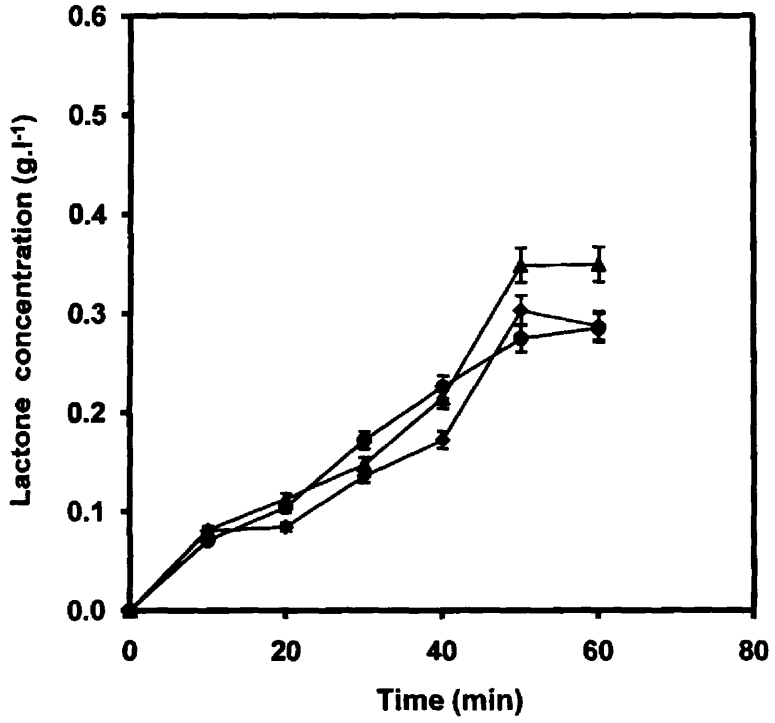

Figure 3.12 Effect of liquid fill volume on whole cell *E. coli* TOP10 [pQR239] bioconversion kinetics. The bioconversion was carried out in 96 DSW using an initial concentration of 1 $g.l^{-1}$ bicycloketone within each well, 30°C and 1000 rpm. Three different volumes were explored, 1000 µl (♦), 500 µl (▲) and 200 µl (•). Experiments performed as described in Section 2.6.1.5. Error bars represent the range of measured values about the mean.

3.5.3 Effect of temperature and substrate concentration

Doig et al. (2003) studied the influence of temperature on the bioconversion and at which BVMO has the highest specific activity using an initial concentration of bicycloketone of 0.5 $g.l^{-1}$. They investigated a range of temperatures between 20°C and 45°C. They found that BVMO had a broad optimum temperature range at which activity would be highest. Temperatures ranging from 28 to 37 °C were found to have an approximate constant specific CHMO activity; while the highest activity was found at 37 °C the drop of activity from this temperature onwards was steep and sudden. The temperature across microwell plates is not always homogenous by about 1 degree, and a temperature that allowed more stable conditions and control across the plate was chosen. Bicycloketone also becomes toxic to cells at higher concentrations. According to Doig et al. (2003), there is significant inhibition of the bioconversion at reactant concentrations above 0.2 to 0.5 $g.l^{-1}$.

Based on these findings, in order to optimise the bioconversion stage of the process and to achieve a high rate of product formation, and to overcome evaporation (Figure 3.11), experiments were carried out using a lower temperature of 30°C during the bioconversion stage and a lower initial concentration of bioconversion substrate, 0.5 $g.l^{-1}$ within each well. These conditions were tested at two different working volumes: 500 and 1000 µl.

Bioconversion was carried out using ≈ 5 $g.l^{-1}$ biomass concentration and a shaking speed of 1000 rpm. Figure 3.13 shows that lower working volumes produce better bioconversion performance due to the increased efficiency of oxygen mass transfer (Duetz et al., 2001). After 60 minutes the bioconversion achieved a 92% w/w

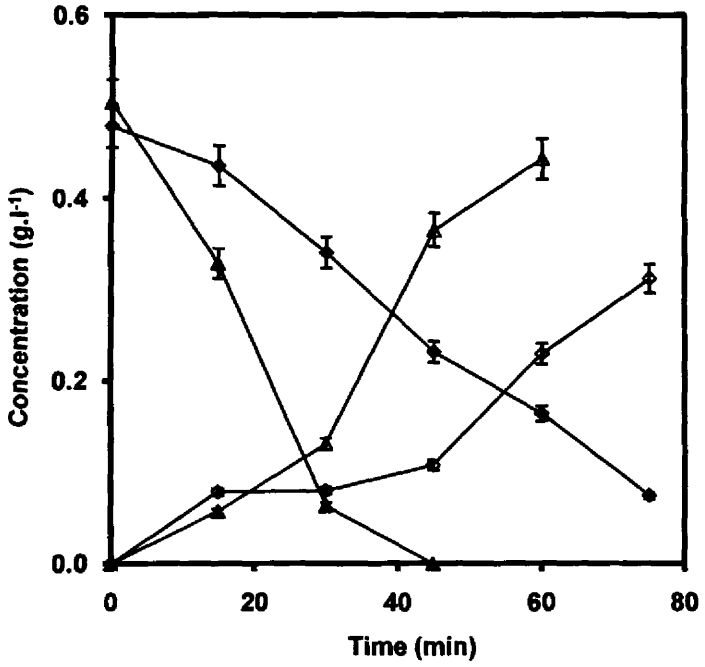

Figure 3.13 Effect of initial bicycloketone concentration and temperature on whole cell *E. coli* TOP10 [pQR239] bioconversion kinetics. The bioconversion was carried out using 0.5 $g.l^{-1}$ of bicycloketone within each well at 30°C and 1000 rpm. The solid symbols represent the bicycloketone utilisation kinetics, while the open symbols represent the bicyclolactone. Two different volumes were tested, 500 µl (▲) and 1000 µl (♦). Experiments performed as described in Section 2.6.1.5. Error bars represent the range of measured values about the mean.

conversion, a RPF of 72.4 ± 3.6 μmol.l^{-1}.min^{-1} and a specific activity (SA) of 16.2 ± 0.5 U.g_{DCW}^{-1} in the case of 500 μl, while at a fill volume of 1000 μl only reached 60% conversion, a RPF of 30.9 ± 1.6 μmol.l^{-1}.min^{-1} and a SA of 7.5 ± 0.3 U.g_{DCW}^{-1}. At lower initial concentrations of bicycloketone, cells are more likely to take in and convert the substrate, which is less likely to evaporate, also higher transfer rates promoted higher conversion rates as there was enough oxygen supply for the oxidative reaction. This compares well with the findings of Doig et al. (2002) as they calculated an specific activity of 30 U.g_{DCW}^{-1} for the conversion of bicycloketone into its corresponding bicyclolactone product using 8 g.l^{-1} biomass concentration of *E. coli* TOP10 [pQR239] as whole cell biocatalyst. Subsequent bioconversions were carried out at 30 °C and 0.5 g.l^{-1} initial bicycloketone concentration, with a working volume in the well of 500 μl unless stated otherwise.

3.6 Dry cell weight estimation at the microwell scale

Throughout this work optical density measurements were used as a surrogate measure of biomass concentration using a calibration curve. Microwell plate spectrophotometers are designed to work with clear bottom plates, such as the 96 Standard Round Well plate, and with a similar height to the 96 SRW of approximately 10 mm. Taller or not clear wells cannot be directly measured with such devices and hence samples must be taken to be measured off line for growth and biomass concentration; however, the sampling volumes of microwell plates are small and indirect ways of measuring biomass content must be devised. Such is the case for calibration curves of biomass against the optical density values measured in such microwell plate readers.

Optical density (OD) measurements are based on the Beer – Lambert law. Lambert's law states that the proportion of radiant energy absorbed by a substance is independent of the intensity of the incident radiation. Beer's law states that the absorption of radiant energy is proportional to the total number of molecules in the light path. Beer's law describes the basic relationship between the concentration of the absorbing substance and the measured value of absorbed radiation. The amount of radiation absorbed by a substance cannot be measured directly and it is usually determined by measuring the difference in intensity between the radiation falling on the sample and the residual radiation which finally emerges from the sample (Holm and Peck, 1998). The combination of both laws is known as the Beer-Lambert law usually used in UV-visible absorbance spectophotometry. It is characterised by Equation (3.2):

$$A = \epsilon c l \qquad \text{[Eq. 3.2]}$$

Where A is the absorbance, c is the concentration of the substance, ϵ is the extinction coefficient for the substance, l is the light path in cm. Absorbance values can be translated into concentration values by determining the mass extinction coefficient. From a stock solution, a series of accurate dilutions are prepared and the absorbance of each dilution is measured at the required wavelength. A plot of absorbance against concentration will give an indication of the validity of the Beer-Lambert relationship for the compound and the absorption coefficient may be calculated from the slope of the linear portion of the graph.

Biomass concentration is one of the most important measurements in fermentation and cell culture studies. Biomass concentration is typically measured by one of two off-line methods, wherein a small sample of the fermentation broth is extracted from the bioreactor.

- Total Cell Density (TCD): Counting the number of cells within a known volume of sample. In this process, the number of cells can be counted either by successively diluting the original sample and plating on a Petri dish, with the help of a microscope and a counting chamber, or with an automated cell counter such as a Coulter counter or a flow cytometer. The plating method detects viable cells; whereas, the automated cell counters detect the total number of cells. This value is typically reported in units of M cells.ml^{-1} (millions of cells/millilitre). This method requires a substantial investment in time or expensive equipment (Prescott et al., 2004).

- Cell Weight (CW), which can be either dry cell weight (DCW) or wet cell weight (WCW), involved weighing the cells in a known volume of sample. In this process, the cells in a sample are separated from the broth and weighed while they are wet, or the cells may be thoroughly dried before weighing. The dry weight measurement usually gives a much more consistent result than the wet weight. This value is typically reported in units of g.l^{-1} (grams/litre) (Prescott et al., 2004).

Both of these methods can be difficult and unreliable. Both are also susceptible to operator error in dilution or evaluation/counting and neither method provides real-time information for process control. For example, dry/wet weight methods and automated counting equipment fail completely if the broth contains other insoluble particulate matter, which is often the case in industrial fermentation media. Furthermore, cell weight methods cannot distinguish the viable cells from the dead ones. On the other hand, the standard plate count can detect viable cells among other particulate matters. However, the method requires elaborate preparations, and it takes 24-48 hours for the cells to be incubated and counted (Prescott et al., 2004). Consequently, the utility of direct plate count is limited for feedback control of a fermentation process.

Particulate objects such as bacteria scatter light in proportion to their number. The turbidity or optical density of a suspension of cells is directly related to cell mass or cell number, after construction and calibration of a standard curve. The method is simple and nondestructive, but the sensitivity is limited. The correlation of absorption to dry weight is very good for dilute suspensions of bacteria, and this relationship seems to hold regardless of cell size. In more concentrated suspensions this correlation (absorption to dry weight) no longer holds (Koch, A. 1970).

As there are several factors that can affect an optical density calibration curve (quality of lamp output, size of slit, condition of filter, condition of detector, microorganism characteristic, etc) this calibration should be confirmed every time the conditions of the assay change. Despite the inherent inaccuracy of the method, if the procedure is adequately controlled and calibrated the estimation of microbial numbers by optical density is sufficiently accurate for use in preparing inoculum for QC testing and offers the overwhelming advantages of being rapid, low cost and non-destructive.

The turbidity of a culture is dependent upon the shape and internal light-absorbing components of the microorganism and therefore turbidity readings are species-specific and cannot be compared between different microbes or even between different strains of the same species. There are microbes that change cell size or shape at different stages of growth, which introduces some inaccuracy to this method of cell counting. Also both living and dead cells scatter light and are therefore counted. However, the method is very rapid and simple to perform and provides reliable results when used with care, so it is an extremely common method of real time analysis of prokaryotic populations. Care must be taken however to take into consideration changes in the cell during such cell changes and measure the changes in optical density when cell morphology changing events occur.

In most applications however, the simplest off-line method for estimating cell density is to monitor the optical density of the sample. Optical density and cell density readings can be related by a set of calibration curves that are generated from several bioreactor runs (Turner et al., 2003). Once optical density measurements are mapped to biomass values, optical density readings can provide useful feedback immediately. While OD_{600} provides a simple and rapid method for determining cell density, it has significant disadvantages at high cell concentrations. This method is extremely dependent on both the sampling and manual dilution techniques therefore the dilution method often becomes the governing parameter in determining the error of the off-line OD_{600} value, higher dilution levels result in greater error; however the dilution rates used in this work was up to ten. Still the more reliable method for cell mass determination is dry cell weight (DCW).

There are several commercial *in situ* probes for the online measurement of cell growth, but while they are available they are not compatible with microwell plate work. Also, these probes have problems as biomass and protein build-up on the probe tip plagues most on-line in-situ cell mass sensors and susceptible to bubble interferences and surface fouling, they can influenced by aeration and agitation conditions (Junker et al., 1994).

Despite the known setbacks of the optical density method bioprocess design and bioprocess miniaturisation research largely employs this method ((Duetz et al., 2001; Doig et al., 2002, 2005). Weuster-Botz et al. (2005) estimated dry cell mass of *E. coli* BL21(DE3)-pLysS from OD_{650} measurements making use of a second order polynomial function allowing a measuring range of undiluted samples between 0.16 and 1.74 OD_{650} units with a linearity R^2=0.995 while developing milliliter scale devices for high-throughput bioprocess design. It is important to notice that they considered measurements closer to an optical density value of 2 to be still accurate and representative and thought they maintained a linear relationship

between optical density and biomass concentration. This is a relevant difference to the work presented here, where the linearity of the values were kept under more traditional optical density values of up to 0.8.

There are many reported absorbance-based assays used to assess microorganism growth; there are some studies where results are often based directly on recorded absorbance fluctuations (Das et al., 1998; Pitts et al., 2003; Turcotte et al., 2004). Such methods predict the bioactive effect of a sample accurately if biomass growth trends share a linear relationship with absorbance/turbidity fluctuations, or if efforts are made to linearise the relationship, or work within a linear region of response. Casey et al. (1998) required a method that allowed the conversion of turbidity values from microtiter plate wells to biomass concentrations in order to accurately determine the bioactive effect of a sample from turbidity data. They achieved this by using biomass conversion standard curves established for all their test organisms. This method was also used by Amanullah et al. (2002, 2003) to monitor the fed-batch bioconversion of indene to *cis*-indandiol using *Rhodococcus* I24 and asses the substrate and product effect on the membrane integrity using multiparameter flow cytometry. Stone et al. (1992) found little variation between using a whole sample for the measurement of dry cell weight or using only a fraction of the sample for this purpose.

Although it would be ideal to measure the biomass concentration using DCW measurements, in this work the volume of the samples that can be acquired from a well (<0.8 ml) is too small to reliably measure DCW. Whilst using more than one well to make a sufficient sample would seriously compromise the throughput of experiments, thus detracting from the overall goal of the project.

3.7 Summary

As stated in Section 3.1, the aim of this chapter was to establish microscale fermentation and bioconversion methodologies and to optimise conditions to facilitate the highest growth rates and bioconversion yields using whole cell *E. coli* TOP10 [pQR239]. The key findings are summarised below.

- A microwell fermentation process using *E. coli* TOP10 [pQR239] has been established (Section 3.3) and the work presented here has gone some way toward enabling parallel fermentation optimisation.

- Optimal conditions for microwell fermentation in terms of the highest biomass concentration and fastest growth rates were found using the 96 DSW plate geometry, incubated at 37 °C and shaking at 1000 rpm, using a fill volume of 1000 µl and 5% v/v inoculum. This well geometry appears to provide the best compromise between liquid fill volume (to provide enough material for sampling) and experimental throughput.

- The use of commercially available 96 SRW plates for parallel on line monitoring of biomass growth kinetics and DOT levels has also been illustrated. However, due to the limitations in the oxygen mass transfer capacity of this microwell format these plates were deemed unsuitable for further bioprocess studies.

- Optimal conditions for the whole cell bioconversion of bicyclo[3.2.0]hept-2-en-6-one (bicycloketone) in 96 DSW plates, using *E. coli* TOP10 [pQR239] as biocatalyst were found to be 500 µl fill volume in each well at a temperature of 30 °C during the biocatalysis stage and an initial

bicycloketone concentration of 0.5 $g.l^{-1}$. These conditions allowed experimental product formation rates of up to 72.4 $\mu mol.l^{-1}.min^{-1}$ and specific activity of 16.2 $U.g_{DCW}^{-1}$, comparable to previously published work (Doig et al., 2002) in 2 l stirred bioreactors.

All of the work presented in this chapter has focused on establishing the microwell experimental methodologies and has been largely performed manually. The advantage of the microwell approach is that it can easily be automated using a variety of laboratory robotic platforms (Lye et al., 2003). In Chapter 4, the automation of these methods is considered along with the linked operation of fermentation and bioconversion in a micoscale process sequence.

4.0 Parallel microscale process sequences: fermentation, bioconversion and biocatalyst recovery

4.1 Aims of the chapter

In Chapter 3, the basic microwell methodologies were established for performing fermentations and bioconversions using *E. coli* TOP10 [pQR239] as a whole cell biocatalyst. As mentioned in Section 1.4, the aim of this chapter was to establish automated microscale process sequences for the operation of linked fermentation, bioconversion and primary product recovery stages and to apply these to a focused library of whole cell CHMO biocatalysts. Specific objectives were to:

- Examine the accuracy and reproducibility of microscale data collection for the quantification of fermentation and bioconversion process kinetics.
- Illustrate the potential of the established microscale methods to quantitatively discriminate between the performance of a small library of different whole cell CHMO biocatalysts in automated fermentation-bioconversion process sequences.
- Extend the automated microscale process to include analysis of different unit operations for primary product recovery and biocatalysts removal.

As described in Section 2.6, three different strains were used for this work, *E. coli* TOP10 [pQR239], *E. coli* JM107 [pQR210] and *A. calcoaceticus* NCIMB 9871 each expressing cyclohexanone monoxygenase (CHMO). Each strain was used in combination with three different ketone substrates: bicyclo[3.2.0]hept-2-en-6-one (bicycloketone), cyclohexanone and cyclopentanone. The utility of each host strain

was investigated in an automated sequence of operations comprising fermentation, enzyme induction and bioconversion. Additionally microscale filtration and centrifugation steps were evaluated as primary steps for biocatalyst recovery.

The majority of the results presented in this chapter have previously been published as: C. Ferreira-Torres, M. Micheletti and G. J. Lye "Microscale process evaluation of recombinant biocatalyst libraries: application to Baeyer–Villiger monooxygenase catalysed lactone synthesis" *Bioproc. Biosyst. Eng.* (2005) **28**, 83 – 93.

4.2 Microscale processes calculations and evaluation

4.2.1 Automation of microscale processing techniques

As explained in Section 1.2.5, automation of microscale processing techniques can reduce labour intensity and enable a wider range of process variables to be examined in a given time. A key aspect of microscale processing is the use of laboratory liquid handling robots to reduce error and increase throughput. The small volumes used with microwell formats also optimise the use of often scarce and expensive chiral pharmaceutical intermediates.

The equipment used for this study was a Perkin Elmer Multiprobe II EX liquid handling robot (Figure 4.1). This system had four washable, independent fixed tips to handle different liquids and could dispense from 500 nl to 5 ml. These could be fitted with disposable tips, able to handle volumes from 500 nl to 150 µl to eliminate cross contamination. The error in the accuracy and precision of all liquid additions was expected to be less than 5% based on previous optimisation of the robot's performance files (Nealon et al., 2005). Each tip has a liquid level sensor incorporated at its end. Liquid transfers can be performed in a multi-tipped mode

from many combinations of laboratory containers including 24, 96 and 384-well. The robot was controlled by a PC with the WinPREP software supplied by the manufacturer.

Several custom programs were created using the software provided. Each program controlled an individual stage of the microscale process. Details of the individual programs can be seen in Appendix IV, while the steps involved in the overall programme can be seen in Figure 4.2.

Figure 4.1 The Multiprobe II EX liquid handling robot from Perkin Elmer and the Packard Instrument Company (Meriden, Connecticut, US). Image obtained from the Advanced Centre of Biochemical Engineering (ACBE) facilities in UCL. In this picture the robot is dispensing liquids into a 96 SRW plate using disposable tips.

Figure 4.2 Illustration of the WinPrep programme used to perform the microscale fermentation and bioconversion sequence described in Section 4.2.1. The left hand window illustrates the timed sequence of events involved in setting up the experimental protocol and shows user prompts at key stages in the process. The right hand window shows the deck layout used and the different labware geometries that can be addressed.

4.2.2 Quantitative analysis of process performance

The process parameters chosen to characterise the microscale fermentation processes presented in this work were:

i. Maximum specific growth rate.
ii. Final biomass concentration.

Those used to characterise the bioconversion processes were:

i. Initial rate of lactone product formation.
ii. Specific CHMO activity.
iii. Final bioconversion yield (% w/w).

According to Monod's model, maximum growth rate or μ_{max} is measured in h^{-1} and is defined as "a first order autocatalytic reaction" by Doran (1995); it is measured during fastest cell division or mass increment. The final biomass concentration is an indication of the yield of biomass on substrate ($Y_{X/S}$) and the amount of whole cell biocatalyst produced. Together, these parameters will facilitate an assessment of the performance of the different CHMO host strains during fermentation.

The initial rate of lactone (product) formation is defined as the micromoles of product formed at a given time per volume of bioconversion medium ($\mu mol.l^{-1}.min^{-1}$) (Doig et al., 2002). The specific activity is defined as the rate of reaction multiplied by the volume of reaction per unit mass of whole cell biocatalyst ($U.g_{DCW}^{-1}$). Bioconversion yield was calculated as a ratio based on the concentrations of lactone and ketone determined after a fixed bioconversion period of 90 minutes.

Quantification of all five of these parameters was considered necessary to give an accurate indication of how both the fermentation and bioconversion stages impact on the whole process performance for each of the different host strains. This would

enable discrimination between several process scenarios, such as slow growth or low biocatalyst concentration but high specific activity versus fast product formation, or high biocatalyst concentration but low specific activity.

4.2.3 Reproducibility of microscale fermentation and bioconversion

Reproducibility studies were first carried out with the model process involving the fermentation of *E. coli* TOP 10 [pQR239] with 10 $g.l^{-1}$ of glycerol as carbon source and induction of CHMO activity three hours after inoculation, as described in section 2.6.1.3 and 2.6.1.5. Each fermentation was followed by a bioconversion stage using an initial concentration of bicycloketone of 0.4 $g.l^{-1}$. Therefore, the reproducibility of the linked fermentation and bioconversion stages was assessed.

Figure 4.3 shows representative profiles of replicate *E. coli* TOP10 [pQR239] fermentations carried out in 96 DSW plates. Apart from some differences in initial inoculum levels and lag phase duration, all the growth curves showed similar kinetics during the exponential phase and similar final biomass concentrations. For the five fermentations shown, the growth rate was calculated to be 0.53 ± 0.05 h^{-1} and the mean biomass concentration at the end of the fermentation was 5.6 ± 0.2 $g.l^{-1}$. Standard deviations of this magnitude are generally considered acceptable for microbial fermentations.

Figure 4.4 shows representative profiles for the bioconversion of bicyclo[3.2.0]hept-2-en-6-one by *E. coli* TOP10 [pQR239] in 96 DSW plates at a relatively low initial substrate concentration of 0.4 $g.l^{-1}$. The results show excellent agreement between the three data sets. The mean initial rate of lactone formation was calculated to be 115 ± 3.5 $\mu mol.l^{-1}.min^{-1}$ while the final bioconversion yield was 89 ± 2 % w/w. The profiles shown in these figures were obtained using different batches of cells grown independently on different dates. They thus

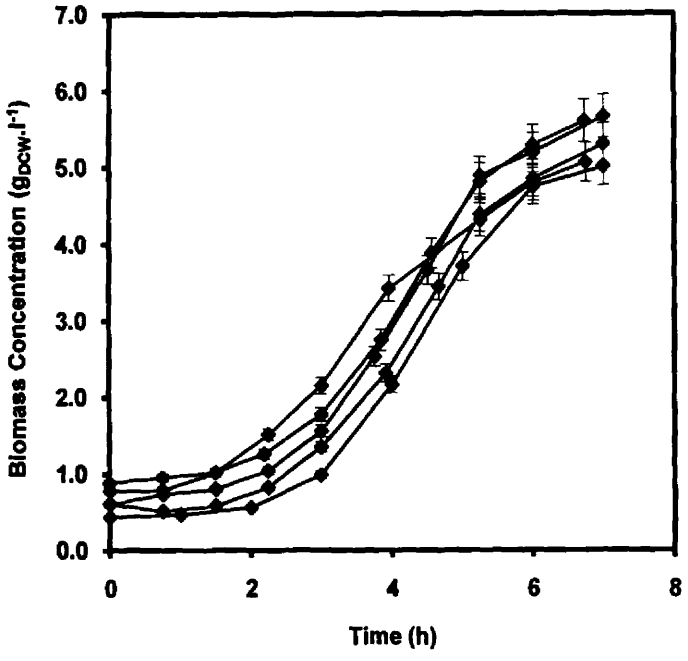

Figure 4.3 Reproducibility of independently replicated *E. coli* TOP10 [pQR239] batch microscale fermentations in a 96 DSW plate. All fermentations were induced by addition of L-arabinose 15% w/v three hours after inoculation. Experiments performed as described in Section 2.6.1.3 and 2.6.1.5. Error bars represent the range of measured values about the mean.

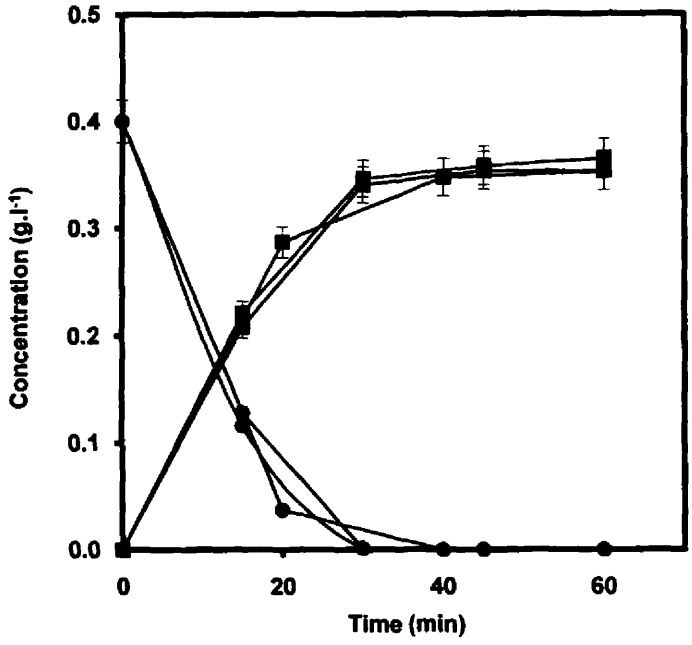

Figure 4.4 Reproducibility of independently replicated bioconversion kinetics of bicyclo[3.2.0]hept-2-en-6-one in 96 DSW plates using *E. coli* TOP10 [pQR239] as whole cell biocatalyst. Bioconversions were carried out at an initial ketone concentration of 0.4 $g.l^{-1}$: ketone depletion (●) and lactone formation (■). Experiments performed as described in Section 2.6.1.3 and 2.6.1.5. Error bars represent the range of measured values about the mean.

demonstrate quantitative reproducible data can be consistently achieved.

Figure 4.5 shows the reproducibility of bioconversion performance across the wells on a single microwell plate. Ten microwells were used under similar conditions and were harvested after 15 minutes into the bioconversion stage in order to measure both bicycloketone and bicyclolactone concentrations. Similar concentrations of bicycloketone and lactone were measured across the plate. The product formed during this time was on average 0.18 ± 0.02 $g.l^{-1}$. These results demonstrate the validity of "sacrificial well" approach described in Section 3.3.1, and the absence of significant variations across wells.

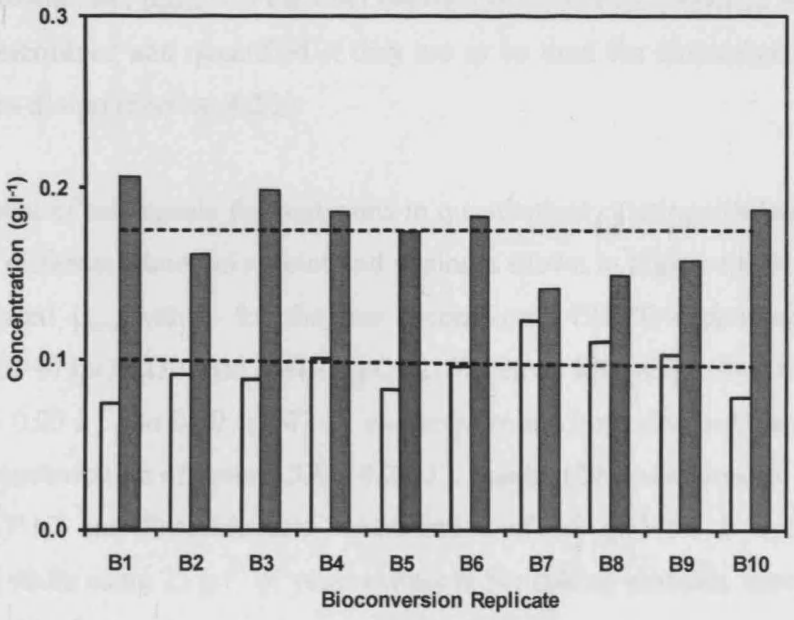

Figure 4.5 Reproducibility of bioconversion kinetics (past fermentation) across a single 96 DSW plate. After fifteen minutes of bioconversion the average bicycloketone concentration (□) remaining across the plate was 0.1 ± 0.015 $g.l^{-1}$, while the average bicyclolactone (■) produced was 0.18 ± 0.02 $g.l^{-1}$. The error in product formation was of 12%. Experiments performed as described in Section 2.6.1.5. Dashed lines indicate the mean for ketone and lactone concentrations.

4.3 Evaluation of different CHMO host strains

4.3.1 Microscale fermentation

The first stage of the overall process sequence involves production of the various whole-cell biocatalyst by aerobic fermentation. Whole cell biocatalyst growth kinetics and yields are well known to be species and strain dependent and to be affected by a number of factors, in particular the type and concentration of the main carbon and energy source and the minimum dissolved oxygen tension, DOT, reached during cell growth (Doran, 1999). Here, parameters such as the maximum specific growth rate, μ_{max}, and the final biomass concentration obtained need to be reliably determined and quantified if they are to be used for biocatalyst selection and process design (Section 4.2.2).

The potential of microscale fermentations to quantitatively distinguish between the growth of different microbial species and strains is shown in Figure 4.6. In this case the calculated μ_{max} values for the two recombinant CHMO-expressing *E. coli* strains, TOP10 [pQR239] and JM107 [pQR210], grown in glycerol-limited cultures are 0.53 ± 0.05 h^{-1} and 0.30 ± 0.07 h^{-1} respectively and both strains achieve a final biomass concentration of around 5.8 ± 0.2 $g.l^{-1}$. Lander (2001) determined a growth rate of 0.7 h^{-1} and final biomass concentration of 7.9 $g.l^{-1}$ for *E. coli* TOP10 [pQR239] while using 25 $g.l^{-1}$ of yeast extract in her culture medium, instead of the 10 $g.l^{-1}$ used in this work.

The wild-type *A. calcoaceticus* NCIMB 9871 grown in monosodium glutamate and cyclohexanol-limited culture, grew approximately ten times slower displaying a μ_{max} of 0.043 h^{-1} and only reached a final biomass concentration of 4.6 $g.l^{-1}$ after 92 hours (Figure 4.6). The final biomass concentration obtained for *A. calcoaceticus* is comparable to that found previously by Barclay (2001) in shake flasks using the

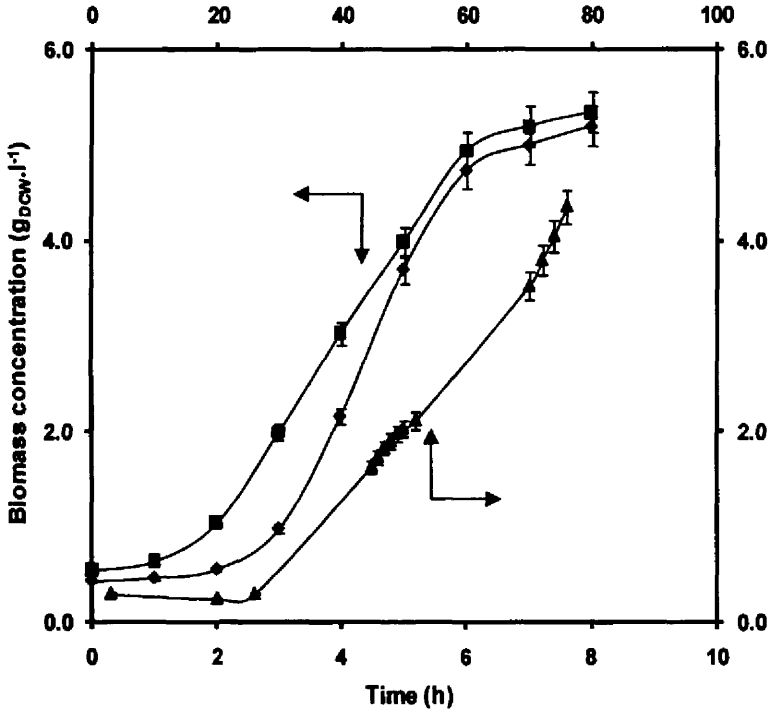

Figure 4.6 Comparative growth kinetics of different CHMO whole cell biocatalysts: *E. coli* TOP10 [pQR239] (♦), *E. coli* JM107 [pQR210] (■), *A. calcoaceticus* NCIMB 9871 (▲). Experiments performed as described in Sections 2.6.1.3, 2.6.2.2 and 2.6.3.2 respectively. *E. coli* TOP10 [pQR239] was induced by addition of L-arabinose 15% w/v three hours after inoculation. Error bars represent the range of measured values about the mean.

same medium formulation.

During fermentations of *A. calcoaceticus* NCIMB 9871, due to the length of time required for its growth, different mechanisms to cover the microwell plate to avoid evaporation and cross contamination while allowing high oxygen transfer were tested, such cotton wool caps, parafilm and gas permeable adhesive seals (Art. No. AB-0718, Abgene, Hamburg, Germany). However, they were found to reduce oxygen permeation (Zimmermann et al., 2003) as there was little or no growth of cells. These covers also increased the likelihood of contamination as condensation droplets formed on the interface between the well and the cover. The covers did not prevent evaporation and 24 hours after inoculation the wells had significant volume loss. Consequently *A. calcoaceticus* NCIMB 9871 fermentation was finally carried out in glass shake flasks and not microwells due to this and other constrains. This strain required regular additions of cyclohexanol which acted as both carbon source and inducer; cyclohexanol is highly volatile thus impeding the use of open wells. Also, when this fermentation was attempted in microwell plates, during the earlier stages when cell concentration was not high, cyclohexanol evaporated before it could be used by the cells. As growth took up to 100 hours, sterility became a problem with open well fermentations.

The issues found during *A. calcoaceticus* NCIMB 9871 fermentations display some of the practical problems associated with microscale processes, as lengthy fermentations can be difficult, though not impossible. Elmahdi et al. (2003) have demonstrated successful growth of *Saccharopolyspora erythraea* CA340 in fermentations of 100 hours in custom made microwell plates. These fermentations were carried out at 28 °C in closed wells. However, this temperature is less likely to promote evaporation and the rate of evaporation was reported to be in the range of 4.5 to 8% (v/v) though any liquid losses were offset by the addition of NaOH to the wells for pH control. Unfortunately Elmahdi et al. (2003) did not ascertain further mass transfer conclusions in order to draw further comparisons with this work.

4.3.2 Microscale whole cell bioconversion

Following biocatalyst production by fermentation and induction of CHMO activity (Section 4.3.1), the next step in the overall process is the actual bioconversion. Bioconversions of bicycloketone were carried out using whole cells of the strains *E. coli* TOP 10 [pQR239], *E. coli* JM107 [pQR210] and *A. calcoaceticus* NCIMB 9871. For the bioconversion using *A. calcoaceticus* NCIMB 9871 produced in shake flask, the fermentation culture broth was first dispensed into microwell plates prior to addition of the bioconversion substrate. All bioconversions were studied in 96 DSW plates.

Figure 4.7 shows bicyclolactone production kinetics using bicyclo[3.2.0]hept-2-en-6-one as substrate at an initial concentration of 1.0 $g.l^{-1}$. This high initial concentration of substrate was selected based on the concentrations representative of industrial bioconversion conditions and is a concentration at which the wild type CHMO host, *Acinetobacter calcoaceticus* NCIMB 9871 has shown to work well (Carnell et al., 1991). In this case, the calculated initial rate of product formation of the two *E. coli* strains, TOP10 [pQR239] and JM107 [pQR210] are very similar at 58 and 60 $\mu mol.l^{-1}.min^{-1}$ respectively, while the rate for *A. calcoaceticus* NCIMB 9871 was higher at 111 $\mu mol.l^{-1}.min^{-1}$. While it may appear that the original wild type host is a better choice due to its capacity to convert higher concentrations of ketone at a greater rate, the strain has a growth rate 10 times slower than *E. coli* TOP10 [pQR239] as described earlier in Section 4.3.1. *A. calcoaceticus* NCIMB 9871 also contains an active lactone hydrolase that further metabolises the lactone produced by the bioconversion which would make product recovery and isolation, difficult. The selective inhibition of the hydrolase would require the use of a toxic inhibitor such as tetraethyl-pyrophosphate (Alphand et al., 1990).

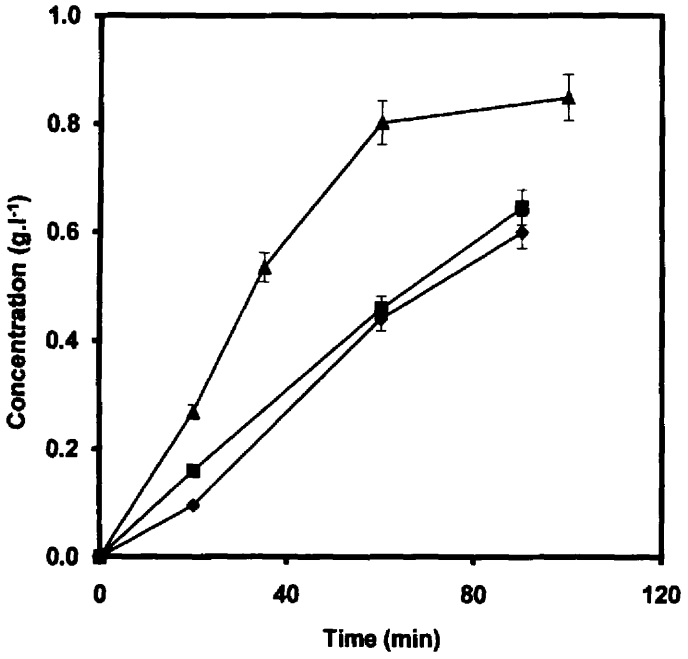

Figure 4.7 Comparative kinetics of bicyclolactone formation in 96 DSW plates using three different whole cell CHMO biocatalysts, *E. coli* TOP10 [pQR239] (♦), *E. coli* JM 107 [pQR210] (■) and *A. calcoaceticus* NCIMB 9871 (▲). Experiments performed using an initial concentration of bicycloketone of 1 $g.l^{-1}$. Experiments performed as described in Sections 2.6.1.5, 2.6.2.3 and 2.6.3.3 respectively. Error bars represent the range of measured values about the mean.

4.3.3 Parallel fermentation and bioconversion process analysis

4.3.3.1 Microscale fermentation

Having established the quantitation and reproducibility of the individual microscale fermentation and bioconversion operations (Section 4.2.3), in this section they were linked together in an automated microscale whole process sequence. A combinatorial approach to experimental design involving the study of three different whole cell biocatalysts, each produced by fermentation at two different initial carbon source concentrations. Biocatalysts produced from fermentation then evaluated on three different ketone substrates at two initial substrate concentrations. Both, *E. coli* TOP10 [pQR239] and *E. coli* JM107 [pQR210] were grown in 96 DSW plates using the culture medium described in Table 2.2. The only variation was the level of glycerol used. All fermentations were induced as described in Sections 2.6.1 and 2.6.3.

Figure 4.8 shows the growth rate of the two *E. coli* strains at the different carbon source concentrations investigated. It is also a representation of the degree of parallelisation possible when using the microwell approach. However, the analytical values required for each graph were obtained using several wells with the "sacrificial well strategy" described in Section 3.3.1. The growth rate of *E. coli* TOP10 [pQR239] grown on 10 $g.l^{-1}$ of glycerol was 0.56 ± 0.03 h^{-1} while at 20 $g.l^{-1}$ of glycerol it was little different at 0.58 ± 0.04 h^{-1}. This represents a difference of $\approx$ 3% and falls within the range of the standard deviation. *E. coli* JM107 [pQR210], in contrast, had a growth rate of $0.30 \pm .02$ h^{-1} when grown on 10 $g.l^{-1}$ of glycerol, but was significantly higher at 0.47 ± 0.03 h^{-1} when grown on 20 $g.l^{-1}$ of glycerol, a difference of $\approx$ 57%. The final biomass concentration obtained was around 5.7 ± 0.3 $g.l^{-1}$ for both strains at each glycerol concentration.

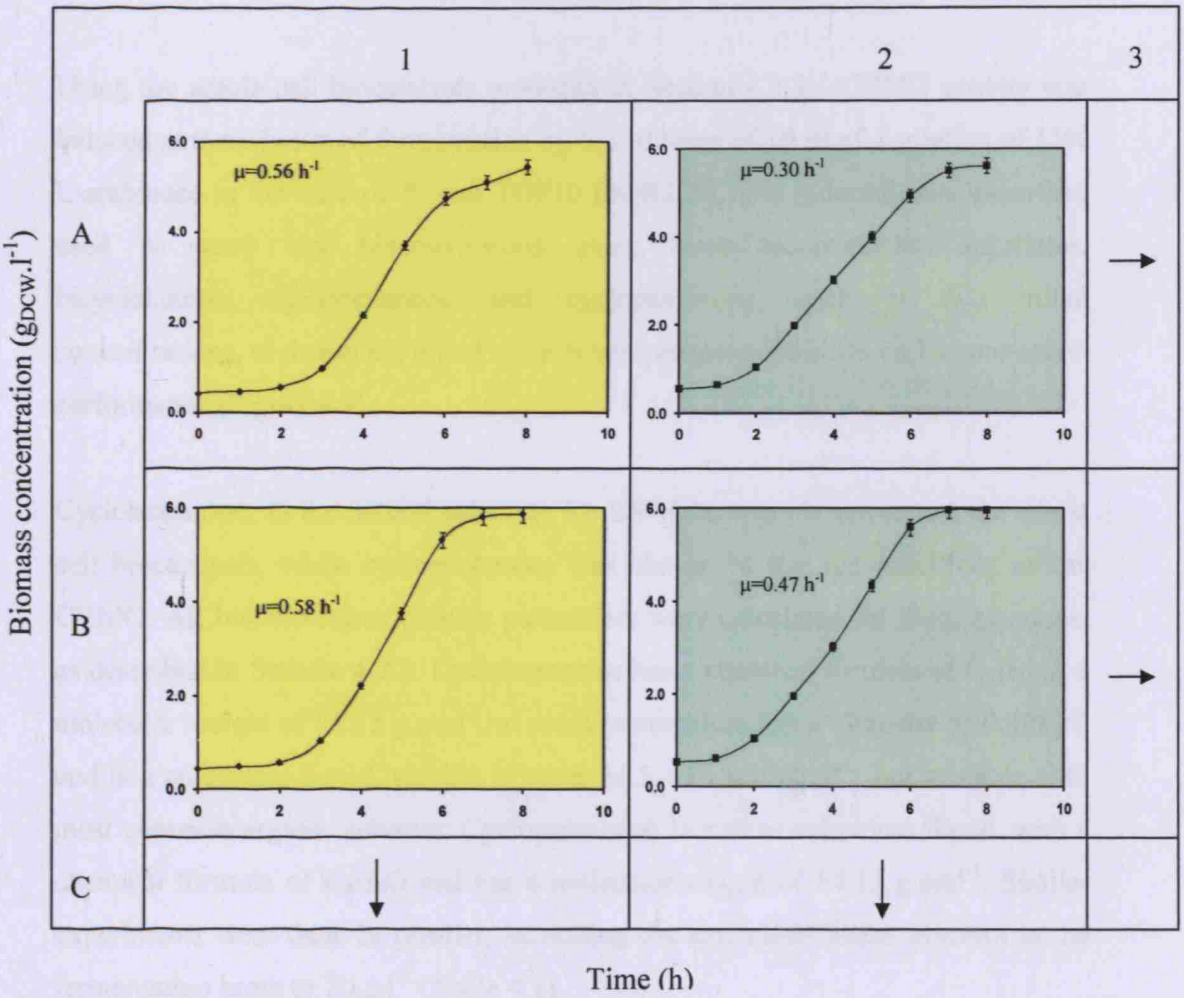

Figure 4.8 Parallel collection and evaluation of fermentation kinetic data in 96 DSW plates. Column 1 shows the growth curves of *E. coli* TOP10 [pQR239] (♦, yellow background), Column 2 shows the growth curves of *E. coli* JM107 [pQR210] (■, green background). Row A was filled with culture media containing 10 $g.l^{-1}$ of glycerol, while Row B was filled with culture media containing 20 $g.l^{-1}$ of glycerol. Experiments performed as described in Section 2.6. Error bars represent the range of measured values about the mean.

4.3.3.2 Microscale bioconversion

Using the whole cell biocatalysts produced in Section 4.3.3.1 CHMO activity was induced at three hours of fermentation by the addition of 10 µl of a solution of 15% L-arabinose in the case of *E. coli* TOP10 [pQR239]. The induced cells were then used to carry out bioconversions using three bioconversion substrates: bicycloketone, cyclohexanone and cyclopentanone, each at two initial concentrations, to assess the effect of upstream process conditions on bioconversion performance (Figure 4.9).

Cyclohexanone, as the natural substrate for BVMOs, was chosen to test the whole cell biocatalysis, while cyclopentanone was chosen to test the specificity of the CHMO. All bioconversion process parameters were calculated for these reactions, as described in Section 4.2.2. Cyclohexanone has a chemical formula of $C_6H_{10}O$, a molecular weight of 98.15 $g.mol^{-1}$, at room temperature has a viscosity of 0.898 cP and is a colourless liquid, soluble in water at 5 - 10 $g.100\ ml^{-1}$, but miscible with most common organic solvents. Cyclopentanone is a clear colourless liquid, with a chemical formula of C_5H_8O and has a molecular weight of 84.12 $g.mol^{-1}$. Similar experiments were done in parallel, increasing the amount of initial glycerol in the fermentation broth to 20 $g.l^{-1}$ (Table 4.1).

Table 4.1 presents a summary of microscale process results for sequential fermentation and bioconversion operations using three different CHMO-expressing whole cell biocatalysts. Results of bioconversion using *A. calcoaceticus* NCIMB 9871 are not presented in Figure 4.9, however they are present at the end of Table 4.1, this is because no bioconversion product could be recovered during the whole cell biocatalysis of cyclohexanone or cyclopentanone as they were further metabolised by the lactone hydrolase, as mentioned in Section 4.3.2. Only bicycloketone kinetics were determined and the results are shown in Table 4.1.

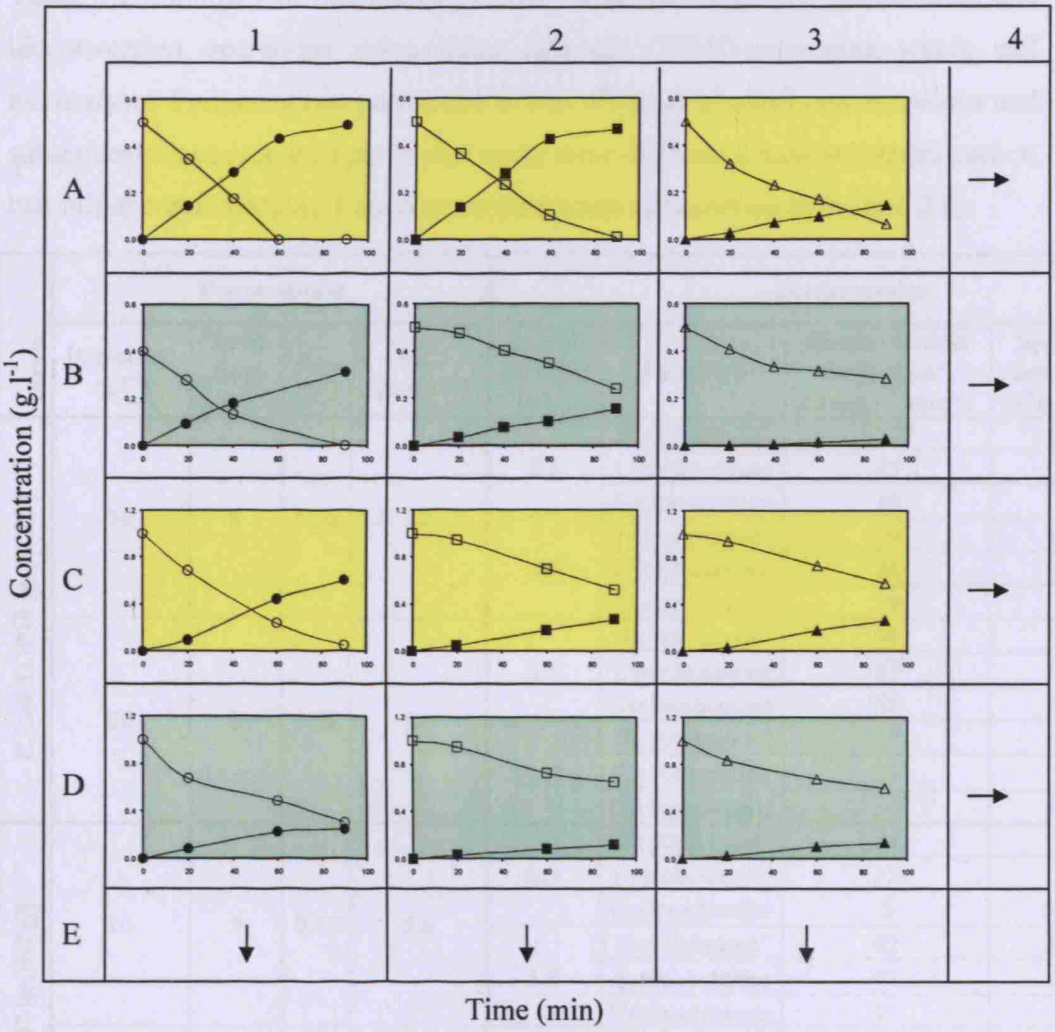

Figure 4.9 Parallel characterisation of whole cell CHMO bioconversion. Rows A and C contain fermentations of *E. coli* TOP10 [pQR210] (yellow background), while rows B and D contain fermentations of *E. coli* JM107 [pQR210] (green background). Initial ketone substrate concentrations of 0.5 $g.l^{-1}$ (Rows A and B) and 1.0 $g.l^{-1}$ (Rows C and D) were used. Three different ketones (open symbols) were converted into their respective lactones (solid), bicycloketone (○, column 1), cyclohexanone (□, column 2) and cyclopentanone (△, column 3). Experiments performed as described in Section. 2.6. All bioconversions were carried out at an initial glycerol concentration of 10 $g.l^{-1}$ during the fermentation.

Table 4.1 Summary of microscale process results for sequential fermentation and bioconversion operations using three different CHMO-expressing whole cell biocatalysts. Fermentations performed at two different glycerol concentrations and subsequent bioconversions performed using three different ketone substrates each at two initial concentrations. Experiments performed as described in Section 2.6.

Strain	Fermentation				Bioconversion				
	[Glycerol] ($g.l^{-1}$)	Total time (h)	μ_{max} (h^{-1})	X_{final} ($g_{DCW}.l^{-1}$)	Initial [ketone] ($g.l^{-1}$)	Substrate	Rate of lactone formation* ($\mu mol.l^{-1}.min^{-1}$)	Specific activity* ($U.g_{DCW}^{-1}$)	Yield+
E. coli TOP10 [pQR239]	10	8	0.56	5.6	0.5	Bicycloketone•	62**	11**	0.92
						Cyclohexanone	45	8	0.50
						Cyclopentanone	16	3	0.29
					1.0	Bicycloketone•	59	11	0.60
						Cyclohexanone	26	5	0.27
						Cyclopentanone	29	5	0.26
	20	8	0.58	5.9	0.5	Bicycloketone•	90	18	0.95
						Cyclohexanone	87	16	0.98
						Cyclopentanone	51	9	0.62
					1.0	Bicycloketone•	57	10	0.58
						Cyclohexanone	29	5	0.36
						Cyclopentanone	59	11	0.49
E. coli JM107 [pQR210]	10	8	0.30	5.6	0.5	Bicycloketone•	14	3	0.36
						Cyclohexanone	15	3	0.31
						Cyclopentanone	2	0.5	0.06
					1.0	Bicycloketone•	62	12	0.65
						Cyclohexanone	32	6	0.28
						Cyclopentanone	17	3	0.13
	20	8	0.42	6.0	0.5	Bicycloketone•	71	12	0.52
						Cyclohexanone	7	2	0.13
						Cyclopentanone	35	7	0.42
					1.0	Bicycloketone•	30	7	0.25
						Cyclohexanone	12	3	0.12
						Cyclopentanone	4	1	0.03
A. calcoaceticus	30x	92	0.04	4.6	1.0	Bicycloketone•	111	24	0.82
						Cyclohexanone	0	0	0
						Cyclopentanone	0	0	0

(*) Calculated over first 60 min of bioconversion. (+) Calculated after 90 minutes of bioconversion. (**) Calculated over 20 minutes of bioconversion in this case. (•) Bicycloketone = bicyclo[3.2.0]hept-2-en-6-one. (x) Carbon source = 30 $g.l^{-1}$ monosodium glutamate.

For *E. coli* TOP10 [pQR239] the two concentrations of glycerol used in the initial fermentation stage showed little effect on either μ_{max} or final biomass concentration (X_{final}). In contrast, there were significant differences in the rate and yield of the bioconversion step for the three substrates tested. For biocatalyst produced on 10 $g.l^{-1}$ glycerol, and subsequent bioconversions performed at an initial substrate concentration of 0.5 $g.l^{-1}$, bicyclo[3.2.0]hept-2-en-6-one was converted at a faster rate and had a higher conversion yield than the natural CHMO substrate cyclohexanone. This has been observed previously and is due to the faster uptake of the larger substrate into the whole cell biocatalyst, *E. coli* TOP10 [pQR239], due to its solubility in aqueous and organic phases (Wang et al., 2003). Cyclopentanone, as expected, is seen to be a poor substrate for the cyclohexanone monooxygenase (Wang et al., 2003), resulting in the lowest bioconversion rate and yield.

Table 4.1 shows that at the higher initial substrate concentration of 1.0 $g.l^{-1}$, the bioconversion rates and yields for both bicyclo[3.2.0]hept-2-en-6-one and cyclohexanone are significantly reduced compared to 0.5 $g.l^{-1}$ and are in line with the substrate inhibition characteristics previously reported for these two compounds (Doig et al. 2003). No inhibitory effects can be seen in the case of cyclopentanone although the rate of product formation and yield values remain low.

For biocatalyst produced on 20 $g.l^{-1}$ glycerol during the initial fermentation stage, the effects of substrate type and initial concentration on bioconversion rate and yield follow the same trends as described above. The main difference, however, is the generally higher specific activity of the biocatalysts which could be a consequence of higher NADPH availability, as glycerol was added prior bioconversion to allow its regeneration (Section 2.6.1.5). Proof that the glycerol was used for regeneration is that the growth rate does not increase. In the case of bicyclo[3.2.0]hept-2-en-6-one this results in the process with the highest overall rates and yields.

The results for *E. coli* JM107 [pQR210] suggest this is a less good CHMO host than *E. coli* TOP10 [pQR239]. At higher glycerol concentration does the bioconversion kinetics improve and become comparable to those of *E. coli* TOP10 [pQR239]. Also at higher ketone concentrations do the *E. coli* JM107 [pQR210] results bioconversion kinetics approach those *E. coli* TOP10 [pQR239], but only in the case of bicycloketone. Overall *E. coli* JM107 [pQR210] grows more slowly and displays consistently lower bioconversion yield.

Yield was defined as the fraction at conversion of lactone to ketone after a period of time, typically 90 minutes (Table 4.1). The yields in this work changed under different bioconversion conditions, but in many cases this could be simply due to poor bioconversion substrates, as most of the ketone remained in the medium, without being converted or evaporated further when it was not taken by the cells. Figure 4.9 demonstrates that with the exception of *E. coli* TOP10 [pQR239] and 0.5 $g.l^{-1}$ initial substrate concentration, in most cases substrate concentration remained close to half of the initial ketone concentration after 100 minutes of bioconversion. This is further demonstrated in Table 4.1; however, trends in the behaviour of yield can be seen. Cyclohexanone conversion, for example, seems to benefit from an increase in carbon source concentration to process 0.5 $g.l^{-1}$ of cyclohexanone, using *E. coli* TOP10 [pQR239] as whole cell biocatalyst; however, this was achieved as long as ketone concentration remained below inhibitory levels. On the other hand, when using *E. coli* JM107 [pQR210] as whole cell biocatalyst, cyclohexanone bioconversion yields remained similar regardless of the initial ketone concentration, but seemed negatively affected by the increase in carbon source concentration; nonetheless this bioconversion never achieved levels above 40%. Cyclopentanone also remained in the liquid phase; this was expected as cyclopentanone is a poor substrate for BVMOs and therefore should produce very low yields (as low as 3 to 6%), but also demonstrates that unused ketone is more likely to remain in the aqueous phase and either remain there or evaporate, rather than be absorbed but not

catalysed by the whole cell biocatalyst. Hilker et al. (2005) assessed how to increase the yields of *E. coli* TOP10 [pQR239] whole cell bioconversion of bicycloketone using a resin based *in situ* substrate feeding and product removal (SFPR) strategy. They found that within the first 12 h, 30% of ketone was converted to the expected lactones mixture. However, from 12 to 24 h, the reaction hardly proceeded, and apparently the CHMO activity was totally lost after this time period.

In the case of *A. calcoaceticus* NCIMB 9871 the μ_{max} and X_{final} values determined during fermentation are significantly lower than for both of the *E. coli* strains. For subsequent bioconversions at an initial substrate concentration of 1 $g.l^{-1}$, lactone formation is only detected for the bicycloketone substrate. In the case of cyclohexanone and cyclopentanone substrate uptake was observed. However, *A. calcoaceticus* NCIMB 9871 is known to possess a lactone hydrolase (Donoghue et al., 1976) which results in the immediate degradation of the lactone compounds produced (the bicyclic lactones produced from bicycloketone are presumably poor substrates or inhibitors of the lactone hydrolase). The slow growth and potential for product degradation make the wild type *Acinetobacter* strain a poorer industrial biocatalyst compared to either of the two *E. coli* strains. Overall these results demonstrate the capacity of microscale processing techniques to generate quantitative data for host strain selection and early stage definition of bioprocess conditions.

4.4 Evaluation of biocatalyst recovery options

4.4.1 Microscale centrifugation

In this section previously established approaches to microscale centrifugation and microfiltration (Jackson et al, 2006) were evaluated for biocatalyst recovery from

the bioconversions described in Section 4.3.2. Microwell plate centrifuges were first used to perform clarification experiments and measure the amount of product that could be recovered at the end of a whole cell biocatalytic process sequence. The fraction of cell removal (or fractional clarification) as well as the fractional recovery of bicycloketone and bicyclolactone was measured. Centrifuge effect or g-number (Z) a measurement of a particle acceleration when subjected to centrifugal forces. Z values from 4 to 249, equivalent to 500 to 4000 rpm, were tested at different time intervals of 5, 10 and 15 minutes.

As shown in Figure 4.10, optimal g-numbers were found to be between 16 (for long centrifugation times) and 97 as they showed high levels of cell removal and good clarification. The figure also indicates that at g-numbers lower than 4 there is low clarification and poor product recovery making this condition unsuitable. For g-numbers equal to or higher than 16, product recovery is higher but clarification is poor unless longer periods of time are used for the centrifugation; for g-numbers equal or above to 97 both cell removal and product recovery were high, regardless of the time used to achieve this. The latter would be better centrifugation conditions as the time required for efficient clarification is low, even though a high g-number is required to achieve this. There was no evidence of cell disruption, which is desirable at this stage, since it enables biocatalysts recycle while it avoids its contamination, it also enables whole cell biocatalysis product recovery from the supernatant.

4.4.2 Microfiltration

Jackson et al. (2006) (see Section 1.2.6) have previously reported a microscale normal flow filtration (NFF) technique, established for the automated high throughput evaluation of complex biological feed streams. A commercially

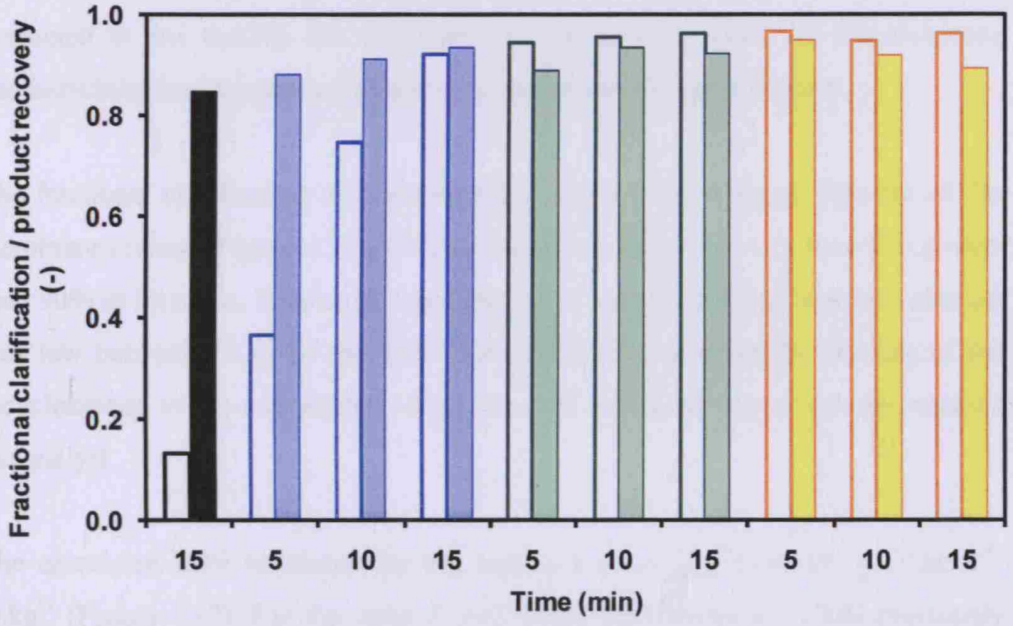

Figure 4.10 Fractional clarification (open bars) and product recovery (solid bars) by microcentrigation to harvest cells following whole cell bioconversion in a 96 DSW plate. Four gravitational forces or g-numbers (Z) were investigated, Z = 4 (black), Z = 16 (blue), Z = 97 (green) and Z = 249 (yellow) after three centrifugation times. Experiments performed as described in Section 2.7.1.

available 96 well filter plate (0.3 cm^2 per well) and a custom designed 8 to 24-well filter plate (0.8 cm^2 per well) were used to quantitatively study the microfiltration characteristics of an *E. coli* TOP10 [pQR239] fermentation broth. The suitability of microfiltration as a primary product recovery and biocatalyst removal technique following the whole cell bioconversion process reported in Section 4.3.2 is evaluated in this section. Six different membranes were tested for bicycloketone and bicyclolactone transmission as well as cell removal or clarification.

The fractional clarification or biocatalyst removal remained above 96% for all the membranes tested (Figure 4.11). Product (bicyclolactone) recovery was also greater than 90% in all cases. In contrast transmission of unreacted bicycloketone substrate was low between 75 to 85 %. This could be due to non specific binding of the bicycloketone to the membranes or the removal of the substrate with the retained biocatalyst.

The calculated cake resistance for the experiments ranged from 10 – $13x10^{-12}$ $m.kg^{-1}$ (Figure 4.12). For the same *E. coli* strain, Jackson et al. (2006) previously reported a cake resistance of approximately $150x10^{-12}$ $m.kg^{-1}$. However, the culture broth used had been aged for four hours before being processed which is known to lead to an increase in cake resistance. Also, bicycloketone is known to damage cell integrity (Doig et al., 2002) thus decreasing the cake resistance. As with the microscale centrifugation described in Section 4.4.1, this work was done to demonstrate the potential of further microscale downstream processing in an integrated process sequence.

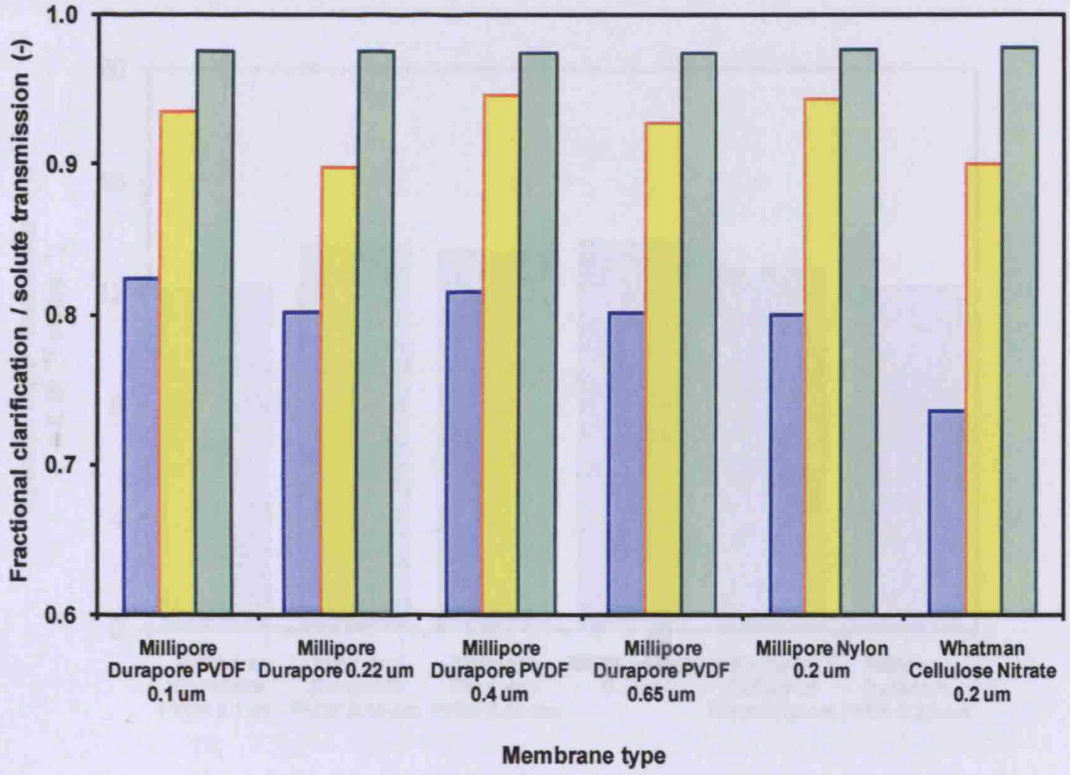

Figure 4.11 Microscale microfiltration of *E. coli* TOP10 [pQR23] following whole cell bioconversion in a 96 DSW plate. Experiments performed at 25 °C as described in Section 2.7.2. The results illustrate the fractional clarification (green bars), ketone (blue bars) and lactone transmission (yellow bars) using a variety of filters. Experiments performed as described in Section 2.7.2.

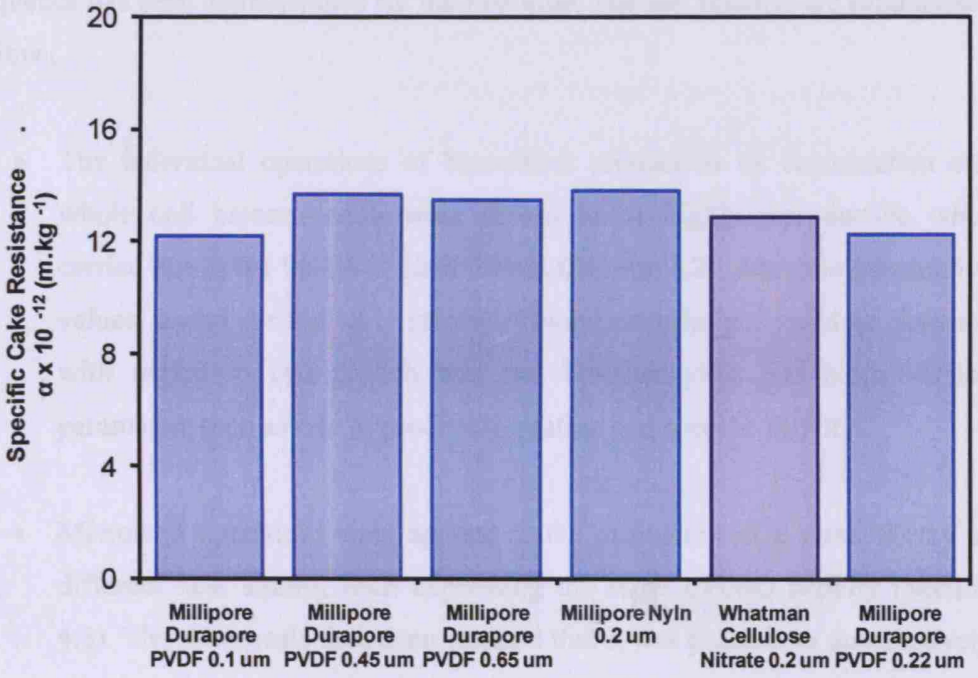

Figure 4.12 Specific cake resistance of *E. coli* TOP10 [pQR239] calculated for the use of different microfiltration membranes based on the data presented in Figure 4.11. Experiments performed as described in Section 2.7.2.

4.5 Summary

In this chapter, the potential of microwell based approaches for the automated high throughput evaluation of different CHMO host strains in multi – step process sequence has been demonstrated for the first time. The key findings are summarised below.

- The individual operations of biocatalyst production by fermentation and whole cell bioconversion were shown to be highly reproducible when carried out in the 96 DSW plate format (Section 4.2). Accurate quantitative values, useful for the early stages of bioprocess design, could be obtained with regard to cell growth rate and biomass yield and bioconversion parameters such as rate of product formation and specific activity.

- Microwell operations were applied to the evaluation of a small library of different host strains, each expressing the same CHMO activity (Section 4.3). The microscale data demonstrated that it was possible to quantitatively discriminate between the fermentation (Section 4.3.1) and bioconversion (Section 4.3.2) kinetics of each strain.

- The performance of each biocatalyst was next evaluated in a fully automated and linked sequence of operations comprising fermentation, enzyme induction (when required) and bioconversion using a combinatorial approach to experimental design (Section 4.3.3). The strain *E. coli* TOP10 [pQR239] was shown to be the best overall catalyst in terms of a high yield of biocatalyst with a high specific activity.

- The automated *E. coli* TOP10 [pQR239] microscale process sequence was finally extended to include analysis of different unit operations for primary

product recovery and biocatalyst removal (Section 4.4). Centrifugation and microfiltration operations, each operated in microwell formats over a range of operating conditions, indicated high product recovery levels (close to 100 %) and almost complete biocatalyst removal.

The work presented here and in the previous chapter have now demonstrated the quantitative and reproducible nature of microscale operations for the evaluation of multistep bioconversion sequences. In the next chapter the possibility to use the microscale data generated for the prediction of larger scale performance will be explored.

5.0 Predictive scale-up of microwell results

5.1 Aims of the chapter

In the previous chapters, it was shown that quantitative kinetic data can be obtained from fermentation and bioconversion processes carried out at the microwell scale. As described in Section 1.4, the aim of this chapter was to establish a suitable basis for the scale-up of microwell results so that the results obtained can be predictive of larger scales of operation. Given that companies most likely already have established scale-up criteria from laboratory to pilot and process scales, the challenge for microwell scale processes is to show that they can be predictive of data generated in conventional laboratory scale stirred bioreactors. This would involve scale-up factors of the order of 2800 fold based on the experimental methodologies established in Chapter 3.

In Section 4.3, it was shown that an automated microscale process sequence comprising of fermentation and bioconversion could quantitatively distinguish between different biocatalyst-substrate combinations. Here the microwell results obtained with the most extensively studied biocatalyst, *E. coli* TOP10 [pQR239], will be compared to those obtained from an equivalent laboratory scale process performed in a 1.4 l working volume stirred tank bioreactor. Details of the bioreactor geometry and its operation were given in Section 2.6.1.6 and Section 2.6.1.7 respectively. Given the different geometries at the two scales of operation and that both the fermentation and bioconversion stages require molecular oxygen, it was proposed that similar performance at the two scales can be achieved if the processes are operated at matched k_La values. In order to test this hypothesis, the specific objectives of this chapter were to:

- Establish methods for the measurement of k_La values at the microwell scale and to explore how microwell and stirred bioreactor agitation/aeration conditions influence the measured k_La values.

- Establish experimental methods for the *in-situ* monitoring of DOT during microwell fermentation and bioconversion in order to provide insight into how DOT values vary during processes performed at the two scales and how they influence bioconversion performance.

- Perform a series of linked fermentation and bioconversion processes over a range of matched k_La values at the two scales to validate the use of k_La as a basis for scale-up.

The process studied was the production of the whole cell *E. coli* TOP10 [pQR239] biocatalyst at an initial glycerol concentration of 10 $g.l^{-1}$ with CHMO induction using 0.15% v/v L-arabinose 3 hours after inoculation. This followed by examination of the oxidative bioconversion of bicyclo[3.2.0]hept-2-en-6-one at an initial concentration of 0.5 $g.l^{-1}$, as previously described in Sections 3.5 and 4.3.2.

5.2 k_La as a basis for scale-up

5.2.1 Prediction of k_La values

The Oxygen Uptake Rate (OUR) of *E. coli* TOP10 [pQR239] during bioconversion has previously been investigated in a 55 l pilot-scale stirred bioreactor by Doig et al.

(2002). They found that the rate of oxygen utilisation was stoichoimetrically 6.91 times the rate of lactone formation due to the additional requirement of oxygen for glycerol oxidation and co-factor recycling. The rate of lactone formation obtained for the bioconversion of 0.5 $g.l^{-1}$ bicycloketone in the 96 DSW plate geometry used here was 62 $\mu mol.l^{-1}.min^{-1}$ (Table 4.2), therefore, an OUR of 25 $mmol.l^{-1}.h^{-1}$ can be estimated assuming the same reaction stoichiometry.

The corresponding Oxygen Transfer Rate (OTR) of the different vessels can be calculated from the Equation 5.1:

$$OTR = K_L a\left(C_L^* - C_L\right) \qquad \text{[Eq. 5.1]}$$

Where K_L is the overall oxygen mass transfer coefficient, approximately equal to the liquid phase mass transfer coefficient, k_L, in the case of poorly soluble gases such as O_2 in aqueous systems; a is the specific gas-liquid interfacial area; C_L is the oxygen concentration in the liquid phase and C_L^* is the saturation concentration of oxygen.

According to Quicker et al. (1981), a typical value for O_2 solubility in aqueous systems such as culture medium, at atmospheric pressure and T = 30°C is around 8.05×10^{-3} $kg.m^{-3}$. For the laboratory scale bioconversion process it is known from on-line measurements of DOT that C_L is close to zero during the initial stages of the reaction (Doig et al., 2002). A minimum k_La value of 100.8 h^{-1} is therefore necessary if oxygen limited conditions are to be avoided.

For the laboratory scale stirred bioreactor process (Section 2.6.1.6) it has previously been reported that optimum CHMO activity is obtained when the dissolved oxygen tension is in the range 5 – 10 % during enzyme induction (Doig

et. al., 2001). This corresponds to an impeller speed of 900 rpm and an air supply of 0.7 vvm in the stirred bioreactor used for this work. Van't Riet (1979) has reviewed a large number of investigations on gas-liquid mass transfer in stirred vessels and has correlated the results to an accuracy of 20-40% using Equation 1.2, where v_s is the superficial gas velocity (0.0014 $m.s^{-1}$ in this case).

$$k_L a = 2.0x10^{-3}\left(\frac{P_g}{V}\right)^{0.7} v_s^{0.2} \qquad \text{[Eq. 1.2]}$$

The stirred bioreactor details and dimensions can be seen in Table 2.3. The unaerated power number in a dual Rushton impeller system (T = 0.56 m, D = T/3) has been measured by Hudcova et al. (1989). The unaerated power number for a spacing between the impellers $\Delta C/D = 1$ was found to be 8.3, while the gassed to ungassed power ratio at a gas flow number (FL_G) of 0.017 yielded a value equal to 0.95. For the impeller speed of 900 rpm used in this work, an estimated k_La value of 360 h^{-1} was thus calculated based on this power number and Equation 1.2.

For the microwell-based process, Hermann et al. (2002), showed how k_La values for microwells vary with the shaking speed and diameter and the liquid fill volume. Doig et al. (2005) has also reported k_La values for various microwell geometries, based on dynamic gassing out measurements and on the growth kinetics of an obligate aerobe. They proposed the correlation shown in Equation 1.4 to enable prediction of k_La values in several well geometries (Section 1.3.5):

$$k_La = 31.35\, D_{O2}\, a_i\, Re^{0.68}\, Sc^{0.36}\, Fr^{Y}\, Bo^{Z} \qquad \text{[Eq. 1.4]}$$

The values taken for Y was 0.64 and for Z was 0.15, which are those reported for 96 SRW plates. Based on the shaking radius (ϕ = 3 mm), speed (1000 rpm) and liquid fill volume (V_L = 500 µl) used in this work, and as described in Section 2.6.1.4 and 4.2, the estimated k_La value is 198 h^{-1}.

5.2.2 Measurements of k_La values

5.2.2.1 96 DSW plate k_La values

In order to confirm the k_La values calculated in Section 5.2.1 and to determine the range of k_La values it is possible to achieve in microwell processes, it was necessary to experimentally measure them. The dynamic gassing out method was used to carry out these measurements as described in Section 2.4.1. This method involves de-oxygenating the media with nitrogen until the DOT is zero. Air is then reintroduced and the change in the DOT from zero to steady state is recorded. The rate of change of the DOT during this period is equal to the rate of oxygen transfer from gas to liquid. A modified well from a 96 DSW plate was created as described in Section 2.4.1. This incorporated a fibre optic oxygen sensor in order to enable these k_La measurements to be made. Figure 5.1 shows typical gassing out curves obtained at different shaking speeds and liquid fill volumes in a 96 DSW plate.

The culture medium described in Table 2.2 was used during measurements of k_La values over a variety of shaking speeds and liquid fill volumes. Figure 5.2 demonstrates that, as expected, k_La values increase with the increase of shaking speeds (rpm) and with decreases in liquid fill volume. This is also demonstrated by the raw DOT data shown in Figure 5.1. These experimental k_La values were determined with the actual culture medium used for all fermentations because it is

most representative of the conditions under which actual fermentation and bioconversion processes are performed (Table 5.1a). 10 $g.l^{-1}$ of sodium chloride was also used to investigate any coalescence effects on k_La in microwells (Table 5.1b). Van't Riet (1979) does not recommend the use of sodium chloride solutions for the measurement of k_La because as with the sodium sulphite methods, it is not representative of biological systems. However this concern mainly applies to mechanically stirred vessels where oxygen is transferred via a dispersed gas phase rather than via surface aeration in microwells (where no disperse gas has been observed). The results presented in figure 5.2 are not calibration curves and should not be considered as such, it only demonstrates trends; it is recommended that k_La value are calculated with the vessel and conditions to be used in further experiments.

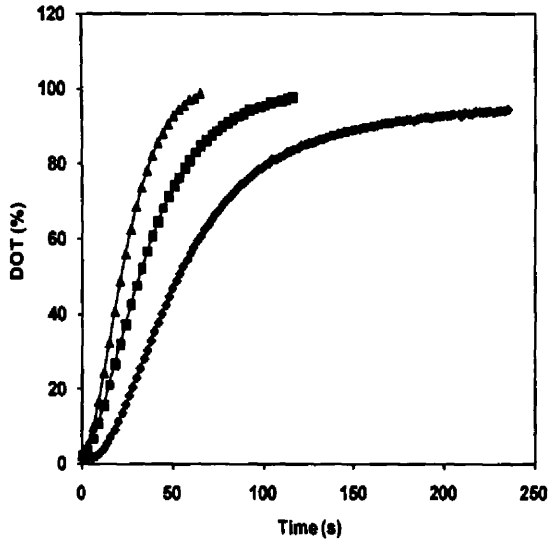

Figure 5.1 Measurements of oxygen transfer rate in 96 DSW plates based upon the dynamic gassing out method. Representative curves are shown for various agitation speeds and liquid fill volumes: 1000 rpm, 1000 µl (♦), 1000 rpm, 600 µl (■), 1200 rpm, 200 µl (▲). Experiments performed in culture medium as described in Section 2.4.1.

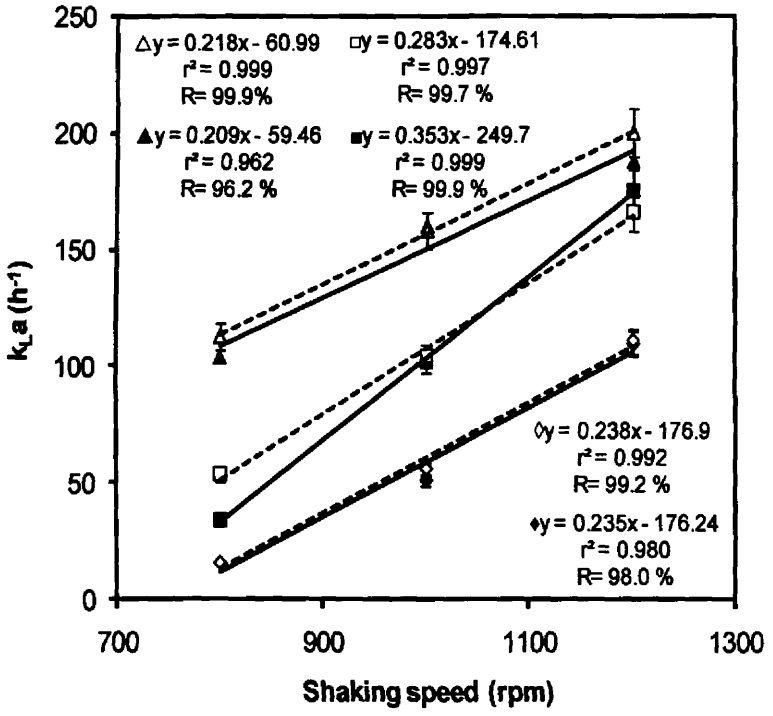

Figure 5.2 Measured k_La values in a 96 DSW plate as a function of shaking speed. Figure shows k_La values measured with culture medium (solid line, solid symbols) and 10 $g.l^{-1}$ NaCl solution (dotted line, open symbols) at different liquid fill volumes: 1000 µl (♦), 600 µl (■) and 200 µl (▲). Lines were fitted by linear regression. Experiments performed as described in Section 2.4.1 and k_La values calculated according to Equations 2.1 and 2.2. Error bars represent the range of measured values about the mean.

Table 5.1a Experimentally determined k_La values (h^{-1}) in 96 DSW plates measured using fermentation media described in Table 2.2. Experiments performed as described in Section 2.4.1.

Liquid fill volume (µl)	Shaking speed (rpm)		
	800	1000	1200
200	104	160	186
600	34	102	175
1000	16	51	110

Table 5.1b Experimentally determined k_La values (h^{-1}) in 96 DSW plates measured using a 10 $g.l^{-1}$ sodium chloride solution. Experiments performed as described in Section 2.4.1.

Liquid fill volume (µl)	Shaking speed (rpm)		
	800	1000	1200
200	113	158	200
600	53	105	166
1000	16	56	111

In the area of shaken microwells no significant difference in k_La values was found between culture medium and sodium chloride solution (Figure 5.2). The major resistance in stirred vessels to oxygen mass transfer is the liquid film surrounding the gas bubbles, while in microwells mass transfer is more closely related to diffusion and the superficial aeration velocity (Doig et al., 2005) than bubble size as no visible bubbles are produced in the liquid. For mass transfer in microwell plates key operating variables in shaken microscale fermentations are shaking pattern (orbital or linear), shaking frequency and amplitude, microwell diameter, liquid fill volume, fluid properties such as diffusivity, density, viscosity and surface tension (Büchs et al., 2001; Doig et al., 2005). Surface forces are paramount at this scale and shaking must overcome the force required to break the surface tension of the liquid for oxygen to diffuse to the bottom of the well. This is better described in Table 1.1. In stirred vessels, superficial aeration is considered low and mass transfer is more dependent on bubble size. Therefore, the influence on k_La of ions or surfactants could not be observed in microwells. While the use of sodium chloride over estimates k_La in stirred vessels, in microwells it does not have any influence in the mass transfer rate therefore the action of bubbles is minimal. Culture medium was used to determine the k_La values for scale comparison, as it closer replicates the conditions of the fermentation.

Table 5.2 shows microwell k_La values reported for different well geometries, fill volumes, shaking speed and orbital shaking diameter. This demonstrates that the k_La values measured in this work fall within the range of previously reported values. Kensy et al. (2005) measured k_La using 24 Standard Round Well (24 SRW) microwell plates with a similar PreSens oxygen probe to the one used in this work. They used the chemical sulphite method to measure the volumetric mass transfer coefficient and found a similar correlation between fill volume and mass transfer coefficient. While the typical fill volume of one well from a 24 SRW plate is 2000

µl, the k_La values established by Kensy et al. (2005) were within the range of 60 h^{-1} for 1200 µl fill volume to 240 h^{-1} for 400 µl fill volume which are again similar to those found here for a 96 DSW plate. The studies presented by Kensy et al. (2005) and the ones described here indicate the importance of matching microwell shaking conditions in order to match the oxygen uptake rate of growing cultures within the wells. They also demonstrate the importance of suiting culture oxygen needs by varying oxygen transfer conditions by adjusting fill volume and shaking conditions.

Table 5.2 Literature k_La values reported for a variety of microwell plates and shaking conditions determined using a number of conditions and techniques.

Well geometry	Filling Vol. (µl)	Shaking Diameter (mm)	Shaking speed (RPM)	k_La value (h^{-1})	Method	Reference
DSW (8 mm)	500	25	300	60	Horseradish peroxidase Rx*	Duetz et al. (2004)
DSW (8 mm)	500	50	300	132	Horseradish peroxidase Rx*	Duetz et al. (2004)
DSW (8 mm)	750	50	300	95	Growth of strict aerobe+	Duetz et al. (2001)
96 DSW	500	50	300	188	Sulfite oxidation	Duetz et al. (2000)
96 SRW	200	3	1100	150	Cathecol Oxidation Rx*	Ortiz-Ochoa et al. (2005)
96 SRW	200	3	1000	90	Sulfite oxidation	Hermann et al. (2003)
96 SRW	200	3	1100	198	Gassing out technique with culture medium	Doig et al. (2005)

(*) Rx indicates reaction; (+) based on growth kinetics of *Pseudomonas putida*.

5.2.2.2 Stirred bioreactor k_La values

In order to verify the calculated bioreactor k_La values in Section 5.2.1, k_La values were also measured at this scale using culture medium and a 10 $g.l^{-1}$ sodium chloride solution over a range of agitation conditions. The gassing out method was again used for these experiments as described in Section 2.4.2, although there are others such as the oxygen enriched method developed by Chang et al. (1989) for larger vessels.

Using a similar approach to the experiments in Section 5.2.2.1, two different solutions were examined: sodium chloride 10 $g.l^{-1}$ and the culture medium described in Table 2.2. Sodium chloride solution was used to assess the effect of bubble coalescence on k_La. Mechanically stirred and aerated vessels are susceptible to changes in mass transfer rates according to the fluid composition and especially the presence of surfactants (Doran, 1995). Figure 5.3 shows that k_La increases in relatation to the agitation speed regardless of the liquid used, while the numerical values of k_La are related to the type of liquid inside the vessel. Both trend lines, however, have a similar slope. The k_La values for the stirred bioreactor range from 40 to 168 h^{-1} (Table 5.3), which is a similar range to those shown by the 96 DSW plates from 16 h^{-1} to 186 h^{-1} (Table 5.1).

Table 5.3 Experimental k_La values in a 2 l stirred bioreactor measured using fermentation media as described in Table 2.2 and a solution of 10 $g.l^{-1}$ of sodium chloride. Experiments performed as described in Section 2.4.2.

Liquid medium	Agitation speed (rpm)			
	700	800	900	1000
10 $g.l^{-1}$ NaCl	89	131	196	255
Culture medium	40	77	126	168

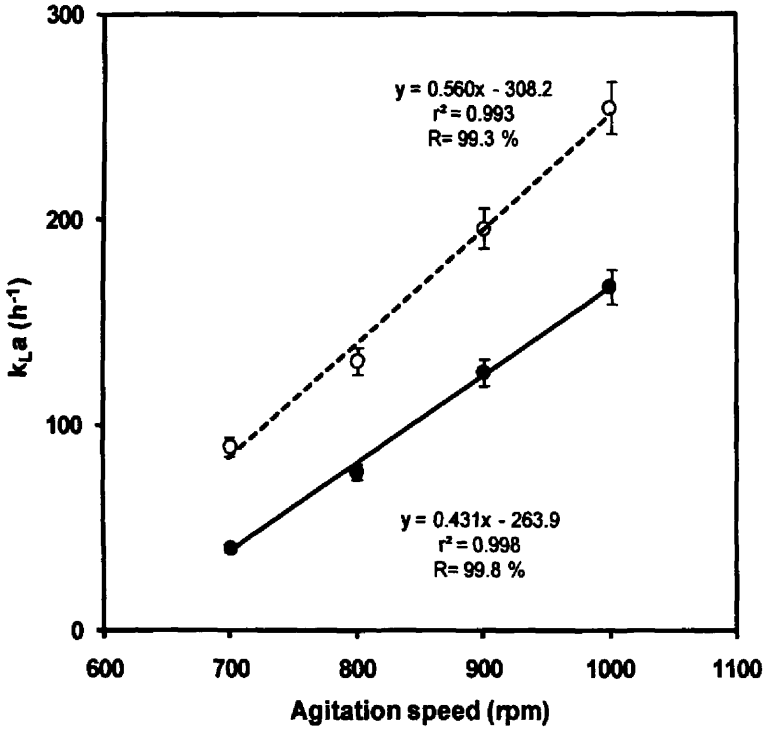

Figure 5.3 Measured k_La values in a 2 l stirred bioreactor with culture media (solid line, solid symbols) and 10 $g.l^{-1}$ NaCl (dotted line, open symbols). Lines were fitted by linear regression. Experiments performed as described in Section 2.4.2 and k_La values calculated according to Equations 2.1 and 2.2. Error bars represent the range of measured values about the mean.

The results presented in figure 5.3 are not calibration curves and should not be considered as such, they only demonstrate trends; it is recommended that k_La value are calculated with the vessel and conditions to be used in further experiments. The 2 l stirred bioreactor oxygen mass transfer measurements indicated that when measuring the k_La, there is a much larger difference between water with a high ionic strength and culture medium compared to microwell k_La measurements. Oxygen solubility is decreased by ions and sugars in the culture medium (Doran, 1995). However, the k_La measured in the presence of sodium chloride yielded higher k_La values even though bubble coalescence would be expected to increase the bubble size in high ionic strength solutions and therefore decreases the total transfer area *a*. The lower k_La values measured with culture medium were probably a consequence of proteins contained in the culture medium that can act as surfactants. Surfactants have been shown to decrease oxygen mass transfer rates, for example the addition of 10 ppm sodium lauryl sulphate reduced k_L for oxygen transfer by 56% versus pure water (Bailey and Ollis, 1989). Rosso et al. (2006) also found that k_La decreased when experiments were carried out using SDS. They surmised that by accumulating at the interface, surfactants lower the surface tension, but act as a barrier to oxygen transfer. Rosso et al. (2006) concluded that there was a direct correlation between the decrease in surface tension and the corresponding decrease in oxygen mass transfer coefficient

The most important property of air bubbles that affect oxygen mass transfer in bioreactors is their size; in most fermentation broths, if the bubbles have diameters less than 2-3 mm, surface tension effects dominate the behaviour of the bubble surface. As a result, the bubbles behave as rigid spheres with immobile surfaces and there is no internal gas circulation. A rigid bubble surface gives lower k_L values. However, the coalescence of small bubbles into bigger bubbles is generally

undesirable in a bioreactor as it reduces the total interfacial area, *a*, and the gas hold up (Doran, 1995).

Garcia-Ochoa et al. (2005) contemplated that the decrease of k_La values observed by addition of glucose to water must be due mainly to a change in viscosity. They also considered that the addition of a surfactant or antifoam, substances commonly present in culture medium cause a larger decrease of k_La values with respect to water, as also found by other authors (Kawase et al., 1992). This can be due to the effect of surfactant molecules affecting the hydrodynamic parameters (average bubble size may increase due to induced bubble coalescence which, in turn, will affect the gas hold-up, hence, the mass transfer area) (Arjunwadkar et al., 1998).

The accumulation of surface active agents at the gas-liquid interface could become a spread film on the bubble surface inhibiting oxygen diffusion and introducing an additional barrier to gas phase mass transfer resulting in a decrease in the mass transfer coefficient. Other authors have pointed out this barrier effect due to a mono-layer of the surfactants formed at the interface which can offer a resistance to the transfer of the gas molecules (Vasconcelos et al., 2003; Linek et al., 2005).

Pursell et al. (2004) encountered this same effect during liquid-liquid extraction, where the soluble components produced during fermentation were found to reduce the overall mass transfer coefficient by up to 70%. After fractionation, they established that components in the weight range from 10–30 kDa had the greatest effect on mass transfer. Protein and phospholipid compounds of similar size were found to reduce the overall k_La in comparable way to the broth components at concentrations of around $0.001 mg.l^{-1}$.

5.3 Process variation at matched k_La values

Because of the high oxygen demand during fermentations a number of authors (Karrow et al., 1953; Bartholomew, 1960) proposed in the early 1950s that the volumetric oxygen mass transfer coefficient k_La be maintained constant on scale-up. They concluded that as long as k_La was maintained above a certain value reasonably comparable results could be obtained at two different scales.

Values of k_La for microwell and bioreactor scales can be estimated from correlations, such as Equations 1.2 and 1.4. It is important when using k_La as scale comparison tool is that the k_La is determined in a consistent manner. k_La must be custom set for individual processes to achieve optimal results, usually when process yield no longer increases with the increment of oxygen mass transfer (Wang et al., 1979).

5.3.1 Fermentation and bioconversion kinetics at typical k_La values

For processes performed under typical operating conditions, k_La values of an average of 115 ± 10 h^{-1} can be calculated for both microwell and bioreactor geometries. Figures 5.4 and 5.5 respectively show the measured fermentation and bioconversion kinetics at the two different scales operating under conditions that give matched k_La values of this magnitude. For the fermentation stage (Figure 5.4), this data represents a 1400-fold scale translation (from 1000 µl to 1.4 l) showing that both scales achieved similar growth rates and final biomass concentrations.

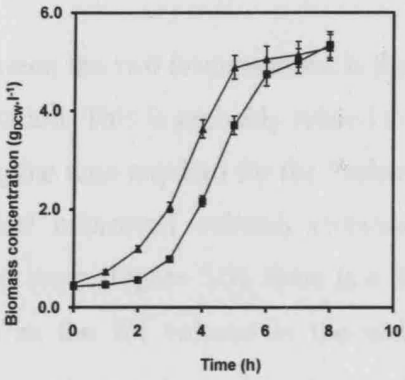

Figure 5.4 Fermentation kinetics of *E. coli* TOP10 [pQR239] biocatalyst at a matched k_La value of 115 ± 10 h^{-1}: 96 DSW plate with 1000 µl fill volume (■) and 2 l stirred bioreactor (▲). Experiments performed as described in Sections 2.6.1.3 and 2.6.1.6 respectively. Error bars represent the range of measured values about the mean.

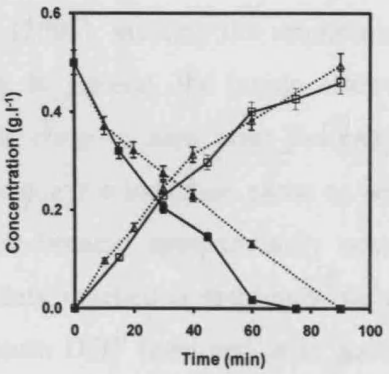

Figure 5.5 Bioconversion kinetics of bicyclo[3.2.0]hept-2-en-6-one at a matched k_La value of 115 ± 10 h^{-1} using a whole cell *E. coli* TOP10 [pQR239] biocatalyst: 96 DSW plate with a liquid fill volume of 500 µl (solid lines) showing bicycloketone (■) and bicyclolactone concentrations (□), 2 l stirred bioreactor (dotted lines) showing bicycloketone (▲) and bicyclolactone (Δ) concentrations. Experiments performed as described in Section 2.6.1.5 and 2.6.1.6 respectively. Error bars represent the range of measured values about the mean.

The main difference between the two fermentations is the slightly longer lag phase in the microwell fermentation. This is probably related to partial oxygen starvation of the seed culture during the time required for the Packard robot to pipette aliquots of inoculum into parallel microwell cultures (Nealon et. al. 2005). For the subsequent bioconversion stage (Figure 5.5), there is a 2800-fold scale translation (from 500 µl to 1.4 l) as the fill volume in the wells was reformatted after fermentation and induction reducing the well working volume from 1000 µl to 500 µl for the bioconversion stage. Excellent agreement is seen between the kinetics of bicyclolactone formation at the two scales.

Figure 5.6 shows the corresponding DOT profiles throughout the fermentation and bioconversion processes at the two scales. These are similar to that previously published by Doig et al. (2003), meeting the requirement for low oxygen levels during enzyme induction. In general, the trends observed at the two scales are similar in that DOT falls close to zero prior the enzyme induction. The DOT increased at the end of the enzyme induction phase as cell growth was arrested and the biomass concentration became approximately constant (Figure 5.4). In the stirred bioreactor OUR data reached a maximum value of 40 $mmol.l^{-1}.h^{-1}$ that coincided with the minimum DOT level and is in good agreement with the data published by Doig et al. (2001). Through the fermentation kinetics, pH oscillated between 7 and 7.5.

DOT also increased after the bioconversion substrate was added. This would be expected based on the k_La values calculated in Section 5.2.1. At the rates of lactone formation seen in Figure 5.5 bioconversion performed at the two scales would both be predicted to occur under non oxygen limited conditions as shown in Figure 5.6. One factor which may contribute to DOT sharp increase is that bicyclo[3.2.0]hept-

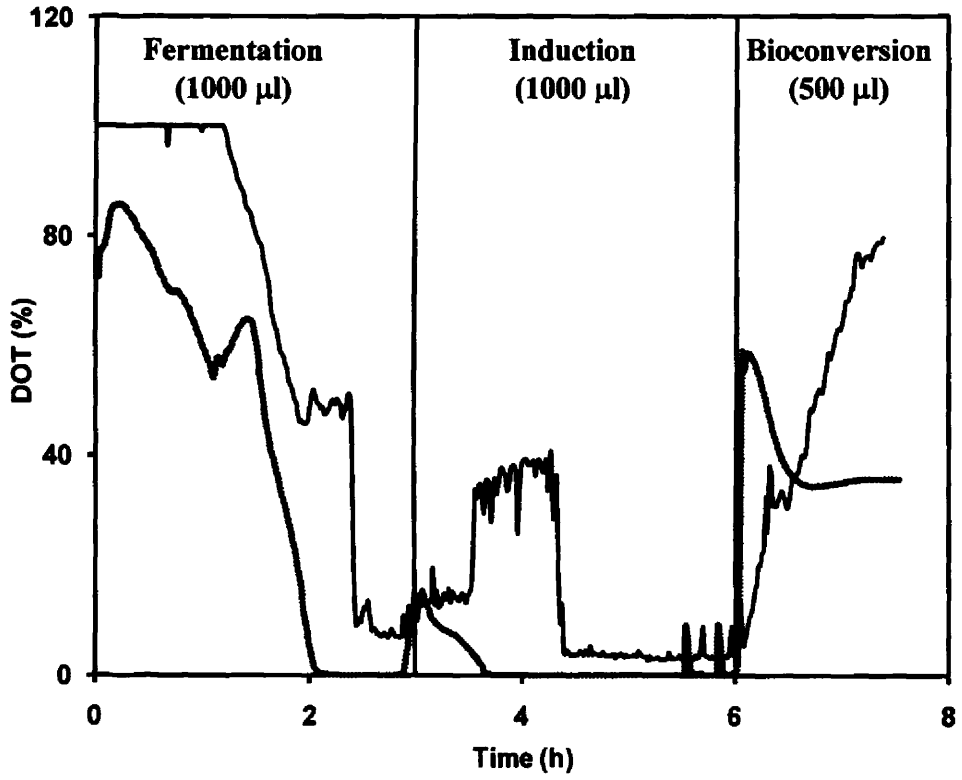

Figure 5.6 DOT profiles measured throughout the 96 DSW plate scale (gray line) and the 2 l stirred bioreactor scale (black line) fermentation and bioconversion processes operated at a matched k_La value of 115 ± 10 h^{-1}. Experiments performed as described in Section 2.4.3.

2-en-6-one (bicycloketone) has been found to be harmful to the cell membrane integrity (Doig et al., 2002). Figure 5.6 shows that this rise occurs after 6 hours of fermentation and coincides with the addition of bicycloketone.

The increase in DOT after the addition of bicycloketone substrate was also observed by Doig et al. (2002) during the bioconversion of the same substrate using similar process conditions but in a 55 l bioreactor. Gomes et al. (2007) encountered a similar effect during the bioconversion of methyl ricinoleate into γ-decalactone by the yeast *Yarrowia lipolytica* using a 2 l bioreactor (Biolab, BRAUN; h_t =21 cm, D_t = 11 cm), however they do not attempt to explain this phenomenon in their work.

Kensy et al. (2005) carried out *Escherichia coli* JM109 (ATCC 53323, DSMZ, Braunschweig, Germany) fermentations in 24 SRW plates using similar PreSens oxygen probes for continuous monitoring as used here. The fermentation broth was incubated at 30°C, a shaking speed of 250 rpm and at a shaking diameter of 25 mm, using LB2.5G medium which contained 2.5 $g.l^{-1}$ of glycerol as carbon source. Similar to Gomes et al. (2007) the DOT profile presents a sharp increase from near zero DOT after some hours of fermentation (the length of these periods vary proportionally with the fill volume). They attribute the spontaneous increase in DOT to the depletion of the primary carbon sources (glycerol together with yeast extract). Weuster-Botz et al. (2005) also used the PreSens probe for monitoring *E. coli* BL21(DE3)-pLysS (P9811, Promega GmbH, Mannheim, Germany) fermentations for parallel control of 48 miniature stirred bioreactors with a liquid-handling system for automation of titration and sampling.

Based on results presented in Figures 5.4 to 5.6 the key kinetic parameters for both fermentation and bioconversion operations are summarised in Table 5.4. In the case of the initial fermentation stage, there is excellent agreement in the calculated

maximum specific growth rates (0.56 and 0.55 h^{-1}) and similar final biomass concentrations of 5.3 and 5.6 $g.l^{-1}$ are achieved. For the bioconversion stage the initial rates of lactone formation were determined as 62 and 64 $\mu mol.l^{-1}.min^{-1}$, respectively again indicating excellent agreement.

The fermentation and bioconversion results obtained at the two different scales of operation also show good agreement with earlier laboratory scale studies performed by Doig et al. (2003) using an AD2 series 2 l stirred tank fermenter (working volume 1.5 l) (Charing, Kent, UK).

Table 5.4 Comparison of kinetic parameters from microwell and laboratory scale processes performed at a matched k_La of 115 ± 10 h^{-1}. Fermentation parameters calculated from Figure 5.4. Bioconversion parameters calculated from Figure 5.5.

Fermentation			**Bioconversion**			
Scale and geometry	μ_{max} (h^{-1})	X_{final} ($g_{DCW}.l^{-1}$)	**Initial [ketone]** ($g.l^{-1}$)	**Rate of lactone formation**[1] ($\mu mol.l^{-1}.min^{-1}$)	**Specific activity**[1] ($U.g_{DCW}^{-1}$)	**Yield**[2]
96 DSW (1000 µl)	0.56	5.6	0.5	62	11	0.92
1.5 l Bioreactor (Doig et. al., 2003)	----	5.5	0.4	52	10	0.60[3]
1.4 l Bioreactor	0.55	5.3	0.5	64	12	0.99

(1) Calculated over first 20 minutes of bioconversion. (2) Defined as the fraction at conversion of lactone to ketone. (3) Calculated over first 30 minutes of bioconversion.

5.3.2 The need to investigate processes at different k_La values

In Section 5.3.1 it was demonstrated that for fermentation and bioconversion processes performed at a matched k_La value of 115 ± 10 h^{-1} there was good agreement in the measured growth rates and bioconversion rates and yields (Table 5.4). This gives initial confidence that the results obtained in microwell geometries can be predictive of those at larger scales. To further verify the use of k_La as a basis for scale-up for microwell plates, processes have been compared at two extreme k_La values in order to assess if the processes at the two scales respond in the same way to k_La variation.

Based on the results shown in Figures 5.2 and 5.3, a k_La value of 45 h^{-1} ± 5 h^{-1} was taken to represent the "low k_La" process while a k_La value of 180 h^{-1} ± 10 h^{-1} was taken to represent the "high k_La" process. To determine how these changes affect the desired process performance, it should be noted that Doig et al. (2001, 2002) reported optimal process performance when induction was carried out at a fermentation DOT of between 5 – 10% and biomass concentrations of ≈ 5 $g.l^{-1}$ was used during the bioconversion stage.

5.3.3 Fermentation and bioconversion at "low" k_La value

Experiments were carried out to determine whether at a "low" k_La value of 45 h^{-1} ± 5 h^{-1} comparable results for key fermentation parameters such as growth rate and final biomass concentration, and bioconversion parameters such as rate of product formation, specific activity and yield could be achieved.

Figure 5.7 shows the fermentation profile of *E. coli* TOP10 [pQR239] grown in the 96 DSW plates and 2 l stirred bioreactor under these "low" k_La conditions. These results show a good agreement in terms of fermentation kinetic data such as growth rate and biomass yield. The average maximum growth rate in the stirred bioreactor was 0.52 ± 0.04 h^{-1}, while the 96 DSW plate achieved a maximum growth rate of 0.54 ± 0.04 h^{-1}. The average final biomass concentration achieved in the stirred bioreactor was 4.4 ± 0.4 $g.l^{-1}$ while in the 96 DSW plate it was 4.1 ± 0.2 $g.l^{-1}$. From these results it can be seen that there is no considerable difference between the two scales.

For the bioconversion step (Figure 5.8), the average rates of product formation were 16.0 ± 0.5 $\mu mol.l^{-1}.h^{-1}$ in the stirred bioreactor and 13.3 ± 2.1 $\mu mol.l^{-1}.h^{-1}$ in the 96 DSW plate. The average specific activities were 3.6 ± 0.1 $U.min^{-1}.g_{DCW}^{-1}$ in the stirred bioreactor and 3.2 ± 0.5 $U.min^{-1}.g_{DCW}^{-1}$ in the 96 DSW plate. Bioconversion yields of 19.2 ± 0.3 % in the stirred bioreactor and 23.3 ± 0.7 % in the 96 DSW plate were achieved under the same low k_La values (Figure 5.8). No significant difference was observed between the kinetic data of the bioconversion stage under the same low k_La values as the fermentation.

Figure 5.9 shows DOT measured profiles at both scales for these processes operations and this "low" k_La value. The DOT profiles, though noisy, show that induction was carried out during the early exponential phase when the DOT was less than 10% as recommended by Doig et al. (2002). However, there was poor biomass production due to the lack of oxygen during the later stages of the fermentation. The subsequent bioconversions were also adversely affected by the low levels of biomass produced during fermentation and the lack of oxygen available to maintain bioconversion activity.

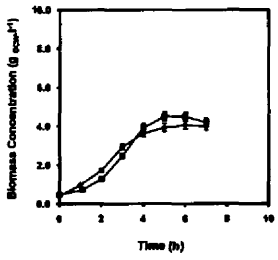

Figure 5.7 Fermentation kinetics of *E. coli* TOP10 [pQR239] biocatalyst at a matched k_La value of 45 ± 5 h^{-1}: 96 DSW plate with 1000 µl fill volume (■) and 2 l stirred bioreactor (♦). Experiments performed as described in Sections 2.6.1.3 and 2.6.1.6 respectively. Error bars represent the range of measured values about the mean.

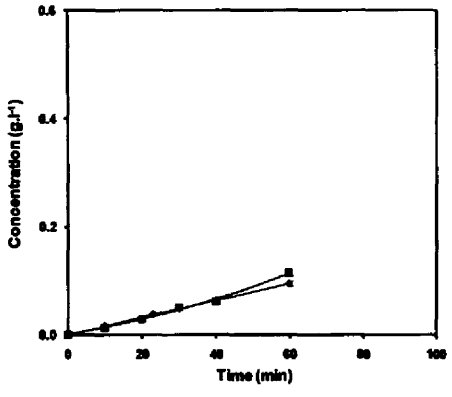

Figure 5.8 Bioconversion kinetics of bicyclo[3.2.0]hept-2-en-6-one at a matched k_La value of 45 ± 5 h^{-1} using a whole cell *E. coli* TOP10 [pQR239] biocatalyst: 96 DSW plate with 1000 µl fill volume (■) and 2 l stirred bioreactor (♦). Experiments performed as described in Section 2.6.1.5 and 2.6.1.6 respectively. Error bars represent the range of measured values about the mean.

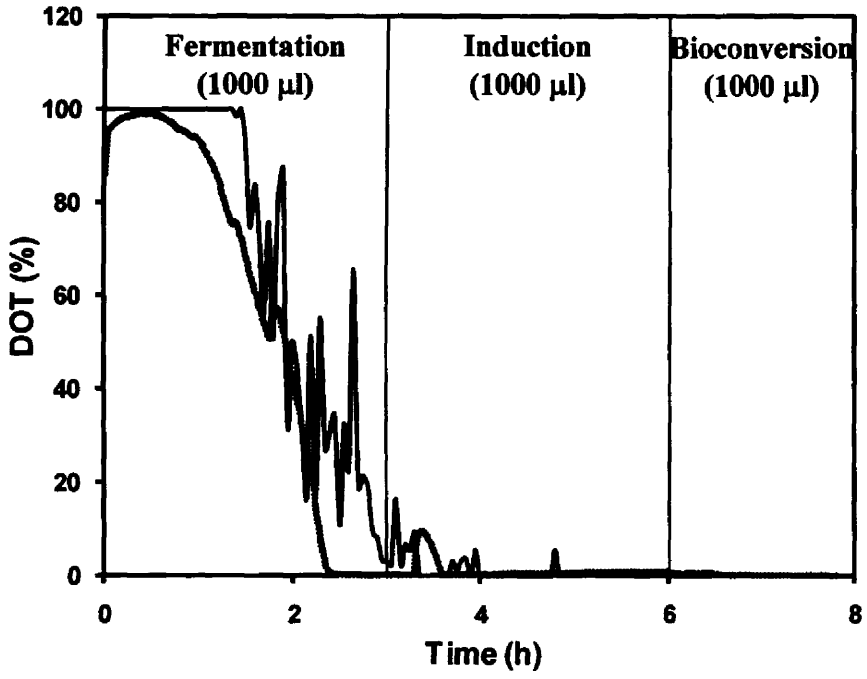

Figure 5.9 DOT profiles measured throughout the 96 DSW plate scale (gray line) and the 2 l stirred bioreactor scale (black line) fermentation and bioconversion processes performed at matched k_La of 45 ± 5 h^{-1}. Experiments performed as described in Section 2.4.3.

The fermentations carried out under "low" k_La conditions did not show any sudden rise on DOT after hours of fermentation, not even after the addition of the biocatalysts substrate. It is likely that mass transfer of oxygen caused it to become the limiting substrate early on in the fermentation, retarding cell growth and later enzyme production. As oxygen became limited early on the fermentation, the carbon source used for growth and other nutrients were most likely consumed at a slower pace and did not become limited during the either the fermentation or bioconversion stages (Kensy et al., 2005). An aerobic fermentation that becomes oxygen limited is likely to become a mixed acid fermentation resulting in the production of compounds such as acetate, formate and succinate (Lee, 1996), as pockets of culture broth are anaerobic and others are aerobic; this was previously explored in section 3.4.2. In the stirred bioreactor, pH values steadily decreased 3 hours after inoculation, from 7 to 6 within one hour, remaining at the latter value for remaining of the fermentation. This drop coincides with the time when oxygen became limited in the fermentation, demonstrating that it became a mixed acid fermentation (Section 3.4.2).

5.3.4 Fermentation and bioconversion at "high" k_La value

Experiments were also carried out to determine how "high" k_La values would affect the kinetic parameters for fermentation (such as growth rate and final biomass) and bioconversion (such as rate of product formation, specific activity and yield). The fermentation was carried out at a matched k_La value of 180 h^{-1} ± 10 h^{-1} in the stirred bioreactor and 96 DSW plate.

The fermentation profile of *E. coli* TOP10 [pQR239] grown in 96 DSW plates and the 2 l stirred bioreactor under these "high" k_La values can be seen in Figure 5.10.

These results show a good agreement between the two scales in terms of fermentation kinetic data, such as growth rate and biomass yield. The average final biomass concentration achieved in the stirred bioreactor was 7.8 ± 0.5 $g.l^{-1}$ while in the 96 DSW plate it was 8.1 ± 0.8 $g.l^{-1}$. The average final growth rate for the fermentations carried out in the stirred bioreactor was 0.49 h^{-1} ± 0.01 h^{-1}, while the 96 DSW plate fermentations achieved 0.53 ± 0.01 h^{-1}. From these results it can be observed that there is no significant difference between scales.

The whole cell bioconversion profile of bicycloketone also presents good agreement in terms of biocatalysis kinetic parameters at the two scales under matched "high" k_La conditions. The average reaction rates were 18.2 ± 2.3 $\mu mol.l^{-1}.h^{-1}$ in the stirred vessel and 13.6 ± 2.8 $\mu mol.l^{-1}.h^{-1}$ in the 96 DSW plate. The average specific activities were 2.8 ± 1.2 $U.min^{-1}.g_{BDW}^{-1}$ in the stirred vessel and 1.6 ± 0.3 $U.min^{-1}.g_{BDW}^{-1}$ in the 96 DSW plates while yields of 30.0 ± 1.3 % in the stirred vessel and 27.1 ± 0.6 % in the 96 DSW plates under the same high k_La value conditions were obtained (Figure 5.11).

Previous work (Doig et al., 2000) has demonstrated that higher than 5 to 10% DOT levels during induction reduce enzyme activity, with the highest activity levels achieved when induction is carried out near zero DOT conditions. Figure 5.12 shows the DOT profile of fermentations at these "high" k_La values. The fermentations were seen not to be oxygen limited and so the requirement for low DOT values at induction was not met. This was then likely to have negatively affected enzyme production and so the measured rate of product formation was lower than that for the low and medium k_La values. The high biomass concentrations at the end of the fermentations might also explain the decrease in CHMO activity.

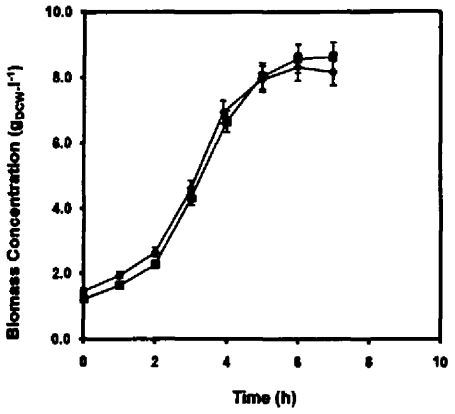

Figure 5.10 Fermentation kinetics of *E. coli* TOP10 [pQR239] biocatalyst at a matched k_La value of 180 ± 10 h^{-1}: 96 DSW plate with 500 µl fill volume (■) and 2 l stirred bioreactor (♦). Experiments performed as described in Sections 2.6.1.3 and 2.6.1.6 respectively. Error bars represent the range of measured values about the mean.

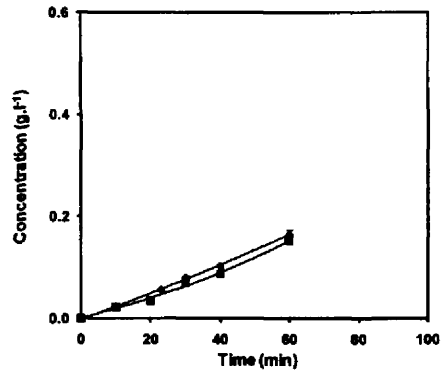

Figure 5.11 Bioconversion kinetics of bicyclo[3.2.0]hept-2-en-6-one at a matched k_La value of 180 ± 10 h^{-1} using a whole cell *E. coli* TOP10 [pQR239] biocatalyst: 96 DSW plate with 200 µl fill volume (■) and 2 l stirred bioreactor (♦). Experiments performed as described in Section 2.6.1.5 and 2.6.1.6 respectively. Error bars represent the range of measured values about the mean.

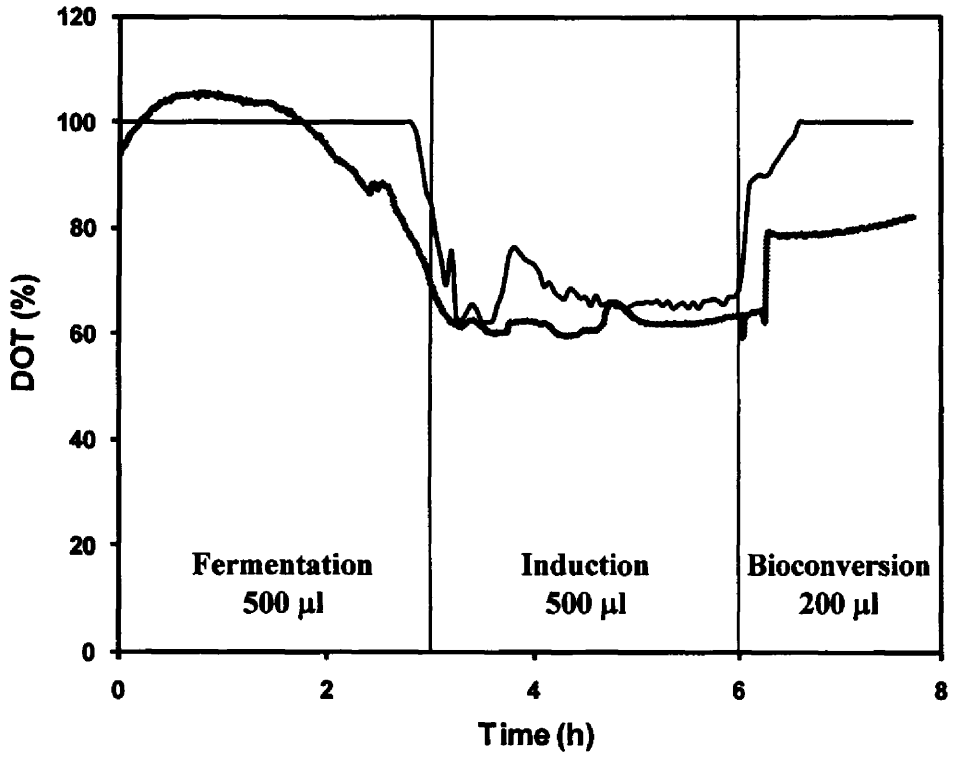

Figure 5.12 DOT profiles measured throughout the 96 DSW plate scale (gray line) and the 2 l stirred bioreactor scale (black line) fermentation and bioconversion processes performed at matched k_La of 180 ± 10 h^{-1}. Experiments performed as described in Section 2.4.3.

As shown in Figure 5.12 the fermentations carried out at "high" k_La values did show the sudden rise in DOT after 6 hours of fermentation upon commencement of the bioconversion. It is likely that although oxygen was sufficient for growth, the combined effects of carbon source and other nutrients depletion and the addition of biocatalysts substrate, which is known to be hazardous to the cell membrane (Doig et al., 2002) promoted this effect (Kensy et al., 2005); this was previously explored in section 5.3.1.

5.3.5 Process comparison at different k_La values

Table 5.5 compares the performance of the combined fermentation and bioconversion processes at the different k_La values and scales in terms of the key kinetic parameters. These values were selected to represent extremes as well as standard operating conditions that can be achieved in both the 96 DSW plate and the 2 l stirred bioreactor scales. The results indicate that there was generally very good agreement in the various kinetic parameters between the two scales when these processes are performed at matched k_La values.

Comparisons between fermentation and bioconversion the processes operated at "low" and "high" k_La values show that the fermentations performed at "high" k_La values displayed an almost two fold increase in the final biomass yield compared to the process at "low" k_La values. However, growth rates remained similar. The bioconversion process was negatively affected at both "low" and "high" k_La values. The "low" k_La process stages were both oxygen limited and so hindered the ability of the biocatalyst to grow and to carry out the oxidation reaction. Conversely, the "high" k_La process resulted in high levels of oxygen in the fermentation culture medium resulting in low levels of BVMO activity as high oxygen concentrations

during induction have been proved to have adverse effects on enzyme activity. Therefore although the fermentation produced more cells their capacity to carry out the bioconversion was limited.

Overall however, it is clear that both microscale and bench scale processes respond in similar ways to variations in key process parameters, such as k_La and oxygen transfer rate.

Table 5.5 Comparison of kinetic parameters from microwell and laboratory scale processes performed at matched k_La values. Fermentation and bioconversion parameters calculated as described in Section 2.6.1. "Low", "medium" and "high" kinetic data taken from Figures 5.7 and 5.8, 5.4 and 5.5, 5.10 and 5.11 respectively.

Matched k_La value (h^{-1})	Vessel	Fermentation		Bioconversion		
		μ_{max} (h^{-1})	X_{final} ($g_{DCW}.l^{-1}$)	Rate of lactone formation ($\mu mol.l^{-1}.min^{-1}$)	Specific activity ($U.g_{DCW}^{-1}$)	Yield (%)[1]
Low 45	96 DSW plate	0.54	4.1	13	3	23
	2 l bioreactor	0.52	4.4	16	4	19
Medium 115	96 DSW plate	0.56	5.6	62	11	92
	2 l bioreactor	0.55	5.3	64	12	99
High 180	96 DSW plate	0.53	8.1	14	2	30
	2 l bioreactor	0.49	7.8	18	3	27

(1) Defined as the fraction at conversion of lactone to ketone.

5.4 Summary

In this chapter the microscale whole cell bioconversion process sequence established in Chapters 3 and 4 was successfully replicated at a larger laboratory scale (2800 fold scale translation) in a stirred tank bioreactor. Key process parameters were comparable to those previously reported by Doig et al. (2003) at both microwell and stirred tank bioreactor scales (Table 5.4). The key findings are summarised below.

- Gassing out was suitable method to measure k_La in both stirred bioreactors and 96 DSW plates. It was demonstrated to be a flexible method in order to replicate the measurement conditions in both vessels making it comparable across scales. This method also highlighted the different mechanisms of oxygen transfer in microwell plates (liquid height, diffusivity) and sparged and stirred vessels (bubble size, partial pressure) whilst still producing comparable process performances.

- A range of k_La values could be obtained in 96 DSW plates, which were comparable to those measured in stirred vessels by using different liquid fill volumes and shaking speeds in the case of the 96 DSW plate and stirring speeds in the stirred vessel.

- The need for miniaturised online monitoring probes was emphasised when oxygen concentration was found to have adverse effects to process performance, particularly in the case of high k_La processing, when high oxygen concentrations appeared to have reduced the enzyme activity. This

result would have been harder to conclude without the DOT profiles provided by appropriate tools.

- Kinetic data for both fermentation (growth rate and final biomass yield) and bioconversion operations (rate of product formation, specific activity) performed at matched k_La vales showed that the processes responded in almost identical fashion, particularly to the measured DOT profiles presented for each set of operating conditions for the linked process sequences. This validates k_La as a reliable basis for scale-up and translation of shaken microwell plates results to stirred laboratory scale bioreactors.

The wider implications of these results and suggestions for further work will be discussed in the following chapter.

6.0 Conclusions and future work

6.1 Microscale process design, characterisation and parallelisation

In this final chapter the main **conclusions** drawn based upon the experimental data obtained in this thesis are described. These are indicated in **bold** text in the following two sections. Finally in Section 6.3 specific suggestions for future work are made.

Microscale processing techniques are rapidly emerging as a means to increase the speed of bioprocess design and to reduce the material requirements for development. Their potential application in bioprocessing has inspired work regarding microwell mixing and fluid mechanics (Nealon et al., 2006), oxygen transfer (Hermann et al., 2001, 2003; Duetz et al., 2004; Kensy et al., 2005), oxygen sensing (Gernot et al., 2003; Arain et al., 2005), fermentations (Duetz et al., 2000, 2001; Puskelier et al., 2005; Harms et al., 2006), microfiltration (Jackson et al. 2005) and process optimization (Jansen et al., 2003). Automation of these techniques can reduce labour intensity and enable a wider range of process variables to be examined, as well as minimizing human error and maximizing reproducibility (Nealon et al., 2005; Micheletti et al., 2006).

According to Lamsa et al. (2004), when the goal of automated evaluation of enzyme libraries is to identify mutants with a higher specific activity, it is important to design the screening protocol with conditions that will mimic as closely as possible the conditions that the strain would experience in the final large scale process. This consideration was the basis for the work reported in this thesis. An *E. coli* TOP10 [pQR239] whole cell biocatalyst expressing the CHMO from *A. calcoaceticus*

NCIMB 9871 was chosen as the model system for start as the strain has been reasonably researched in this laboratory by Doig et. al. (2001, 2002a, 2002b, 2003) and comparative larger scale data is available up to 55 l scale.

The first stage of the research consisted of identifying the optimal conditions for carrying out microbial fermentations in microwell plates. **As described in Chapter 3, the 96 deep square well format was found to be the most suitable, because of its slightly larger working volume, and its better oxygen transfer compared to 96 SRW.** The results were in agreement with those previously demonstrated by Duetz and Witholt (2001, 2004). This could be because the corners of the wells function as baffles and therefore enhance mass transfer (Doig et al., 2002).

Subsequent studies showed the effects of variations in inoculum concentration, temperature, and shaking speed on fermentation performance in 96 DSW plates. It was possible to quantify the effects of the variables quantitatively in terms of the measured cell growth rate during fermentations and rate of product formation during whole cell bioconversions. **The ability to quantify such changes in process performance makes the 96 DSW format a useful tool for generation of bioprocess design data (Sections 3.3 and 3.5).** The results achieved in the studies reported here were in agreement with previous fermentations carried out with this strain at 55 l scale, where biomass reached $\approx$ 5.5 $g.l^{-1}$ (Doig et al., 2001, 2003). Doig et al. (2002) also reported specific activities in the range of 30 to 35 $U.g_{DCW}^{-1}$ in 96 DSW plates, under similar conditions a specific activity of 22.03 $\mu mol.min^{-1}.g_{DCW}^{-1}$ was achieved in 96 DSW plate in this work (Sections 4.2.3 and 4.2.6).

The bioconversion of bicyclo[3.2.0]hept-2-en-6-one can be product inhibited. The inhibiting concentration of the combined lactone products has been reported as 3.5 $g.l^{-1}$ (Doig et al., 2002). Lander (2002) devised a strategy to increase the productivity the reaction by up to 85% by feeding the ketone under inhibitory

concentrations and removing the product *in-situ* with the use of an activated carbon adsorbent. The design of such bioreactor systems would benefit from the high throughput generation of reaction rate data now possible in microwell plates.

Liquid fill volume is an important factor to be considered when using microwell plates for fermentations and even more so for bioconversions (Section 3.5); oxygen availability is a function of fill volume (Duetz et al., 2004). Limitations in the use of microwell plates were found; the fermentation of *A. calcoaceticus* NCIMB 9871 showed that it is difficult to carry out lengthy fermentations in microwell plates because of excessive evaporation on uncovered wells, while permeable sticky covers used to prevent evaporation affected oxygen mass transfer (Zimmerman et al., 2003) and therefore inhibit the growth of *A. calcoaceticus* while promoting condensation and potential contamination (Section 4.3.1).

The 96 DSW plate format not only achieves good oxygen mass transfer (Duetz et al., 2004), it also has the advantage of higher fermentation throughput, fitting more experiments in the one plate than 24 or 6 well plates. For these reasons this plate format was selected to perform fermentation and bioconversion processes. There are, however, other plate formats in the market with desirable further attributes like the capacity to monitor dissolved oxygen, for example the 96 SRW plates with an integrated fluorescent oxygen sensor, as described in Section 3.4.1 (Figure 1.5). These plates were evaluated to obtain parallel DOT and growth profiles of *E. coli* TOP10 [pQR239]. However in order to give accurate readings, DOT measurements had to be carried out immediately after shaking stops, this prevented fermentations from being carried out in more suitable environments therefore they had to be incubated in the microwell plate reader in order to avoid large transport times between incubator and reader. Microwell plate readers can be unsuitable incubators for fermentations because they have very low agitation rates and therefore cannot achieve k_La values that are representative of other better aerated systems (especially

for aerobic fermentations). Gernot et al. (2003) reached a similar conclusion when they measured k_La values of 10 to 40 h^{-1} using this same type of microwell plates with the same model of plate reader. These are low k_La value when compared to a static well where k_La is $\approx 25\ h^{-1}$ (Hermann et al., 2003).

The possibility of carrying out a whole process sequence in microwell plates was addressed in Section 4.2.1. A microscale sequence at first comprising fermentation, CHMO induction and bioconversion was established and automated. To asses the potential of this approach in bioprocess development, the process was then evaluated over a range of conditions with different CHMO host strains, fermentation media composition as well as the biocatalysis substrate and its initial concentration. A combinatorial approach was used to carry out these experiments, assessing the impact from fermentation to bioconversion of each one of these changes (Figure 4.9 and Table 4.1). **It was shown that the microscale process could differentiate quantitatively between different fermentation and biocatalysis conditions as well as its interactions, such as the effect of changes on carbon source concentration in the bioconversion stage.** For example during the bioconversion of bicyclo[3.2.0]hept-2-en-6-one using *E. coli* JM107 [pQR210] specific activity increased 4 fold with a 2 fold increase in carbon source concentration during fermentation. A similar combinatorial approach was explored previously by Jansen et al. (2003) and Kensy et al. (2005). Jansen et al. (2003) tested the yeast *Zygosaccharomyces rouxii* in 96 SRW microtiter plates, assessing the effects of sodium chloride concentration, pH and temperature on growth and fusel alcohol production. They found similar successful results quantifying and identifying a set of optimal conditions and concluded that microwell plates are a useful initial scale for the generation of early phase bioprocess design data.

6.2 Predictive scale up of microwell results

One of the main challenges for shaken microwell plates is oxygen mass transfer (Section 1.3.3). This is especially relevant for the culture of strict aerobes and oxygen requiring bioconversions. In the case of facultative aerobes, like *E. coli*, enough oxygen needs to be supplied in order to prevent mixed acid fermentation from occurring. It should also be considered that under oxygen limited conditions, growth is slow and product synthesis is limited.

Of the commonly used parameters for scale up, k_La is the most widely researched in microwell scale (Büchs et al., 2001; Hermann et al., 2002; Duetz et al., 2003; Doig et al., 2005 and Kensy et al., 2005). Still, there is a relatively limited amount of research published on k_La values in microwell plates and most deals with new techniques for k_La measurement.

The method to measure k_La used in this work was the gassing out method, reported by Doig et al. (2005) for microwell plates while validating his dimensionless groups' model to calculate mass transfer. This technique was chosen for its robustness, the flexibility to be applied at several scales and for reproducibility. k_La was measured in both 96 DSW microwell plates and 2 l bioreactor using two different fluids; sodium chloride solution and culture medium, in order to assess coalescence in microwell plates and the bioreactor. Coalescence is known to affect mass transfer in stirred vessels, and the degree of coalescence is determined by the presence of additives or contaminants such as surfactant. This was proved in this work, where the absolute k_La values in stirred bioreactors varied with the liquid medium composition. It was necessary to assess the effect of fluid contents on mass transfer in microwell plates, where aeration depends on surface area and surface tension. In microwell plates the fluid contents did not affect the k_La, because there were no bubbles or none that could be seen. Therefore it was concluded that the

coalescence properties of the liquid will have little effect on mass transfer rate at this scale (Section 5.2.2).

The k_La values measured for microwell plates were comparable to those measured in the 2 l bioreactor. The values of k_La in the 96 DSW microwell plate ranged from 16 h^{-1} to 186 h^{-1} (Table 5.1) while the values measured in the 2 l bioreactor ranged from 40 h^{-1} to 168 h^{-1}. Doran (1995) reports that in production fermenters the k_La is typically in the range of 0.02 s^{-1} (72 h^{-1}) to 0.25 s^{-1} (900 h^{-1}) making the measured k_La values in both 96 DSW microwell plates and 2 l bioreactor in range with those observed in much larger vessels. The variations of k_La in microwell plates were dependent on fill volume and agitation conditions (such as rate and orbital shaking diameter) as changes in both parameters have an effect on the surface area (a) by affecting the liquid height (Figures 1.6 and 1.8), therefore a wide range of k_La values can be achieved by the combined variation of the two parameters (Table 1.1), according to the process requirements; this is why the highest k_La values in microwell plates appear much larger than those achieved by the stirred bioreactor. The k_La values found in this work are comparable to those published by other research groups, particularly those researching 96 DSW (Table 5.2). k_La values in microwell plates can be changed by altering the transfer area (a) with modifications to fill volume, well geometry, agitation speed and orbital diameter, while k_L is harder to modify as mass transfer in microwell plates is not really affected by fluid composition. Mass transfer interactions in stirred vessels however are very different and can be affected by the bubble size, which in turn can be affected by the type of sparger, location of the sparger, type of impeller, location of impellers; mass transfer is also affected by fluid properties such as viscosity.

In larger vessels there are ways to reduce the effect of surfactants contained in the fluid. Rosu and Schumpe (2007) established that by adding activated carbon, the liquid-side mass transfer coefficient can be gradually increased. There are other

fluids that can affect mass transfer; oils can increase the oxygen transfer rate by increasing the mass transfer coefficient (k_L), the gas-liquid interfacial area (a), the saturation concentration (C*) or a combination of the three.

One of the main objectives of this work was to investigate the capacity of microwell plates to be used as predictive tools in fermentation and biocatalysis processes, in other words, to investigate if the kinetic data obtained in microscale processes under certain conditions, reflected the events at higher volumes. Table 5.4 demonstrates that it is feasible to use microscale processing as an early indicative tool of how a biocatalyst would behave in a large scale process sequence. Although better yields can be achieved by concentrating the whole cell biocatalyst (Doig et al., 2002; Lander, 2002) or using *in-situ* product removal techniques for the slow release of the biocatalysis substrate (Doig et al., 2002b), it was decided that a better assessment of the use of microwell plates could be obtained using a linked process sequence.

This work also found that microscale bioprocessing can reflect changes in kinetic data that occur as a response to changes in the process set up. Table 5.5 demonstrates good correlation in process performance at different oxygen transfer conditions at both scales in terms of the key kinetic parameters. As previously considered, the changes in fill volume and agitation rates permit a wide range of k_La values to be achieved in microwell plates (Kensy et al., 2005), this in turn allows for the flexibility of meeting particular process requirements regarding oxygen mass transfer. This is demonstrated in Chapter 5, where **dissolved oxygen profiles produce similar patterns, according to their matched k_La values.** One of the main advantages of k_La as a scale up parameter is its flexibility regarding the type and size vessel as long as oxygen requirements are met.

These results show how microscale processing can also reflect larger scales regarding the response of process to changes in its kinetic parameters; this is especially useful when assessing a large number of colonies or a big biocatalyst library as it can help differentiate between the mutations that deliver beneficial phenotypic changes that are applicable at larger scales.

Overall it can be concluded that it is possible to obtain quantitative data from microwells regarding the performance of a process sequence at early stages in development, thus aiding the decision making process for further processing or scale up. There is ongoing research regarding microwells as a scale up tool, mostly focused on k_La measurements in a variety of microwell plate geometries using newly developed methods. It was demonstrated in this work that matching k_La values of microwells with those of higher volumes and different systems, such as a 2 l stirred vessel, can yield comparable process kinetic data for fermentation and bioconversions.

6.3 Future work

The microscale process strategy presented in this work can be applied to a larger biocatalyst library to test for its generic applicability. Jansen et al. (2003) and Kensy et al. (2005) have used similar approaches to test other microorganisms in a array of conditions. This demonstrates the flexibility and robustness of this approach to fit different processes and cellular systems, as well as the possibility to quantify them successfully and reproducibly, despite the small volumes.

While sterility can be maintained in short duration open well fermentations, sterility was hard to guarantee over lengthy ones, even with the use of filter lids in the case of *A. calcoaceticus* NCIMB 9871. Aditionally, these adaptors cannot fully prevent

evaporation and create condensation drops at the top of the well which can encourage contamination. It is therefore necessary to work in better contained environments, such as a robotically encoded cabinet, to overcome these hurdles and to increase the experimental throughput.

More microscale processing research is required in downstream processing on different unit operations such as filtration and centrifugation in order to create microscale linked processes that can give preliminary data regarding the performance of a process sequence. Also new ways to control pH and oxygen transfer during fermentations or reactions that are non intrusive and reliable are needed. Strategies to have continuous feeding to the microwell plate can also be designed. Agitation must be optimised to avoid precipitation of heavy particles, when these are required, and the need for further understanding mass transfer in 3 phase system in microwell plates.

Different parameters, such as momentum, heat and mass transfer of microwell plates of different geometries and volumes must be thoroughly explored, addressing questions such as the impact of culture medium components in oxygen transfer, particularly in the measurement of k_L and a; different type of cultures must be tested, including yeast and filamentous fungus as well as other type of fluids, as these fermentations present an entirely new set of issues such as viscosity, rheology and its effect on oxygen mass transfer; as mass transfer mechanism are different in microwell plates and stirred vessels, these properties have different effects upon it, making microwell plates less able to reflect process performance in larger volumes. Furthermore, recently developed models for the calculations of k_La (Doig et al., 2005) must be put under test with these systems.

In summary shake flasks have been to date the standard choice for early stage bioprocess development work, and have the flexibility of not requiring any new

equipment from what most research laboratories already have. However, microscale processing techniques now look very promising and provide a high throughput, potentially automated development platform that could provide data that reflects larger scales performance.

7.0 References

Alphand, V., Archelas, A., Furstoss R. (1990). Microbiological transformations 13: a direct synthesis of both S and R enantiomers of 5-hexadecanolide via an enantioselective microbiological Baeyer-Villiger reaction. *J Org Chem.* **55**, 347–50.

Alphand, V., Carrea, G., Wohlgemuth, R., Furstoss, R., Woodley, J. M. (2003). Towards large-scale synthetic applications of Baeyer-Villiger monooxygenases. *Trends Biotech.*, **21** (7), 318 – 323.

Amanullah, A., Hewitt, C.J., Nienow, A.W., Lee, C., Chartrain, M., Buckland, B.C., Drewc, S.W., Woodley, J.M. (2002). Fed-batch bioconversion of indene to *cis*-indandiol. *Enzyme and Microbial Tech.* **31**, 954–967.

Amanullah, A., Hewitt, C.J., Nienow, A.W., Lee, C., Chartrain, M., Buckland, B.C., Drewc, S.W., Woodley, J.M. (2003). Measurement of strain-dependent toxicity in the indene bioconversion using multiparameter flow cytometry. *Biotech. Bioeng.* **81** (4), 406 – 420.

Amao, Y., Asai, K., Okura, I. (2000). Oxygen sensing based on lifetime of photoexcited triplet state of platinum porphyrin–polystyrene film using time-resolved spectroscopy. *J. Porphyrins Phthalocyanines* **4**, 292–299.

Arain, S., Weiss, S., Heinzle, E., Gernot, J. T., Krause, C., Klimant, I. (2005). Gas sensing in microplates with optodes: influence of oxygen exchange between sample, air, and plate material. *Biotech. Bioeng.* **90** (3), 271 – 280.

Aucamp, J. P., Cosme, A. M., Lye, G. J., Dalby, P. A. (2005). High-throughput measurement of protein stability in microtiter plates. *Biotech. Bioeng.* **89** (5), 599 – 607.

Bailey, J. E., Ollis, D. F. (1986).Biochemical Engineering Fundamentals, McGraw Hill, Second edition.

Baldwin, C. V. F., Woodley, J. M. (2006). On oxygen limitation in a whole cell biocatalytic Baeyer-Villiger oxidation process. *Biotech. Bioeng.* **95** (3), 362-369.

Baminger, U., Ludwig, R., Galhaup, C., Leitner, C., Kulbe, K. D., Haltrich, D. (2001). Continuous enzymatic regeneration of redox mediators used in bio-transformation reactions employing flavoproteins. *J. Mol. Cat. B: Enz.* **11**, 541 – 550.

Barclay, S. A. (2001). The production and use of cyclohexanone monooxyegenases for Baeyer-Villiger biotransformations. Department of Chemical and Biochemical Engineering. University College London.

Beauhaire, J., Ducrot, P., Malosse, C., Rochat, C., Ndiege, I. O. and Otieno, D.O. (1995). Identification and synthesis of sordidin, a male pheromone emitted by *Cosmopolites sordidus*. *Tetrahedron Lett.* **36**, 1043-1046.

Berg, B., Undisz, K., Thiericke, R., Moore, T., Posten, C. (2000). Miniaturization of an enzyme assay (β-Galactosidase) in the 384- and 1536-well plate format. *J. Biomol. Screen.* **5** (1), 71 – 76.

Berg, B., Undisz, K., Thiericke, R., Zimmermann, P., Moore, T., Posten, C. (2001). Evaluation of liquid handling conditions in microplates. *J. Biomol. Screen.* **6** (1), 47 – 56.

Bocola, M., Schulz, F., Leca, F., Vogel, A., Fraaije, M. W., Reetza, M. T. (2005) Converting phenylacetone monooxygenase into phenylcyclohexanone monooxygenase by rational design: towards practical Baeyer-Villiger monooxygenases. *Adv. Synth. Catal.* **347**, 979 –986.

Boettner, M., Prinz., B., Holz, C., Stahl, U., Lang, C. (2002). High-throughput screening for expression of heterologous proteins in the yeast *Pichia pastoris. J. Biotech.* **99**. 51 – 62.

Brunati, M., Marinelli, F., Bertolini, C., Gandolfi, R., Daffonchio, D., Molinari F. (2004). Biotransformations of cinnamic and ferulic acid with actinomycetes. *Enz. Micro. Tech.* **34**, 3 – 9.

Buckland, B. C., Robinson, D. K., Chartrain, M. (2000) Biocatalysis for pharmaceuticals: status and prospects for a key technology. *Metabolic Eng.* **2**, 42 – 48.

Büchs, J. (2001). Introduction to advantages and problems of shaken cultures. *Biochem. Eng. J.* 7, 91 – 98.

Büchs, J., Lotter, S., Milbradt, C. (2001). Out-of-phase operating conditions, a hitherto unknown phenomenon in shaking bioreactors. *Biochem. Eng. J.* 7, 135 – 141.

Burbaum, J. J. (1998) Miniaturization technologies in HTS: how fast, how small, how soon?. *Drug Discovery Today*, **3** (7), 313 – 322.

Carnell, A.J., Roberts, S.M., Sik, V. and Willets, A.J. (1991). Microbial oxidation of 7endo-Methylbicyclo[3.2.0]hept-2-en-6-one, 7,7-Dimethylbicyclo[3.2.0]hept-2-

en-6-one and 2exo-Bromo-3endo-hydroxy-7,7-dimethylbicyclo[3.2.0]heptan-6-one using *Acinetobacter* NCIMB 9871. *J. Chem. Soc. Perkin. Trans.* **10**, 2385-2389.

Casey, J.T., O'Cleirigh, C., Walsh, P.K., O'Shea, D.G. (2004) Development of a robust microtiter plate-based assay method for assessment of bioactivity. *J. Microbio. Methods*, **58**, 327– 334.

Chae, H. J., DeLisa, M. P., Cha, H. J., Weigand, W. A., Rao, G., Bentley, W. E., (2000). Framework for online optimization of recombinant protein expression in high-cell-density escherichia coli cultures using GFP-fusion monitoring. *Biotech. Bioeng.* **69** (3), 275 – 285.

Chang, H. N., Halard, B., Moo-Young, M. (1989). Measurement of $k_l a$ by a gassing-in method with oxygen-enriched air. *Biotech. Bioeng.* **34**, 1147-1157.

Cheetham, P. (1994). case studies in applied biocatalysis-from ideas to products. *Applied Biocatalysis*, 47-108. Edited by Cabral, J., Best, D., Boross, L. and Tramper, H. Harwood Academic Publishers, London.

Clements, L. D., Miller B. S., Streips, U. N. (2002). Comparative growth analysis of the facultative anaerobes *Bacillus subtilis*, *Bacillus licheniformis*, and *Escherichia coli*. *System. Appl. Microbiol.* **25** (2), 284-286

Corma, A., Nemeth, L.T., Renz, M. and Valencia, S. (2001). Sn-Zeolite Beta as a heterogeneous chemoselective catalyst for Baeyer-Villiger oxidations. *Nature* **412**, 423-425.

Cotter, P. A., Darie, S., Gunsalus, R. P. (1992). The effect of iron limitation on expression of the aerobic and anaerobic electron transport pathway genes in Escherichia coli. *FEMS Microbio. Letters* **100** (1-3), 227 – 232.

Das, J. R., Bhakoo, M., Jones, M. V., Gilbert, P. (1998). Changes in the biocide susceptibility of *Staphylococcus epidermidis* and *Escherichia coli* cells associated with rapid attachment to plastic surfaces. *J. Appl. Microbiol.* **84**, 852 – 858.

Devlin, J.P. (1997). Chemical Diversity and Genetic Equity: Synthetic and naturally derived compounds in high throughput screening: the discovery of bioactive substances, 3-48. Edited by Devlin, J.P. Marcel Dekker Inc., New York

Doig S. D., Avenell P. J., Bird P. A., Gallati P., Lander K. S., Lye G. J., Wohlgemuth R., Woodley J. M. (2002). Reactor operation and scale up of whole cell Baeyer – Villiger catalyzed lactone synthesis. *Biotechnol. Prog.* **18**, 1039-1046.

Doig, S. D., Pickering, S. C. R., Lye, G. J., Woodley, J. M. (2002). The use of microscale processing technologies for quantification of biocatalytic Baeyer – Villiger oxydation kinetics. *Biotech. Bioeng.* **80** (1). 42 – 49.

Doig, S. D., Pickering, S. C. R., Lye, G. L., Baganz, F. (2005). Modelling surface aeration rates in shaken microtitre plates using dimensionless groups. *Chem. Eng. Sc.* **60**, 2741 – 2750.

Doig, S. D., Simpson, H., Alphand, V., Fustoss, R., Woodley, J. M. (2003). Characterization of a recombinant *Escherichia coli* TOP10 [pQR239] whole-cell biocatalyst for stereoselective Baeyer–Villiger oxidations. *Enzyme and Microbial Tech.* **32** 347–355.

Donoghue, N.A. and Trudgill, P.W. (1975). The metabolism of cyclohexanol by *Acinetobacter* NCIB 9871. *Eur. J. Biochem.* **60**, 1-7

Donoghue N.A., Norris D. B., Trudgill P. W. (1976). The purification and properties of cyclohexanone oxygenase from *Nocardia globerula* CL1 and *Acinetobacter* NCIMB 9871. *Eur J. of Biochem* **63** 175-192.

Doran, M. P. (1995). Bioprocess Engineering Principles. *Academic Press*, first edition.

Duetz, W. A., Rüedi, L., Hermann, R., O'Connor, K., Büchs, J., Witholt, B. (2000). Methods for intense aeration, growth, storage, and replication of bacterial strains in microtiter plates. *Appl. Environ. Microbiol.* **66** (6), 2641 – 2646.

Duetz, W. A., Witholt, B. (2001). Effectiveness of orbital shaking for the aeration of suspended bacterial cultures in square-deepwell microtiter plates. *Biochem. Eng. J.* 7, 113 – 115.

Duetz, W. A., Witholt, B., (2004). Oxygen transfer by orbital shaking of square vessels and deepwell microtiter plates of various dimensions. *Biochem. Eng. J.* **17**, 181 – 185.

El-mansi, M., Bryce, C. F. A. (1999) Fermentation microbiology and biotechnology. *Taylor and Francis Ltd.*, first edition.

Elmahdi, I., Baganz, F., Dixon, K., Harrop, T., Sugden, D., Lye, G. J. (2003). pH control in microwell fermentations of *S. erythraea* CA340: influence on biomass growth kinetics and erythromycin biosynthesis. *Biochem. Eng. J.* **16**, 299 – 310.

Fernandes, P., Cabral, J. M. S. (2006). Microlitre/millilitre shaken bioreactors in fermentative and biotransformation processes - a review. *Biocat. Biotrans.* **24** (4), 237 – 252.

Gagnon, R., Grogan, G., Roberts, S.M., Villa, R. and Willets, A.J. (1995). Enzymatic Baeyer-Villiger oxidations of Some Bicyclo[2.2.1]heptan-2-ones using monooxygenases from *Pseudomonas putida* NCIMB 10007: enantioselective preparation of a precursor of azadirachtin. *J. Chem. Soc. Perkin. Trans.* (12), 1505 – 1511

Garcia-Ochoa, F., Gomez, E. (2005). Prediction of gas-liquid mass transfer coefficient in sparged stirred tank bioreactors. *Biotech. Bioeng.* **92** (6), 761 – 772.

Gernot, T. J., Heinzle, E. (2001). Quantitative screening method for hydrolases in microplates using pH indicators: determination of kinetic parameters by dynamic pH monitoring. *Biotech. Bioeng.*, **72** (6) 620 – 627

Gernot, T. J., Klimant, I., Wittmann, C., Heinzle, E. (2003) Integrated optical sensing of dissolved oxygen in microtiter plates: a novel tool for microbial cultivation. *Biotech. Bioeng.* **81** (7). 829 – 836.

Gill, N. K., Appleton, M., Baganz, F., Peacock, M., Lye, G. J. (2006). Design and instrumentation of a novel miniature bioreactor system for high throughput fermentation optimisation. Submited for publication to *Biochem. Eng. J.*

Girard, P., Jordan, M., Tsao, M., Wurm, F. M. (2001). Small-scale bioreactor system for process development and optimization. *Biochem. Eng. J.* 7, 117 – 119.

Gogate, P. R., Beenackers, A. A. C. M., Pandit A. B. (2000). Multiple-impeller systems with a special emphasis on bioreactors: a critical review. *Biochem. Eng. J.* **6**, 109–144.

Gomes, N., Aguedo, M., Teixeira, J., Belo, I. (2007). Oxygen mass transfer in a biphasic medium: Influence on the biotransformation of methyl ricinoleate into γ-decalactone by the yeast *Yarrowia lipolytica*. *Biochem. Eng. J.* **35**, 380–386.

Harms, P., Kostov, Y., French, J. A., Soliman, M., Anjanappa, M., Ram, A., Rao, G. (2006). Design and performance of a 24-station high throughput microbioreactor. *Biotech. Bioeng.* **93** (1), 6 – 13.

Hashimoto, S., Ozaki, A., (1999). Whole microbial cell processes for manufacturing amino acids, vitamins or ribonucleotides. *Current Opinion in Biotech.* **10**, 604–608.

Hermann, R., Lehmann, M., Büchs, J. (2003). Characterization of gas–liquid mass transfer phenomena in microtiter plates. *Biotech. Bioeng.* **81** (2). 178 – 186.

Hermann, R., Walther, N., Maier, U., Büchs, J. (2001). Optical method for the determination of the oxygen-transfer capacity of small bioreactors based on sulfite oxidation. *Biotech. Bioeng.* **74** (5), 355 – 363.

Hibbert, E.G., Dalby, P. A. (2005). Directed evolution strategies for improved enzymatic performance. *Microbial Cell Factories* **4** (29).

Hilker, I., Baldwin, C., Alphand, V., Furstoss, R., Woodley, J. M., Wohlgemuth, R. (2005). On the influence of oxygen and cell concentration in an sfpr whole cell biocatalytic baeyer–villiger oxidation process. *Biotech. Bioeng.* **93** (6), 1138 – 1144.

Hilker, I., Wohlgemuth, R., Alphand, V., Furstoss, R. (2005). Microbial transformations 59: first kilogram scale asymmetric microbial Baeyer-Villiger oxidation with optimized productivity using a resin-based in situ SFPR strategy. *Biotech. Bioeng.* **92** (6), 702 – 710.

Hixson, A. W., Caden, E. L. (1950) Oxygen transfer in submerged fermentation. *Ind. Eng. Chem.* **42** (9), 1792 – 1801.

Holme, D. J., Peck, H. (1998). Analytical Biochemistry. Prentice Hall (third edition).

Hogan, M.C. and Woodley, J.M. (2000). Modelling of two enzyme reactions in a linked cofactor recycle system for chiral lactone synthesis. *Chem. Eng. Sci.* **55**, 2001-2008

Hudcova, W., Machon, W., Nienow, A. W., (1989). Gas-liquid dispersion with dual Rusthon Turbine Impellers. *Biotech. Bioeng.* **34**, 617 – 628.

Ishige, T., Honda, K., Shimizu, S. (2005). Whole organism biocatalysis. *Current Opinion in Chem. Bio.* **9**, 174–180.

Jackson, N. B., Liddell, J. M, Lye, G. J. (2006). An automated microscale technique for the quantitative and parallel analysis of microfiltration operations. Article submitted for publishing to *J. Membrane Sc.*

Jansen, M., Veurink, J. H., Euverink, G. W., Dijkhuizen, L. (2003). Growth of the salt-tolerant yeast *Zygosaccharomyces rouxii* in microtiter plates: effects of NaCl, pH and temperature on growth and fusel alcohol production from branched-chain amino acids. *FEMS Yeast Research* **3**, 313 – 318.

Jaeger, K., Eggert, T. (2004). Enantioselective biocatalysis optimized by directed evolution. *Current Opinion Biotech.* **15**, 305–313.

Junker, B. H., Reddy, J., Gbewonyo, K., Greasham, R. (1994). On-line and *in-situ* monitoring technology for cell density measurement in microbial and animal cell cultures. *Bioprocess Eng.* **10**, 195-207

Kamerbeek N. M., Janssen, D. B., van Berkel, W. J. H., Fraaije, M. W. (2003). Baeyer-Villiger monooxygenases, an emerging family of flavin-dependent biocatalysts. *Adv. Synth. Catal.* **345**, 667 – 678.

Kawase, Y., Halard, B., Moo-Young, M. (1992). Liquid-phase mass transfer coefficients in bioreactors. *Biotech. and Bioeng.* **39**, 1133 – 1140.

Kaya., Schumpe, A. (2005). Surfactant adsorption rather than "shuttle effect"?. *Chem. Eng. Sc.* **60**, 6504 – 6510.

Kensy, F., John, G. T., Hofmann, B., Büchs, J. (2005). Characterisation of operation conditions and online monitoring of physiological culture parameters in shaken 24-well microtiter plates. *Bioprocess Biosyst. Eng.* **75**, 75–81.

Kensy, F., Zimmermann, H. F., Knabben, I., Anderlei, T., Trauthwein, H., Dingerdissen, U., Büchs, J. (2005). Oxygen transfer phenomena in 48-well microtiter plates: determination by optical monitoring of sulfite oxidation and verification by real-time measurement during microbial growth. *Biotech. Bioeng.* **89** (6), 698 – 708.

Koch, A. (1970). Turbidity measurements of bacterial cultures in some available commercial instruments. *Anal. Biochem.* **38**, 252-259.

Konigsberger, K. and Griengl, H. (1994). Microbial Baeyer-Villiger reaction of bicyclo[3.2.0]heptan-6-ones-a novel approach to Sarkomycin A. *Bioorg. Med. Chem.* **2**, 595-604

Lamping, S. R., Zhang, H., Allen, B., Ayazi-Shamlou, P. (2003). Design of a prototype miniature bioreactor for high throughput automated bioprocessing. *Chem. Eng. Sc.* **58**, 747 – 758.

Lamsa, M. H., Jensen, N. B., Krogsgaard, S. (2004). *Enzyme Functionality*, Chapter 25: screen automation and robotics. Marcel Dekker, Inc. Publishers.

Lander, K. S. "In situ removal of bioconversion product by different resins" 2001. Department of Chemical and Biochemical Engineering, University College London.

Lee, S.Y. (1996). High cell-density culture of *Escherichia coli*. *Trends Biotech.* **14**, 98-105.

León, R., Fernandes, P., Pinheiro, H. M., Cabral, J. M. S. (1998). Whole-cell biocatalysis in organic media. *Enzyme Microbial Tech.* **23**, 483–500.

Li, Z., van Beilen, J. B., Duetz, W. A., Schmid, A., de Raadt, A., Griengl, H., Witholt, B. (2002). Oxidative biotransformations using oxygenases. *Current Opinion Chem. Bio.* **6**,136–144.

Liese, A., Villela-Filho, M. (1999). Production of fine chemicals using biocatalysis. *Current Opinion Biotech.* **10**, 595–603.

Linek, V., Kordač, M., Moucha, T. (2006). Evaluation of the optical sulfite oxidation method for the determination of the interfacial mass transfer area in small-scale bioreactors" *Biochem. Eng. J.* **27**, 264 – 268.

Liu D. J., Perdue R. K., Sun L., Crooks R. M., (2004). Inmobilization of DNA onto poly (dimetylsiloxane) surfaces and application to a microelectrochemcial enzyme-

amplified DNA hybridization assay. *The ACS J. of surfaces and colloids.* **20**, 5905-5910.

Lorenz, P., Eck, J., (2004). Screening for novel industrial biocatalysts. *Eng. Life Sci.* **4** (6), 501 – 504.

Lotter, S., Büchs, J. (2004). Utilization of specific power input measurements for optimization of culture conditions in shaking flasks. *Biochem. Eng. J.* **17**, 195 – 203.

Lye, G. J., Ayazi-Shamlou, P., Baganz, F., Dalby, P. J., Woodley, J. M. (2003). Accelerated design of bioconversion processes using automated microscale processing techniques. *Trends. Biotech.* **21** (1). 29 – 37.

Maharbiz, M. M., Holtz, W. J., Howe, R. T., Keasling, J. D. (2004). Microbioreactor arrays with parametric control for high-throughput experimentation. *Biotech. Bioeng.* **84** (4), 376 – 381.

Maier, U., Büchs, J. (2001). Characterisation of the gas–liquid mass transfer in shaking bioreactors. *Biochem. Eng. J.* **7**, 99 – 106.

Maier, U., Losen, M., Büchs, J. (2004). Advances in understanding and modeling the gas–liquid mass transfer in shake flasks. *Biochem. Eng. J.* **17**, 155–167.

Marques, M. P. C., de Carvalho, C. C. C. R., Claudino, J. M. C., Cabral, J. M. S., Fernández, P. (2007) On the feasibility of the microscale approach for a multistep biotransformation: sitosterol side chain cleavage. *J. Chem. Technol. Biotechnol.*, **82** 856 – 863.

Mayr, B., Nagy, E., Horvat, P., Mase, A. (1994). Scale-Up on basis of structured mixing models: a new concept. *Biotech. Bioeng.* **43**, 195 – 206.

Micheletti, M., Barrett, T., Doig, S.D., Baganz, F., Levy, M.S., Woodley, J.M., Lye, G.J. (2006). Fluid mixing in shaken bioreactors: Implications for scale-up predictions from microlitre-scale microbial and mammalian cell cultures. *Chem. Eng. Sc.* **61**, 2939 – 2949.

Micheletti, M., Lye, G. J. (2006). Microscale bioprocess optimisation. *Current Opinion Biotech.* **17**, 611–618

Miyamura, K., Nishio, S., Ito, A., Murata, R., Kono, R. (1974). Micro cell culture method for determination of diphtheria toxin and antitoxin titres using VERO cells. *J. Biological Standardization*, **2** (3). 189 – 192.

Molinari, F., Aragozzini, F., Cabral, J.M.S. and Prazeres, D.M.F. (1997). Continuous production of isovaleraldehyde through extractive bioconversion in a hollow-fiber membrane bioreactor. *Enzyme Microb. Technol.* **20**, 604-611

Moonen, M. J. H., Westphal, A. H., Rietjens, I. M. C. M., van Berkela, W. J. H. (2005). Enzymatic Baeyer--Villiger oxidation of benzaldehydes. *Adv. Synth. Catal.* **347**, 1027 – 1034.

Nealon, A. J., O'Kennedyb, R. D., Titchener-Hooker, N. J., Lye, G. J. (2006). Quantification and prediction of jet macro-mixing times in static microwell plates. *Chem. Eng. Sc.* **61**, 4860 – 4870.

Ni, Y., Chen, R. R. (2004). Accelerating whole-cell biocatalysis by reducing outer membrane permeability barrier. *Biotech. Bioeng.* **87** (6), 804 – 811.

O'Beirne, G.. Hamer, G. (2000). Oxygen availability and growth of Escherichia coli W3110: Dynamic responses to limitation and starvation. *Bioprocess Eng.* **23**, 381 – 387.

Ortiz-Ochoa, K., Doig, S. D., Ward, J. M., Baganz, F. (2005). A novel method for the measurement of oxygen mass transfer rates in small-scale vessels. *Biochem. Eng. J.* **25**, 63 – 68.

Ottolina, G., de Gonzalo, G., Carrea, G., Daniela, B. (2005). Enzymatic Baeyer – Villiger Oxidation of bicyclic diketones. *Adv. Synth. Catal.* **347**, 1035 –1040.

Peter, C. P., Suzukib, Y., Rachinskiya, K., Lottera, S., Büchs, J. (2006). Volumetric power consumption in baffled shake flasks. *Chem. Eng. Sc.* **61**, 3771 – 3779.

Petit, F. and Furstoss, R. (1995). Synthesis of (1S, 5R)-2-8-dioxabicylo[3.3.0]octan-3-one from its enantiomer: a subunit of clerodane derivatives. *Synthesis-Stuttgart* (12), 1517-1520

Pollard, D. J., Woodley, J. M. (2007). Biocatalysis for pharmaceutical intermediates: the future is now. *Trends Biotech.* **25** (2), 66 – 73.

Prescott, L. M., Harley, J. P., Klein, D. A. (2004). Microbiology. *Mc. Graw Hill*, sixth edition.

Pritchard, G.O. and Servedio, F.M. (1975). Excited state kinetics and stern-volmer quenching plots in the photolysis of azoisopropane at 366 nm. *Int. J. Chem. Kinetics* **8**, 99-107.

Pursell, M. R., Mendes-Tatsis, M. A., Stuckey, D. C. (2004). Effect of fermentation broth and biosurfactants on mass transfer during liquid–liquid extraction. *Biotech. Bioeng.* **85** (2), 155 – 165.

Puskeiler, R., Kaufmann, K., Weuster-Botz D. (2005). Development, parallelization, and automation of a gas-inducing milliliter-scale bioreactor for high-throughput bioprocess design (HTBD). *Biotech. Bioeng.* **89** (5), 512 – 523.

Quicker, G., Schumpe, A., Konig, B., Deckwer, W. D. (1981). Comparison of measured and calculated oxygen solubilities in fermentation media. *Biotech. Bioeng.* **23**, 635 – 650.

Renz, M., and Meunier, B. (1999). 100 Years of Baeyer-Villiger oxidations. *Eur. J. Org. Chem.* **4**, 737-750

Roberts, S. M., Willets, A. J. (1993). Development of the enzyme-catalysed baeyer-villiger reaction as a useful technique in organic synthesis. *Chirality* **5**, 334 – 337.

Rosso, D., Huo, D. L., Stenstrom, M. K. (2006). Effects of interfacial surfactant contamination on bubble gas transfer. *Chem. Eng. Sc.* **61**, 5500 – 5514.

Rosu, M., Schumpe, A. (2007). Influence of surfactants on gas absorption into aqueous suspensions of activated carbon. *Chem. Eng. Sc.* **62**, 5458 – 5463.

Rouf, S. A., Moo-Young, M., Scharer, J. M., Douglas, P. L. (2000). Single versus multiple bioreactor scale-up: economy for high-value products. *Biochem. Eng. J.* **6**, 25 – 31.

Samorski, M., Müller-Newen, G., Büchs, J. (2005). Quasi-continuous combined scattered light and fluorescence measurements: a novel measurement technique for shaken microtiter plates. *Biotech. Bioeng.* **91** (1), 61 – 68.

Sardeing, S., Painmanakul, P., Hébrard, G. (2006). Effect of surfactants on liquid-side mass transfer coefficients in gas–liquid systems: a first step to modelling. *Chem. Eng. Sc.* **61**, 6249 – 6260.

Schneider, S., Wubbolts, M. G., Sanglard, D., Witholt, B. (1998). Production of chiral hydroxy long chain fatty acids by whole cell biocatalysis of pentadecanoic acid with an E. coli recombinant containing cytochrome $P450_{BM-3}$ monooxygenase. *Tetrahedron Assymetry* **9**, 2833 – 2844.

Setti, L., Lanzarini, G., Pifferi, P.G. (1997). Whole cell biocatalysis for an oil desulfurization process. *Fuel Process. Tech.* **52**, 145-153.

Shipston, N. F., Lenn, M. J., Knowles, C. J. (1992). Enantioselective whole cell and isolated enzyme catalysed Baeyer-Villiger oxidation of bicyclo[3.2.0]hept-2-en-6-one. *J. Micro. Methods* **15**, 41 – 52.

Sicard, R., Chen, L. S., Marsaioli, A. J., Reymond, J. (2005). A fluorescence-based assay for baeyer –villiger monooxygenases, hydroxylases and lactonases. *Adv. Synth. Catal.* **347**, 1041 – 1050.

Simpson, H. D., Alphand, V., Furstoss, R. (2001). Microbiological transformations 49. Asymmetric biocatalysed Baeyer–Villiger oxidation: improvement using a recombinant Escherichia coli whole cell biocatalyst in the presence of an adsorbent resin. *J. Mol. Cat. B: Enzym.* **16**, 101 – 108.

Stahl, S., Greasham, R. and Chartrain, M. (2000). Implementation of a rapid microbiological screening procedure for biotransformation activities. *J. Biosci. Bioeng.* **4**, 367-371

Steffens, M.A., Fraga, E.S. and Bogle, I.D.L. (2000). Synthesis of bioprocess using physical properties data. *Biotechnol. Bioeng.* **68**, 218-230

Stone, K.M., Roche, F.W., Thornhill, N.F. (1992). Dry weight measurement of microbial biomass and measurement variability analysis. *Biotech. Tech.* **6** (3), 207 – 212.

Sullivan, B. M., Simon, K. D., Nanda, S. K. W., Pocius, J., Scholz, W. K. (2000). Assay development in high density microwell plates: use of well geometries, format, surface modification and optical properties to achieve optimal assay performance. International Symposium for Laboratory Automation and Robotics (ISLAR), Boston, MA, October 15 – 18.

Taschner, M.J. and Chen, Q. (1991). The enzymatic Baeyer-Villiger oxidation: synthesis of the C_{11}-C_{16} subunit of ionomycin. *Bioorg. Med. Chem. Lett.* **1**, 535-538

Tramper, H. (1994). Case studies in applied biocatalysis-from ideas to products. In *Applied Biocatalysis*, 47-108. Edited by Cabral, J., Best, D., Boross, L. and Tramper, H. Harwood Academic Publishers, London

Tramper, J. (1996). Chemical versus biochemical Conversion: when and how to use biocatalysis. *Biotech. Bioeng.* **52**, 290 – 295.

Timmins, M. and Haq, T. "Technical Bulletin #443 Calculating Oxygen Concentration from Fluorescence Data on the BD™ Oxygen Biosensor System"

Turcotte, C., Lacroix, C., Kheadra, E., Grignon, L., Fliss. I. (2004). A rapid turbidometric microplate bioassay for accurate quantification of lactic acid bacteria bacteriocins. *Int. J. Food Microbiol.* **90**, 283– 293.

Turner, C., Rudnitskaya, A., Legin, A. (2003). Monitoring batch fermentations with an electronic tongue. *J. Biotech.* **103**, 87-91.

Urban, P. L, Goodall, D. M., Bruce, N. C., (2006). Enzymatic microreactors in chemical analysis and kinetic studies. *Biotech. Ad.* **24**, 42 – 57.

Van't Riet, K. (1979). Review of measuring methods and results in nonviscous gas-liquid mass transfer in stirred vessels. *Ind. Eng. Chem. Process Des. Dev.* **8** (3), 357 – 364.

Vanags, J. J., Rikmanis, M. A., Ushkans, E. J., Viesturs, U. E. (1990). Stirring Characteristics in Bioreactors. *AIChE J.* **36** (9), 1361 – 1369.

Walsh, C.T. and Chen, Y.C.J. (1988). Enzymic Baeyer-Villiger oxidations by flavin-dependent monooxygenases. *Angew. Chem. Int. Ed. Engl.* **27**, 333-343

Wang, D. I. C., Cooney, C. L., Demain A. L., Dunill, P., Humphrey, A. E., Lilly, M. D. (1979). Fermentations and Enzyme Technologies. John Wiley & Sons Publishers.

Wang S., Kayser M. M., Iwaki H., Lau P. C. K. (2003). Monooxygenase-catalyzed Baeyer–Villiger oxidations: CHMO versus CPMO. *J Mol Cat B Enz* **22**, 211 – 218.

Welch, C.J., Shaimi, M., Biba, M., Chilenski, J.R., Szumigala, R.H., Dolling, U., Mathre, D.J., Reider, P.J. (2002). Microplate evaluation of process adsorbents. *J. Sep. Sci.* **25** (13) 847–850.

Weuster-Botz, D., Puskeiler, R., Kusterer, A., Kaufmann, K., John, G. T., Arnold, M. (2005). Methods and milliliter scale devices for high-throughput bioprocess design. *Bioprocess Biosyst. Eng.* **28**, 109–119.

Willetts, A. (1997). Structural studies and synthetic applications of baeyer-villiger monooxygenases. *Trends Biotechnol.* **15**, 55-62.

Wright, M. A., Taylor, I. N., Lenn, M. J., Kelly, D. R., Mahdi, J. G., Knowles, C. J. (1994). Baeyer-Villiger monooxygenases from microorganisms. *FEMS Micro. Letters*, **116** (1); 67 – 72.

Zambianchi, F., Pasta, P., Carrea, G., Colonna, S., Gaggero, N., Woodley, J. M. (2002). Use of isolated cyclohexanone monooxygenase from recombinant *Escherichia coli* as biocatalyst for Baeyer – Villiger and sulfide oxidations. *Biotech. Bioeng.* **78** (5), 489 – 496.

Zanzotto, A., Szita, N., Boccazzi, P., Lessard, P., Sinskey, A. J., Jensen, K. F. (2004). "Membrane-aerated microbioreactor for high-throughput bioprocessing. *Biotech. Bioeng.* **87** (2), 243 – 254.

Zhang, Z., Szita, N, Boccazzi, P, Sinskey, A. J., Jensen, K. F. (2006). A Well-mixed, polymer-based microbioreactor with integrated optical measurements. *Biotech. Bioeng.* **93** (2), 286 – 296.

Zimmermann, H. F., John, G. T., Trauthwein, H., Dingerdissen, U., Huthmacher, K. (2003). Rapid evaluation of oxygen and water permeation through microplate sealing tapes. *Biotechnol. Prog.* **19**, 1061-1063.

World Wide Web

http://www.bdbiosciences.com/discovery_labware/Products/drug_discovery/polystyrene_microplates/oxygen_biosensor_system/

http://www.presens.de/html/start.html

http://www.bmglabtech.com

Appendix I

Dry Cell Weight Curve for *E. coli* TOP10 [pQR239], *E. coli* JM107 [pQR210] and *A. calcoaceticus* NCIMB 9871

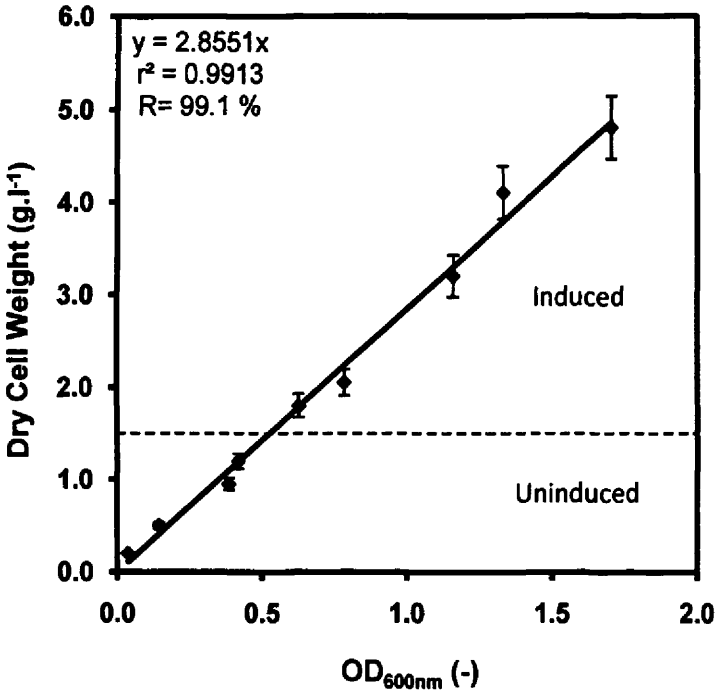

Appendix I.1 Calibration of OD_{600} measurements from an *E. coli* TOP10 [pQR239] fermentation with DCW measurements. OD_{600} was determined as described in Section 2.3.2.2 and DCW was determined as described in Section 2.3.2.1. Linear least squares fitting was carried out and the fitted line had an R^2 value > 0.991. Error bars represent the range of measured values about the mean.

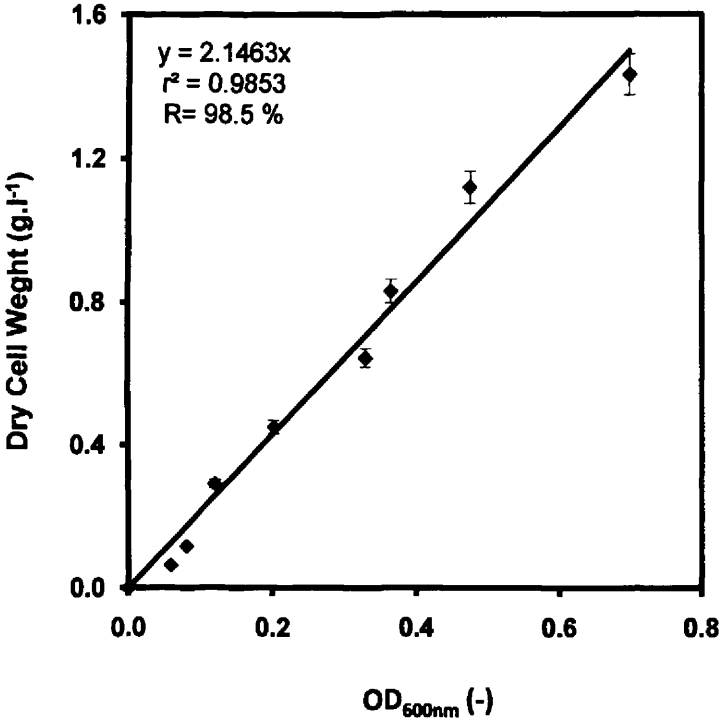

Appendix I.2 Calibration of OD_{600} measurements from an *E. coli* JM107 [pQR210] fermentation with DCW measurements. OD_{600} was determined as described in Section 2.3.2.2 and DCW was determined as described in Section 2.3.2.1. Linear least squares fitting was carried out and the fitted line had an R^2 value > 0.985. Error bars represent the range of measured values about the mean.

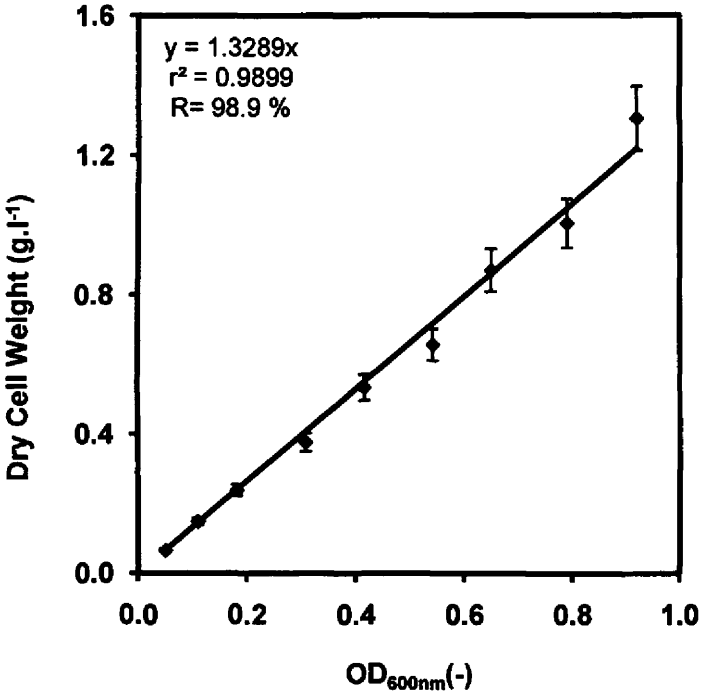

Appendix I.3 Calibration of OD_{600} measurements from *A. calcoaceticus* NCIMB 9871 fermentation with DCW measurements. OD_{600} was determined as described in Section 2.3.2.2 and DCW was determined as described in Section 2.3.2.1. Linear least squares fitting was carried out and the fitted line had an R^2 value > 0.989. Error bars represent the range of measured values about the mean.

Appendix II

Gas chromatography calibration curves for ketones and lactones

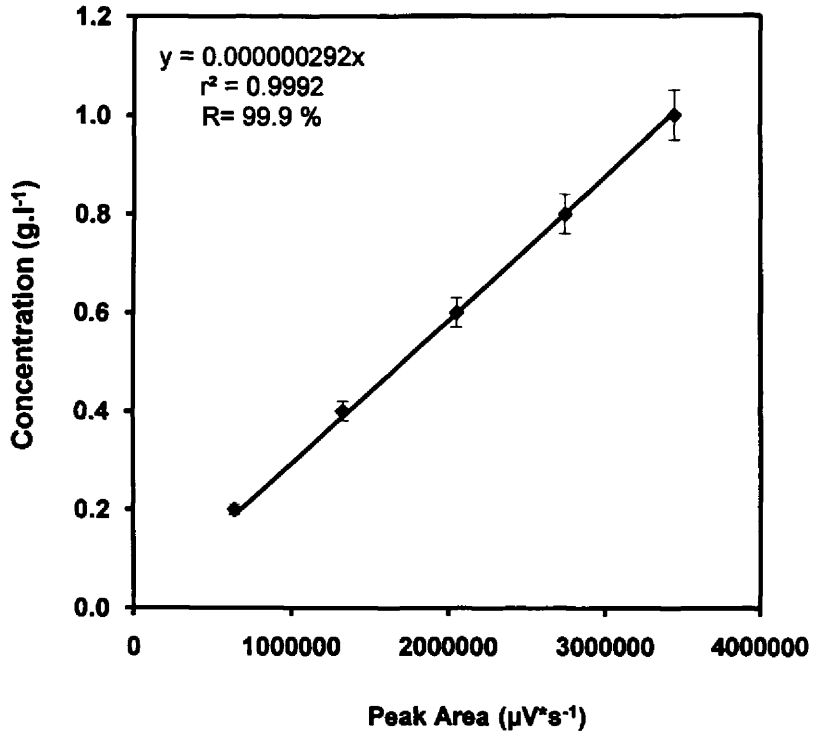

Appendix II.1. Typical calibration curve for bicyclo[3.2.0]hept-2-en-6-one (bicycloketone) in ethyl acetate. Samples were prepared and analysed as described in Section 2.3.1. Linear least squares fitting was carried the fitte lines had an R^2 value > 0.999. Error bars show one standard deviation.

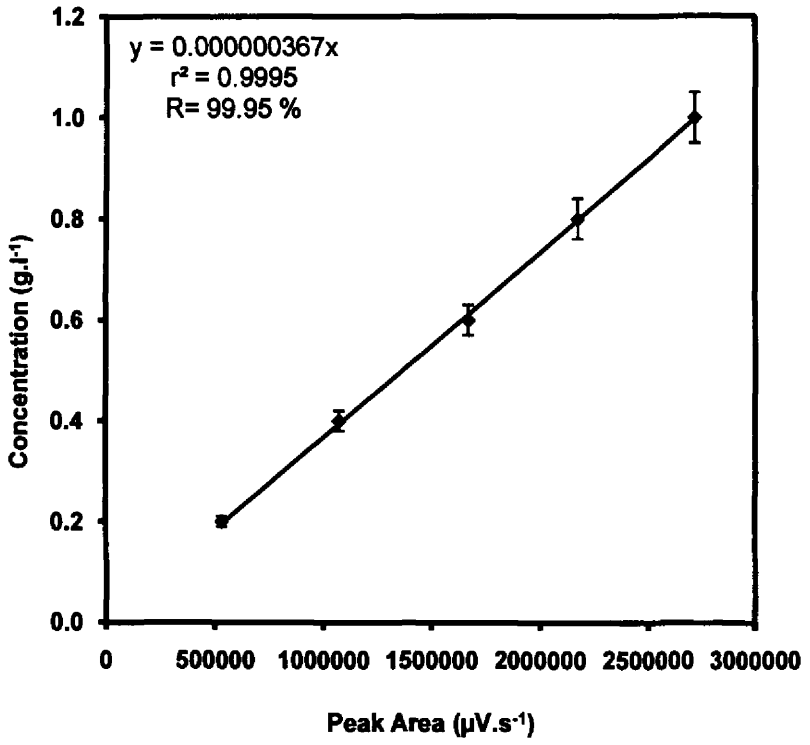

Appendix II.2. Typical calibration curve for (1R, 5S)-2-oxabicyclo[3.3.0]oct-6-en-3-one (bicyclolactone) in ethyl acetate. Samples were prepared and analysed as described in Section 2.3.1. Linear least squares fitting was carried out and the fitted line had an R^2 value > 0.999. Error bars show one standard deviation.

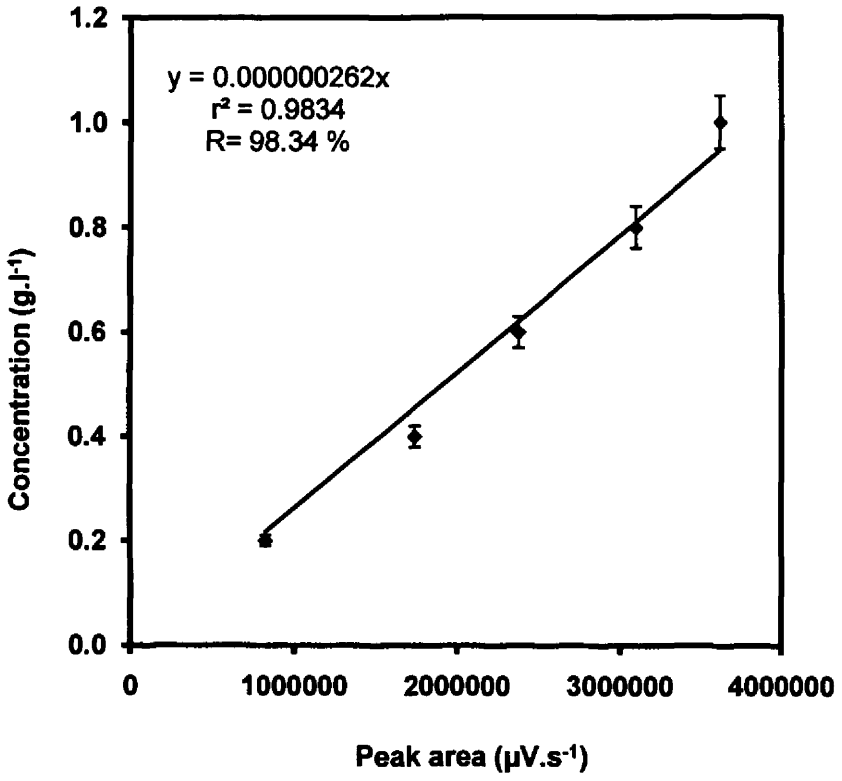

Appendix II.3. Typical calibration curve for cyclohexanone in ethyl acetate. Samples were prepared and analysed as described in Section 2.3.1. Linear least squares fitting was carried out and the fitted line had an R^2 value > 0.98. Error bars show one standard deviation.

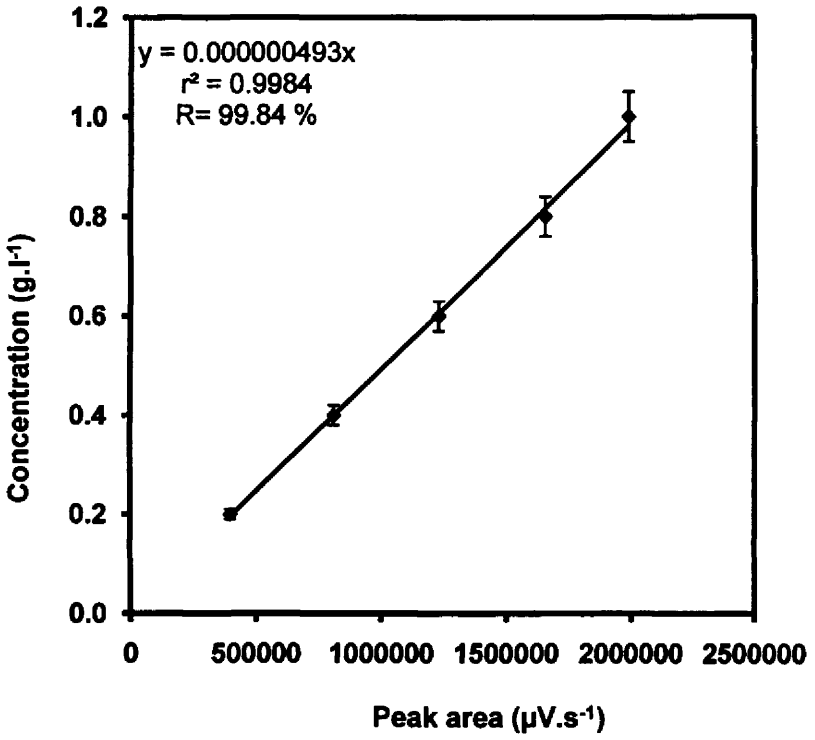

Appendix II.4 Typical calibration curve for caprolactone in ethyl acetate. Samples were prepared and analysed as described in Section 2.3.1. Linear least squares fitting was carried out and the fitted line had an R^2 value > 0.998. Error bars show one standard deviation.

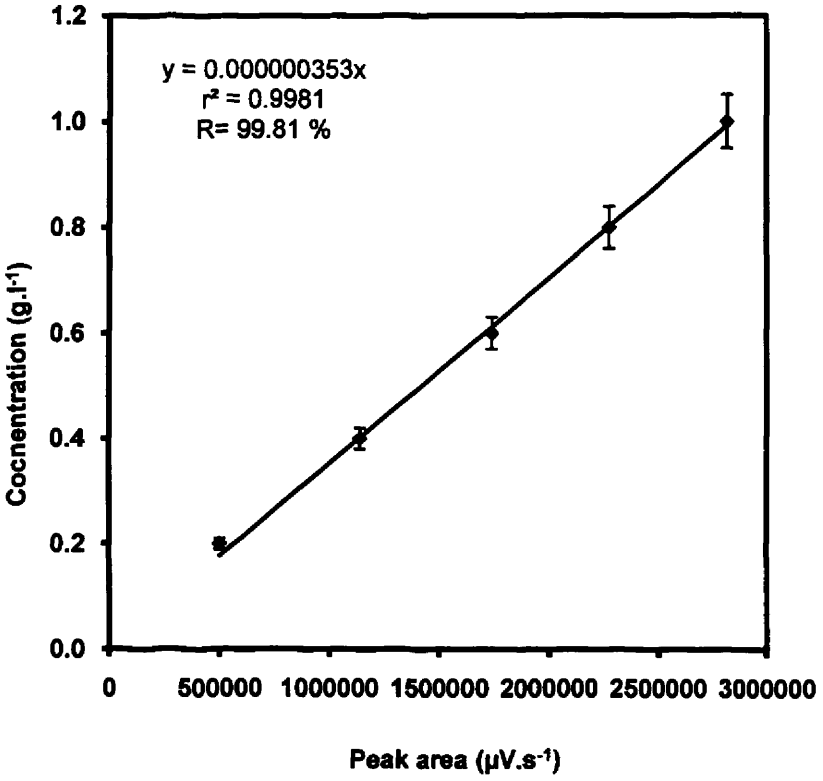

Appendix II.5 Typical calibration curve for cyclopentanone in ethyl acetate. Samples were prepared and analysed as described in Section 2.3.1. Linear least squares fitting was carried out and the fitted line had an R^2 value > 0.998. Error bars show one standard deviation.

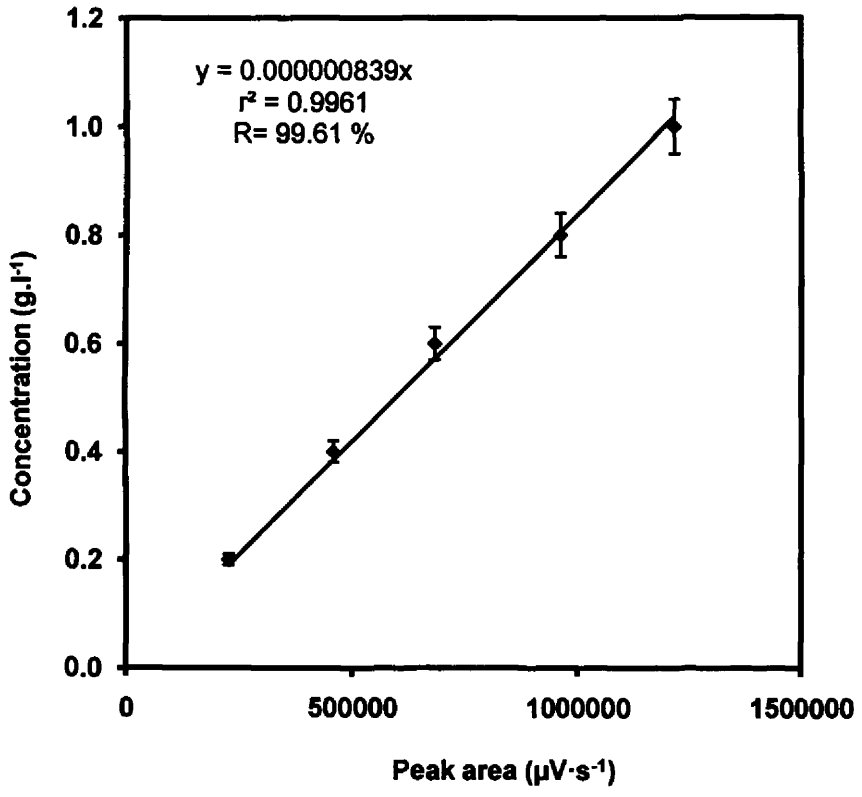

Appendix II.6. Typical calibration curve for δ-valerolactone in ethyl acetate. Samples were prepared and analysed as described in Section 2.3.1. Linear least squares fitting was carried out and the fitted line had an R^2 value > 0.996. Error bars show one standard deviation.

Appendix III

Illustrations of typical chromatograms for ketones and their corresponding lactones

Appendix III.1. Typical GC chromatogram of 1 $g.l^{-1}$ of bicycloketone showing FID response against time. The sample was prepared and analysed as described in Section 2.3.1. The bicycloketone peak is the first major one at 6.39 minutes, while at 12.73 minutes is the naphthalene peak, used as internal standard.

Appendix III.2 Typical GC chromatogram of 1 $g.l^{-1}$ of bicyclolactone showing FID response against time. The sample was prepared and analysed as described in Section 2.3.1. The bicyclolactone peak is the peak at 16.06 minutes, while at 12.71 minutes is the naphthalene peak, used as internal standard.

Appendix III.3 Typical GC chromatogram of 1g.l^{-1} of cyclohexanone showing FID response against time. The sample was prepared and analysed as described in Section 2.3.1. The cyclohexanone peak is the first major one at 6.00 minutes.

Appendix III.4. Typical GC chromatogram of 1g.l^{-1} of caprolactone showing FID response against time. The sample was prepared and analysed as described in Section 2.3.1. The caprolactone peak is the first major one at 14.04 minutes.

Appendix III.5 Typical GC chromatogram of 1g.l^{-1} of cyclopentanone showing FID response against time. The sample was prepared and analysed as described in Section 2.3.1. The cyclopentanone peak is the first major one at 6.36 minutes.

Appendix III.6 Typical GC chromatogram of 1g.l^{-1} of δ-valerolactone showing FID response against time. The sample was prepared and analysed as described in Section 2.3.1. The δ-valerolactone peak is the first major one at 6.36 minutes.

Appendix III.7 Typical bioconversion of bicycloketone using *E. coli* TOP10 [pQR239] as whole cell biocatalyst. The sample was prepared and analysed as described in Section 2.3.1. The bicycloketone peak is marked at 6.07 minutes while the bicyclolactone isomers produced by the bioconversion are marked at 15.48 and 15.64 minutes.

Appendix III.8 Typical bioconversion of cyclohexanone using *E. coli* TOP10 [pQR239] as whole cell biocatalyst. The sample was prepared and analysed as described in Section 2.3.1. The cyclohexanone peak is marked at 5.23 minutes while the caprolactone produced by the bioconversion is marked at 14.53 minutes

Appendix III.8 Typical bioconversion of cyclopentanone using *E. coli* TOP10 [pQR239] as whole cell biocatalyst. The sample was prepared and analysed as described in Section 2.3.1. The cyclopentanone peak is marked at 6.30 minutes while the δ-valerolactone produced by the bioconversion is marked at 15.90 minutes.

Appendix IV

Multiple illustrations from the WinPrep program for automation of microscale processing.

Appendix IV.1 Screenshot of WinPREP program for preparation of the microscale fermentation by adding the culture media and inoculum into individual wells (Section 4.1)

Appendix IV.2 Screenshot of WinPREP program for induction of *E. coli* TOP10 [pQR239] fermentation by addition of 15 µl of 15 % arabinose (Section 4.1).

Appendix IV.3 Screenshot of WinPREP program for the regeneration of NADPH in *E. coli* TOP10 [pQR239] fermentation by addition of 500 $g.l^{-1}$ of glycerol (Section 4.1).

Appendix IV.4 Screenshot of WinPREP program for addition of variable volumes of the ketone substrate to achieve various concentrations within wells.

Appendix IV.5. Screenshot of WinPREP program for preparation of a combinatorial arrange of microscale fermentations by addition of two different culture media and two types of inoculum into individual wells.

Appendix IV.6 Screenshot of WinPREP program for preparation of a combinatorial arrange of bioconversion by addition of multiple ketones substrates to multiple microscale fermentations. These additions were carried out with disposable tips to avoid cross contaminations.

Appendix V

Published Papers

Bioprocess Biosyst Eng (2005) 28: 83–93
DOI 10.1007/s00449-005-0422-4

ORIGINAL PAPERS

C. Ferreira-Torres · M. Micheletti · G. J. Lye

Microscale process evaluation of recombinant biocatalyst libraries: application to Baeyer–Villiger monooxygenase catalysed lactone synthesis

Received: 3 February 2005 / Accepted: 25 April 2005 / Published online: 6 October 2005